

A comprehensive analysis of *Fermi* Gamma-Ray Burst Data: IV. Spectral lag and Its Relation to E_p Evolution

Rui-Jing Lu¹, Yun-Feng Liang², Da-Bin Lin¹, Jing Lü¹, Xiang-Gao Wang¹, Hou-Jun Lü¹, Hong-Bang Liu¹, En-Wei Liang¹, Bing Zhang^{3,1}

ABSTRACT

The spectral evolution and spectral lag behavior of 92 bright pulses from 84 gamma-ray bursts (GRBs) observed by the Fermi GBM telescope are studied. These pulses can be classified into hard-to-soft pulses (H2S, 64/92), H2S-dominated-tracking pulses (21/92), and other tracking pulses (7/92). We focus on the relationship between spectral evolution and spectral lags of H2S and H2S-dominated-tracking pulses. The main trend of spectral evolution (lag behavior) is estimated with $\log E_p \propto k_E \log(t + t_0)$ ($\hat{\tau} \propto k_{\hat{\tau}} \log E$), where E_p is the peak photon energy in the radiation spectrum, $t + t_0$ is the observer time relative to the beginning of pulse $-t_0$, and $\hat{\tau}$ is the spectral lag of photons with energy E with respect to the energy band 8-25 keV. For H2S and H2S-dominated-tracking pulses, a weak correlation between $k_{\hat{\tau}}/W$ and k_E is found, where W is the pulse width. We also study the spectral lag behavior with peak time t_{pE} of pulses for 30 well-shaped pulses and estimate the main trend of the spectral lag behavior with $\log t_{pE} \propto k_{t_p} \log E$. It is found that k_{t_p} is correlated with k_E . We perform simulations under a phenomenological model of spectral evolution, and find that these correlations are reproduced. We then conclude that spectral lags are closely related to spectral evolution within the pulse. The most natural explanation of these observations is that the emission is from the electrons in the same fluid unit at an emission site moving away from the central engine, as expected in the models invoking magnetic dissipation in a moderately-high- σ outflow.

Subject headings: gamma-ray burst: general — methods: statistical

1. Introduction

It was theoretically speculated and observationally confirmed that long gamma-ray bursts (GRBs) are from the collapse of massive stars and short GRBs are from mergers of compact

¹Guangxi Key Laboratory for Relativistic Astrophysics, Department of Physics, Guangxi University, Nanning 530004, China; lindabin@gxu.edu.cn, luruijing@gxu.edu.cn, lew@gxu.edu.cn

²Key Laboratory of Dark Matter and Space Astronomy, Purple Mountain Observatory, Chinese Academy of Sciences, Nanjing 210008, China

³Department of Physics and Astronomy, University of Nevada Las Vegas, NV 89154, USA; zhang@physics.unlv.edu

binaries (e.g., Colgate 1974; Paczynski 1986; Eichler et al. 1989; Narayan et al. 1992; Woosley 1993; Woosley & Bloom 2006; Kumar & Zhang 2015). A spectral lag, defined as the time delay of high-energy photons with respect to low-energy photons, is commonly observed in long GRBs (Norris et al. 1986; Cheng et al. 1995; Band 1997; Norris et al. 2000), but is not in short ones (Yi et al. 2006; Norris & Bonnell 2006). An extensive analysis of the data from the Burst And Transient Source Experiment (BATSE) also shows that long wide-pulse GRBs tend to have long spectral lags (Norris et al. 2005). The distinguished features of spectral lags in these two types of GRBs are proposed to be a phenomenological indicator in GRB classification (Yi et al. 2006; Norris & Bonnell 2006; Gehrels et al. 2006; McBreen et al. 2008; Zhang et al. 2009). An anti-correlation between the spectral lag and peak luminosity is found in a few redshift-known BATSE GRBs (Norris et al. 2000). The low-luminosity GRB 060218 detected with the Burst Alert Telescope (BAT) onboard Swift satellite is consistent with this correlation (Liang et al. 2006). The precursor and main prompt emission in GRB 061121 show different spectral lags, but both are consistent with the above correlation (Page et al. 2007). The above correlation also holds in *Swift*/BAT GRB sample and even in the X-ray flares observed with the X-Ray Telescope onboard *Swift*, albeit with large scatter (Ukwatta et al. 2010; Margutti et al. 2010; Sultana et al. 2012; Sonbas et al. 2013; Bernardini et al. 2015). The relation between spectral lags and peak luminosity was proposed to be a distance indicator of GRBs (Norris et al. 2000; Schaefer 2007) for the purpose of using GRBs to constrain cosmological parameters.

GRB light curves are usually composed of overlapping pulses (Norris et al. 1996; Hu et al. 2014). It is generally speculated that each pulse is related to one individual radiation episode, which represents the fundamental unit of the GRB temporal profile (see, e.g., Fishman et al. 1994). The spectral lags measured in different emission episodes could be different (e.g., Page et al. 2007). However, the measured spectral lag is likely dominated by the wide pulses or the brightest pulse in a light curve. As a result, Hakkila et al. (2008) suggested that the spectral lag is better defined using individual pulses rather than the whole burst light curve profile. Significant spectral evolution is also a common feature of GRB pulses (e.g., Liang & Kargatis 1996; Preece et al. 2000; Lu et al. 2010, 2012; R acz et al. 2018). Two evolutionary patterns have been observed. One is the so-called hard-to-soft (hereafter H2S) pattern, which can be defined as the peak photon energy (E_p) in $\nu\text{-}\nu f_\nu$ spectrum decreasing monotonically within an individual pulse. The second is the so-called intensity tracking pattern, which is defined by E_p tracking the flux (Wheaton et al. 1973; Norris et al. 1986; Golenetskii et al. 1983; Lu et al. 2012). It was suggested that the spectral lag behavior of GRB prompt emission may be related to spectral evolution (Ukwatta et al. 2012; Uhm & Zhang 2016; Preece et al. 2016). Some authors also pointed out that the spectral evolution is related to the pulse profile (Hakkila & Preece 2011; Hakkila et al. 2015, 2018). For example, the hard-to-soft spectral evolution may primarily occur in hard and/or asymmetric pulses, and the intensity-tracking spectral evolution may be more prevalent in soft and/or symmetric pulses (Hakkila et al. 2015, 2018). In addition, Hakkila & Preece (2014) found that the residuals of single pulse fits to GRB lightcurves leave behind a mysterious triple-peaked structure. They argued that the interplay between such a triple-peaked structure and pulse fits may complicate spectral evolution in pulses. In this paper,

we explore the relation between the spectral lags and spectral evolution.

Gamma-Ray Burst Monitor (GBM) onboard the Fermi satellite has established a large GRB sample. We present a comprehensive analysis of the *Fermi* GRB data and report our results in a series of papers. We revealed the spectral components and their temporal evolution of the *Fermi* GRBs in the first two papers of this series (Zhang et al. 2011; Lu et al. 2012) and studied energy dependence of the burst duration in the third paper (Qin et al. 2013). This paper is dedicated to investigating the spectral lag and its relation to spectral evolution within bright GRB pulses. We describe our sample selection and data reduction in Section 2. The relations between the spectral evolution and the spectral lag behavior are studied in Section 3. Based on the results in Section 2, we explore the possible origin of spectral lags by performing simulations within the framework of a phenomenological model in Section 4. We summarize our results in Section 5. Throughout of this paper, a flat Λ CDM cosmology with the parameters $H_0 = 71\text{km} \cdot \text{s}^{-1} \cdot \text{Mpc}^{-1}$, $\Omega_M = 0.3$, and $\Omega_\Lambda = 0.7$ is adopted. The quoted uncertainties are at 1σ confidence level.

2. Samples and Data Reduction

We download the GBM data of GRBs by August, 2015 from Fermi Archive FTP websites¹. The energy-dependent light curves are extracted with the python source package *gtBurst*², the standard HEASOFT tools (version 6.20), and the *Fermi Science Tool* (v10r0p5). The TTE data from the brightest detectors (with the smallest angle between this detector and the source object) are used in our analysis. We select bright and well-shaped pulses for our analysis. To identify such a pulse, we employ an empirical pulse model (Kocevski et al. 2003), i.e.,

$$I(t) = I_m \left(\frac{t + t_0}{t_m + t_0} \right)^r \left[\frac{d}{d+r} + \frac{r}{d+r} \left(\frac{t + t_0}{t_m + t_0} \right)^{r+1} \right]^{-\frac{r+d}{r+1}}, \quad (1)$$

to fit the bright pulses, where t_0 measures the offset of the pulse zero time relative to the GRB trigger time, t_m is the time of the peak flux (I_m), and r and d are the power-law rising and decaying indices, respectively. Note that the values of r and d are degenerated with t_0 and thus one needs to set a t_0 value for estimating the value of r and d for a pulse. In this analysis, we simply set t_0 at the time corresponding to $0.1I_m$ in the rising phase. To obtain the value of t_0 , we first give a trial fit to a pulse profile with Equation (1). With the fitting result, one can easily identify the time of $0.1I_m$, which is set as the value of t_0 . Then, we fit the pulse profile with Equation (1). We would like to select relatively smooth pulses and adopt $\chi_r^2 < 1.5$ as our pulse selection criterion. Owing to the mini-pulses or the triple-peaked structure (e.g., bn0901310901, Hakkila and Preece 2014), a few pulses have larger χ_r^2 . However, the spectral lags of these pulses are dominated by the bright

¹<ftp://legacy.gsfc.nasa.gov/fermi/data/>

²<http://sourceforge.net/projects/gtburst/>.

pulse. Similar to the work of Hakkila et al. (2008), we also include these pulses in our analysis. We finally obtain 92 pulses from 84 GRBs for our analysis. These pulses along with our fittings (red solid lines) are shown in Figures 1 (H2S spectral evolution) and 2 (tracking spectral evolution), where the spectral evolution behavior is identified by eye (see Section 3.1 for detail discussion). The results of our light curve fittings are reported in Tables 1. Note that there might be a triple-peaked structure in the residual of our defined pulses (Hakkila & Preece 2014). Equation (1) only provides a first-order approximation to the pulse profiles.

We then perform an analysis for the spectral evolution and the spectral lag. The Gamma-Ray Spectral Fitting Package (RMFIT, Version 4.3.2)³ is used to extract the time-dependent spectra with a signal-to-noise ratio $\text{SNR} > 40$ and perform joint spectral fitting with the Band function (Band & Trzhaskovskaya 1993). The spectral fitting results are reported in Tables 2. The values of E_p , which are marked as violet “★” and labeled with bottom x - and right y -axis in the left panel and top x - and right y -axis in the right panel of each sub-figure, are plotted Figures 1 and 2. In Figures 1 and 2, the two vertical dotted lines in the left panel of each sub-figure mark the time period (see first column of Table 3) adopted to perform the cross correlation function (CCF) analysis in order to obtain the spectral lag. The procedure to obtain the spectral lag $\hat{\tau}$ and its error is shown as follows. (1) For each energy band, we produce 10^3 sets of simulated light curves with the Monte Carlo method by assuming that the observed flux error is normal distribution. (2) We calculate the $\text{CCF}(\hat{\tau}')$ of our simulated light curve for high-energy photons and that for lowest-energy photons (Band 1997; Norris et al. 2000, 2005; Yi et al. 2006; Ackermann et al. 2010). (3) We fit the $\hat{\tau}' - \text{CCF}$ relation with a Gaussian function and obtain the maximum value of CCF and its corresponding value of $\hat{\tau}' = \hat{\tau}'_p$. (4) The value of $\hat{\tau}$ and its 1σ uncertainty are obtained by fitting the distribution of $\hat{\tau}'_p$ with a Gaussian function for a sample of 10^3 pairs of our simulated light curves. In our analysis, we estimate the spectral lag ($\hat{\tau}$) with respect to 8-25 keV for four energy bands (①: 25-50 keV, ②: 50-100 keV, ③: 100-300 keV, ④: 300-1000 keV) of NaI detectors and two energy bands (⑤: 300-1000 keV, ⑥: 1000-5000 keV) of the BGO detectors if it is available. In some GRBs, especially soft pulses, we also estimate the spectral lag for other energy bands, such as ⑦: 25-40 keV, ⑧: 40-60 keV, ⑨: 60-100 keV, ⑩: 16-25 keV. The same energy band (300-1000 keV) in the NaI (④) and BGO (⑤) detectors is chosen in order to perform cross-check of the lag in different detectors. Our obtained spectral lag $\hat{\tau}$ can be found in Table 3 and is plotted in the right panel of sub-figure of Figures 1 and 2 with the black “●” (bottom x - and left y -axis), where the value of E is the median value of each energy band in the logarithmic space. In this work, we also estimate the spectral lag ($\hat{\tau}_{31}$) between 100-300 keV and 25-50 keV in order to compare our results with those found in the previous works. The value of $\hat{\tau}_{31}$ is reported in Table 4.

³<http://fermi.gsfc.nasa.gov/ssc/data/analysis/rmfit/>

3. Spectral Evolution and Spectral Lag

3.1. Spectral Evolution

In this work, we plan to investigate the possible relation between spectral evolution and spectral lags and identify the main trend of spectral evolution. For this purpose, we make a linear fit to the data sets $(\log(t + t_0), \log E_p)$, i.e., $\log E_p = k_E \log(t + t_0) + b$. A steeper slope (i.e., larger $|k_E|$) indicates a faster softening. The results of our fittings can be found in the right panel of each sub-figure of Figures 1 (for H2S pulses) and 2 (for tracking pulses), and the derived slope k_E of each burst is reported in Table 4. The left panel of Figure 3 shows the distribution of k_E , where we have defined three types of pulses: H2S pulses (the green “/” hatch), H2S-dominated-tracking pulses (blue “\” hatch), and other tracking pulses (“o” hatch). The definitions of the latter two categories are as follows. From Figure 3, we find that all the H2S pulses have a value of $k_E < -0.2$, ranging from -0.23 to -1.55 . In addition, the tracking pulses in Figure 2 with a value of $k_E < -0.2$ (21/28) have essentially the same distribution as the H2S pulses at the 5% significance level by performing the Anderson-Darling test. In these pulses, the dominating feature of E_p evolution is still H2S during their decay phase and the tracking feature is illustrated by only one or two hard spectra in their rising phase. Therefore, we define that these tracking pulses (21/28) with a value of $k_E < -0.2$ as H2S-dominated-tracking pulses. The H2S and H2S-dominated-tracking pulses are included in our statistical analysis about the relationship between spectral evolution and spectral lag. For other pulses in Figure 2, four tracking pulses (4/28), i.e., GRBs 110622158, 120222021, 120402669 and 130612456 have a value of $k_E \simeq 0$, indicating no clear E_p evolution. The other three tracking pulses (3/28), i.e., GRBs 100122616, 131214705 and 120308588, have a positive k_E , indicating that those pulses are dominated by a soft-to-hard spectral evolution pattern. These seven pulses are shown with the black “o” hatches in Figure 3, and are grouped into the category of other tracking pulses.

It is suggested that the spectral evolution may be related to the pulse profile (Hakkila & Preece 2011; Hakkila et al. 2015, 2018). For example, the H2S spectral evolution may primarily occur in hard and/or asymmetric pulses, and the intensity-tracking spectral evolution may be more prevalent in soft and/or symmetric pulses (Hakkila et al. 2015, 2018). We then study the relationship between pulse width (W) and pulse asymmetry (κ_a) in Figure 4, where $\kappa_a = T_d/T_r$ with T_d (T_r) being the time interval between I_m and $0.1I_m$ in the decay (rising) phase and the pulse width $W = T_d + T_r$. From this figure, we find that the tracking pulses are systematically more symmetrical compared with the H2S pulses, which is consistent with those found in Hakkila et al. (2015, 2018). This reveals that pulse asymmetry can be taken as an indicator of its spectral evolution (Norris et al. 1996). Preece et al. (2016) pointed out that pulse asymmetry is directly produced by E_p evolution. Here we only focus on the relationship between spectral evolution and spectral lags.

It should be also noted that the light curve of some GRB pulses may be non-monotonic, i.e., there is an underlying the triple-peaked profile superposed on the simple pulse fits (Hakkila & Preece 2014). The non-monotonicity behavior of the pulses may affect spectral evolution. The triple-

peaked pulse found in the light curve fitting residuals can be decomposed into a precursor peak, a central peak, and a decay peak (Hakkila & Preece 2014). The precursor peak is always harder than the decay profile in which these two peaks can be measured. As a result, the spectral evolution of the pulses would always take on a H2S behavior (Hakkila et al. 2015). However, some pulses often exhibit re-hardening at or around the time of the central/decay peak. These pulses may then take an intensity-tracking behavior, depending on the hardness contribution made by each of these peaks. The spectral evolution in these pulses would be complex and thus the relation of spectral evolution and spectral lags may be difficult to estimate. To avoid these complications, our analysis about the relation of spectral evolution and spectral lags is performed based on the H2S and H2S-dominated pulses.

3.2. Spectral Lag Behavior

In Figure 1, a clear dependence of $\hat{\tau}$ on E can be found. Since $\hat{\tau}$ is almost a linear function of $\log(E)$ in this figure, we estimate the relation of $\hat{\tau} - \log E$ with a linear fit, i.e., $\hat{\tau} = k_{\hat{\tau}} \log E + b$. Our fitting results are shown in Figure 1 and the derived $k_{\hat{\tau}}$ is reported in Table 4. A similar dependence of $\hat{\tau}$ on E can be also found in the H2S-dominated-tracking pulses. We then also estimate the relation of $\hat{\tau} - \log E$ by performing a linear fitting for these pulses. The fitting results can also be found in Figure 2 and the derived value of $k_{\hat{\tau}}$ is also reported in Table 4. The distribution of $k_{\hat{\tau}}$ can be found in the right panel of Figure 3.

In Figure 5, we demonstrate the relations of $k_{\hat{\tau}}-W$ (left panel), k_E-W (middle panel), and $k_{\hat{\tau}}/W-k_E$ (right panel) for H2S pulses (black “•”) and H2S-dominated-tracking pulses (blue “★”). Here, W is the full width at half maximum of the pulse observed at 8keV-1MeV energy band and can be found in Table 4. We perform a Kendall’s tau correlation test to the $k_{\hat{\tau}}-W$ sample and obtain a tau statistic value of 0.578 with the probability $p \ll 10^{-4}$ by testing non-correlation. We then employ a linear fit to the data from the H2S pulses and H2S-dominated-tracking pulses. The relation of $\log k_{\hat{\tau}} = (-0.821 \pm 0.057) + (1.269 \pm 0.088) \log W$ is obtained. This relation indicates that a wider pulse gives a steeper slope for the relation of $\hat{\tau}$ and E . We also notice that the value of the $k_{\hat{\tau}}$ found in the H2S-dominated-tracking pulses is systematically smaller than that found in the H2S pulses (see the left panel in Figure 5). This is owing to the hardening behavior found in the rising phase of the H2S-dominated-tracking pulses. In the middle panel of Figure 5, we do not find any relation between k_E and W in the both H2S pulses and H2S-dominated-tracking pulses. In the right panel of Figure 5, a Kendall’s tau correlation test indicates a weak correlation between $\log(k_{\hat{\tau}}/W)$ and $\log(-k_E)$ with a tau statistic value of 0.307 and the probability $p < 10^{-4}$. We perform a linear fit to the data and obtain the correction of $\log(k_{\hat{\tau}}/W) = (-0.558 \pm 0.032) + (0.594 \pm 0.115) \log(-k_E)$. This relation indicates that a quick evolution of E_p would form a strong evolution of $\hat{\tau}$ relative to the photon energy E .

To compare our analysis with that in the literature, we also study the relations of $\hat{\tau}_{31}$ and W for the H2S pulses (blue “•”) and the H2S-dominated-tracking pulses (violet “★”) in the left panel

of Figure 6. It is shown that the value of $\hat{\tau}_{31}$ is positively related to W . We find a correction of $\log \hat{\tau}_{31} \propto \varepsilon \log(W/s)$ with $\varepsilon = 0.88 \pm 0.03$, which is consistent with that found in Arimoto et al. (2010) ($\varepsilon = 0.86$ in the 6-25 keV band and $\varepsilon = 1.06$ in the 50-400 keV band), but slightly shallower than that obtained by Hakkila et al. (2008) ($\varepsilon = 1.17$) and that of Norris et al. (2005) ($\varepsilon = 1.42$). This relation shows that a wide pulse tends to have a large spectral lag (Norris et al. 2005), but it is not the case in a tracking pulse. We also notice that the value of $\hat{\tau}_{31}$ in the H2S-dominated-tracking pulses is systematically smaller than that found in the H2S pulses. The reason for this behavior is the same as that found in the left panel of Figure 5.

3.3. $t_{\text{PE}}-E$ and W_E-E Relation

To further study the spectral lag behavior, we select the pulses which are well shaped in at least three energy bands. Thirty pulses are obtained. We then plot the t_{PE} (left y -axis) and W_E (right y -axis) as a function of E in Figure 7, where t_{PE} (W_E) is the peak time (full width at half maximum) of the pulse and t_0 is from Table 1. One can find that both t_{PE} and W_E are negatively related to the photon energy E for the H2S pulses (19/30) and H2S-dominated-tracking pulses (4/30). These behaviors suggest that the pulse profile in a lower energy band tends to peak earlier and be wider than that in a higher energy band for the H2S pulses and H2S-dominated-tracking pulses. In 4/30 other tracking pulses (GRBs 100122616, 120222021, 120402669 and 130612456), W_E tends to become narrower with an increasing photon energy E while t_{PE} is positively correlated to E . On the other hand, in the other 3/30 tracking pulses (GRBs 110622158, 120308588 and 131214705), both t_{PE} and W_E are positively related to the energy E . We estimate the E -dependent behavior of t_{PE} and W_E by performing a linear fit to the relations of $\log(t_{\text{PE}} + t_0) - \log E$ and $\log W_E - \log E$, i.e., $\log(t_{\text{PE}} + t_0) = k_{t_p} \log E + b$ and $\log W_E = k_W \log E + c$, respectively. Our best fitting results are plotted in Figure 7. One can find that for smooth H2S pulses (e.g., bn081224887 and bn090922539), a linear model does fit the data well. For tracking pulses (e.g., bn131214705), the rising part is too short and thus the evolution trend of E_p is difficult to estimate. However, a linear fit to the data can roughly estimate the main trend of the spectral evolution. In addition, Uhm & Zhang (2016) found from their pulse modeling that the peak time and the width of a pulse are all linearly related to E in logarithm space. As a result, we perform linear fits to the data in Figure 7. In Figure 8, we show the relations of $k_W - k_{t_p}$ and $k_{t_p} - k_E$ together with k_W , k_{t_p} , and k_E distributions. One can find from this figure that the values of k_W , k_{t_p} , and k_E are distributed at the center of -0.25 , -0.08 , and -0.8 , respectively. In addition, the tentative correlations, i.e., $k_W = (-0.16 \pm 0.02) + (1.03 \pm 0.20)k_{t_p}$ with $(r, p) = (0.77, \ll 0.0001)$ and $k_{t_p} = (-0.46 \pm 0.21) + (0.89 \pm 0.29)k_E$ with $(r, p) = (0.40, 6.09 \times 10^{-2})$, are obtained for H2S and H2S-dominated-tracking pulses, respectively. The relation of $k_{t_p} - k_E$ reveals that the dependence of spectral lag on E is likely related to the spectral evolution.

4. Origin of Spectral Lags

As shown in Section 3, the observed spectral lag behavior is likely related to spectral evolution. To illustrate this, in this section we develop a phenomenological model and investigate the spectral lag behavior based on simulations. We assume the flux density $f(t, E)$ of a GRB observed at a given time t and photon energy E as

$$f(t, E) = I(t)\phi(E, t), \quad (2)$$

where $I(t)$ and $\phi(E, t)$ are the intensity and normalized radiation spectrum, respectively. Equation (1) is adopted to describe the evolution of $I(t)$ ⁴. For the radiation spectrum $\phi(E, t)$, we take the Band function, which is characterized with three parameters, i.e., low photon energy index α , high energy photon index β , and break energy E_b (Band et al. 1993). For the Band function, the value of E_p can be straightforwardly derived using $E_p(t) = (2 + \alpha)E_b$ if $\beta < -2$ is satisfied. We take the observed spectral evolution pattern to model the $E_p(t)$ evolution in our simulations, i.e.,

- Case (I): H2S spectral evolution

$$\log E_p = a + k_E \log t \quad \text{with } k_E < 0, \quad (3)$$

- Case (II): Tracking spectral evolution

$$\log E_p = \begin{cases} b + k_1 \log t, & t \leq t_m + \xi, \\ b + (k_1 - k_2) \log(t_m + \xi) + k_2 \log t, & t > t_m + \xi, \end{cases} \quad (4)$$

where $k_1 > 0$ and $k_2 < 0$ are adopted, and ξ is adopted to describe the difference between the intensity peak and the peak time of $E_p(t)$ evolution pattern.

The simulated light curves for Case (I) are plotted in the left panel of Figure 9, where $F_m = 1$, $t_m = 5$, $r = 1$, $d = 2$, $t_0 = 0$, $\alpha = -1$, $\beta = -2.3$, and $k_E = -1$ are used in our simulations. Eight energy bands are adopted which are uniformly distributed in the logarithm space in the range of $(10, 10^4)$ keV. The spectral lags for different energy bands are estimated based on our simulated light curves and are plotted in the middle panel of Figure 9. It can be found that the value of $\hat{\tau}$ increases with E and saturates at around 10^3 MeV, which is the value of $E_p(t = 0)$. This behavior can be also easily found in the left panel of Figure 9. The relation of $\hat{\tau}_{31}$ and W is also studied in the right panel of Figure 9, where the value of r or d in Equation (1) is changed in order to produce different W from our simulations. We also estimate the values of $k_{\hat{\tau}}$ and k_{t_p} for different values of k_E and $E < 1\text{MeV}$. The relations of $k_{\hat{\tau}}-k_E$ and $k_{t_p}-k_E$ are shown in Figure 10, which indicates strong correlation between $k_{\hat{\tau}}$ and k_E or k_{t_p} and k_E .

For Case (II), our simulated light curves and the E -dependent $\hat{\tau}$ are shown in the left and right panels of Figure 11, respectively. Here, the value of $F_m = 1$, $t_m = 5$, $r = 1$, $d = 2$, $\xi = -1$, $\beta = -2.3$,

⁴ One caveat here is that the results obtained in this section is the first-order approximation. The introduction of the underlying triple-peaked structure may somewhat complicate the situation.

$k_1 = 5$, and $k_2 = -2$ are adopted in the simulations, and the sub-cases with $\xi = -1.5, 0, 1.5$, are adopted in the upper, middle, and lower sub-figures, respectively. One can find that there is no spectral lag for all energy bands in the sub-case with $\xi = 0$ s. However, the value of $\hat{\tau}$ increases with the observed energy band for the sub-case with $\xi = -1.5$ s and decreases with photon energy for the sub-case with $\xi = 1.5$ s. It should be noted that the spectral evolution in the sub-case with $\xi = -1.5$ s is similar to that of H2S-dominated-tracking pulses and that the sub-case with $\xi = 1.5$ s is similar to that of other tracking pulses. The spectral lag behaviors found in these two sub-cases are similar to those found in Section 3.

As shown in the above, our simulations with different spectral evolution patterns can reproduce the observational results. This may indicate that spectral lag is the result of temporal evolution of E_p across energy bands (e.g., Ukwatta et al. 2012). That is to say, spectral lag is associated with spectral evolution. This is also consistent with the physically-motivated simulations within the framework of synchrotron radiation at a large emission radius (Uhm & Zhang 2016).

5. Conclusions and Discussion

This work studies the spectral evolution and spectral lag behavior in 92 bright pulses from 84 GRBs observed by the Fermi GBM telescope. We focus on the relation of spectral evolution and the spectral lag behavior in H2S (64/92) and H2S-dominated-tracking (21/92) pulses. It is found that the spectral lag ($\hat{\tau}$) is usually photon-energy-dependent. In the H2S and H2S-dominated-tracking pulses, the spectral lag increases with increasing photon energy E (given the same reference band in 8-25 keV). In addition, the dependence of spectral lag on E may be different from pulse to pulse, even for those in the same GRB. We then adopt the slope $k_{\hat{\tau}}$ in the relation of $\hat{\tau} \propto k_{\hat{\tau}} \log E$ to describe the behavior of E -dependent $\hat{\tau}$ for different pulses. The main trend of E_p evolution is approximated by performing a log-linear fit to the E_p - t relation with $\log E_p(t) \propto k_E \log(t + t_0)$ and the k_E is used to describe the behavior of spectral evolution. For H2S and H2S-dominated-tracking pulses, a weak relation of $k_{\hat{\tau}}/W$ and k_E is found, where W is the full width at half maximum for the pulses observed at 8-10³ keV energy band. For further studying the relation between spectral evolution and spectral lag, we also investigate the evolution of peak time t_{pE} in different energy bands for 30 well shaped pulses. A log-linear relation of t_{pE} - E is found, i.e. $\log t_{pE} \propto k_{t_p} \log E$, in H2S and H2S-dominated-tracking pulses. In addition, a weak relation between k_{t_p} and k_E is also obtained. The relations of $k_{\hat{\tau}}$ - k_E and k_{t_p} - k_E together with the spectral evolution pattern are reproduced in our simulations within the framework of a phenomenological model that invokes the evolution of a Band-function spectrum with time. Based on these results, we conclude that spectral lag is related to the spectral evolution in GRBs.

The discovery reported in this paper sheds light on the GRB prompt emission mechanism that is highly debated. The fact that the spectrum evolves uniformly within each pulse (which has a typical duration of seconds) suggests that pulses are fundamental units of GRB radiation. Within the framework of GRB models, there are two scenarios to interpret these broad pulses. The

first scenario is that the pulse shape is defined by the central engine activity history, so that each emission epoch in the light curve corresponds to emission from different groups of electrons when they reach a certain radius (e.g., photosphere or internal shocks). The second scenario is that the broad pulse is emission from electrons within the same fluid unit, and different emission episodes correspond to the same fluid unit emitting at different locations as it streams outwards. This second possibility corresponds to an emission radius $R_{\text{GRB,pulse}} \sim \Gamma^2 ct_{\text{pulse}} \sim 10^{15} \text{ cm}(\Gamma/100)^2(t_{\text{pulse}}/3 \text{ s})$. Any model that invokes an emission radius smaller than this radius, e.g., the photosphere model (unless Γ is extremely small) and the internal shock model (unless the variability time Δt is of the order of pulse duration), belong to the first scenario. Our data and simulations suggest that spectral lags are closely related to the spectral evolution of the emission spectrum. This is much easier to realize if emission comes from electrons within the same fluid unit, so that emission properties can evolve continuously as the fluid unit moves in space (so that the magnetic field strength, bulk Lorentz factor, and probably characteristic electron Lorentz factors) can evolve continuously (see the generic physical model discussed by Uhm & Zhang 2016 and Uhm et al. 2018). Such a scenario naturally produces asymmetric pulse profiles and H2S evolution. Under certain conditions, one can also reproduce tracking pulses (most are H2S-dominated)⁵. It is consistent with dissipation of magnetic energy at a radius of the order of $R_{\text{GRB,pulse}}$, as has been invoked in the ICMART model of GRB prompt emission (Zhang & Yan 2011; Lazarian et al. 2018). Within this picture, the smaller variability timescale overlapping on the broad pulses are produced by the local Lorentz-boosted regions due to magnetic reconnection within a moderately-high- σ bulk flow (Zhang & Yan 2011; Zhang & Zhang 2014; Deng et al. 2015). Within the framework of the first scenario, on the other hand, the requirement to have emission spectrum evolves corporately as a function of time is much more demanding, since electrons are from different fluid units. Indeed within the framework of the photosphere model, it has been shown that it is quite challenging to produce H2S evolution pulses (Deng & Zhang 2014). The small-radii internal shock model (which is needed to interpret the rapid variability in the light curves) also faces the similar problem, since it requires that the electron Lorentz factors, magnetic fields, and bulk Lorentz factors in different internal shocks would behave corporately with conspiracy to give rise to the observed spectral evolution.

We thank the referee for a constructive report. This work is supported by the National Basic Research Program of China (973 Program, grant No. 2014CB845800), the National Natural Science Foundation of China (grant Nos. 11573034, 11773007, 11533003, 11673006, 11603006), the Guangxi Science Foundation (grant Nos. AD17129006, 2016GXNSFDA380027, 2016GXNSFFA380006, 2017GXNSFFA198000, 2016GXNSFCB380005), the Natural Science Key Foundation of Guangxi under Grant No. 2015GXNSFDA139002, the Special Funding for Guangxi Distinguished Professors (Bagui Yingcai & Bagui Xuezhe), and the Innovation Team and Outstanding Scholar Program in Guangxi Colleges.

⁵ The mysterious triple-peaked structure claimed by Hakkila & Preece (2014) is, however, difficult to interpret within the framework of any physically oriented models.

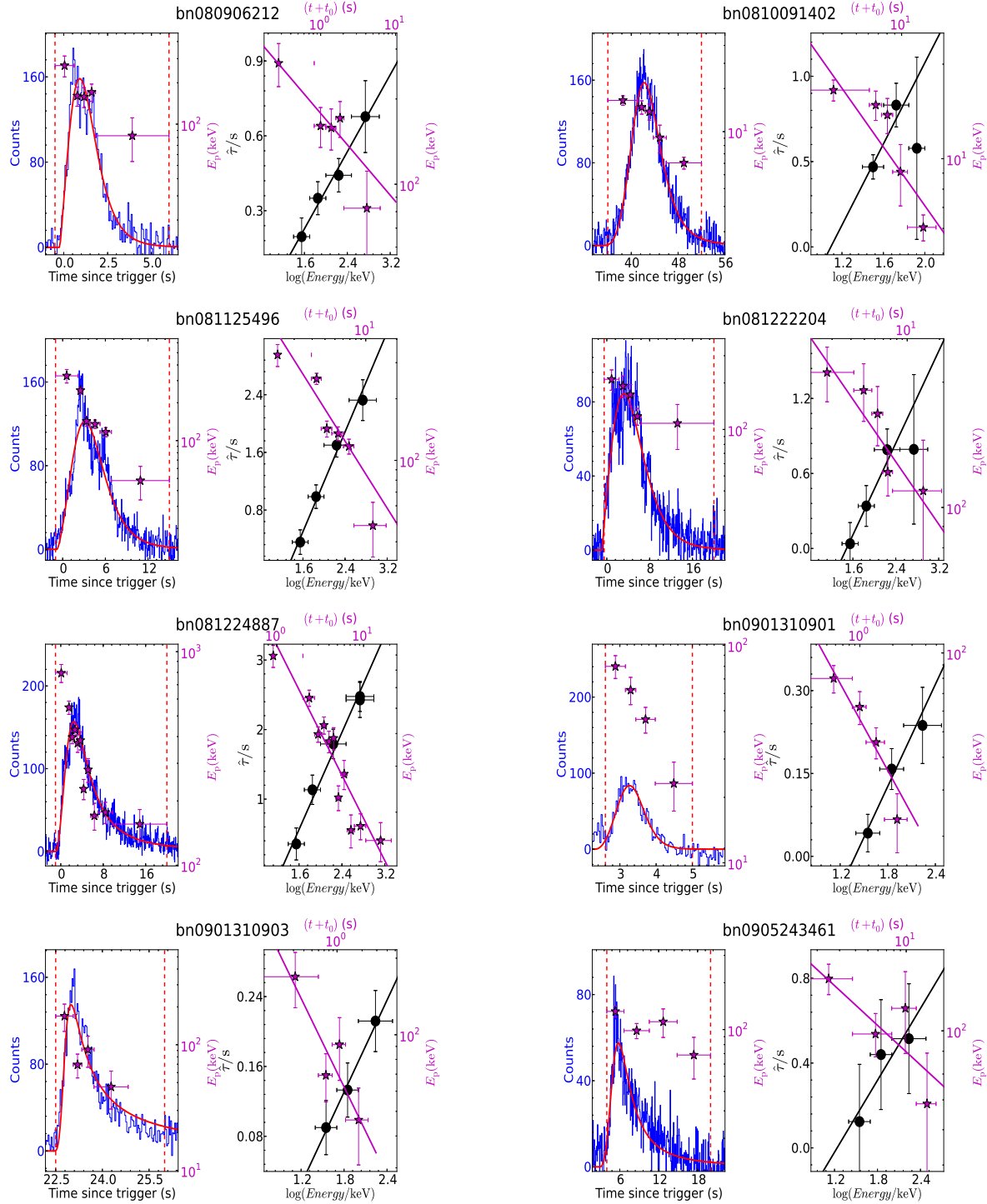


Fig. 1.— Our selected pulses with H2S spectral evolution. The light curve of pulse (blue curves), best light curve fitting result (red solid line) with Equation 1, and E_p (violet “★”) are shown in the left panel of each sub-figure. Here, the two vertical dotted lines mark the time period for performing CCF analysis. The energy dependent $\hat{\tau}$ (black “●”, bottom x - and left y -axis) and time dependent E_p (violet “★”, top x - and right y - axis) are shown in the right panel of each sub-figure, where the solid lines are the best linear fitting result for the spectral lag behavior (black solid line) and spectral evolution (violet solid line).

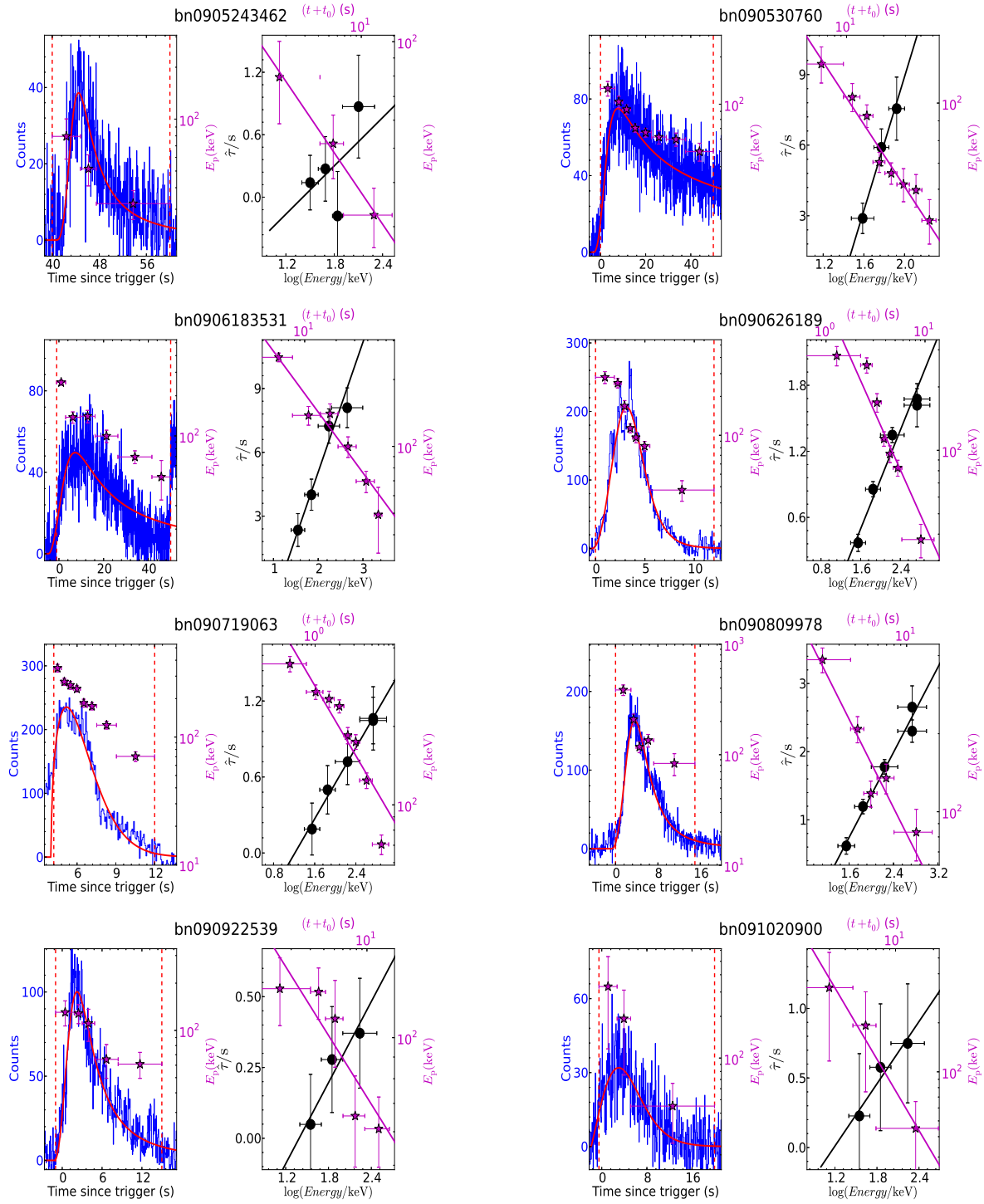


Fig. 1—Continued.

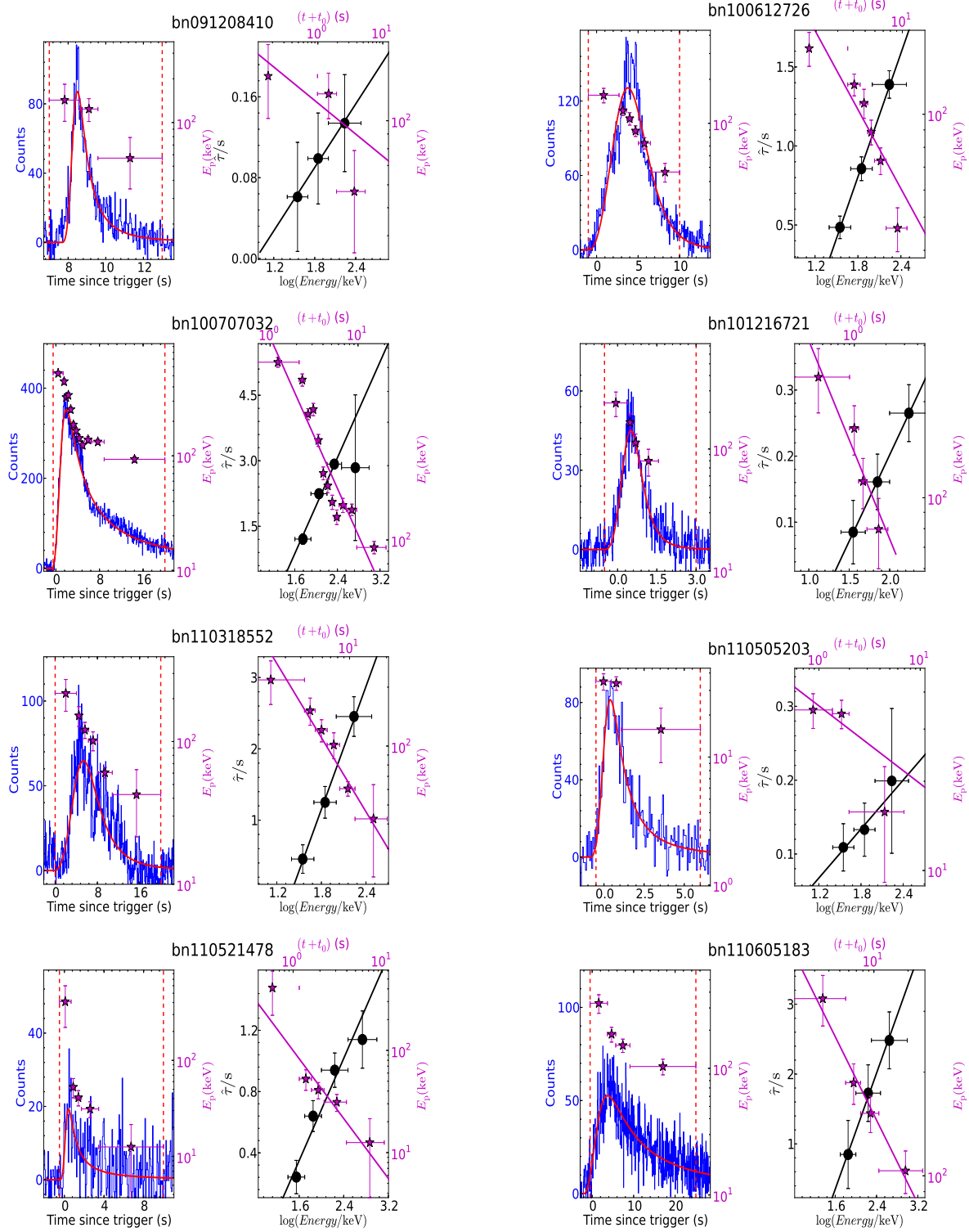


Fig. 1—Continued.

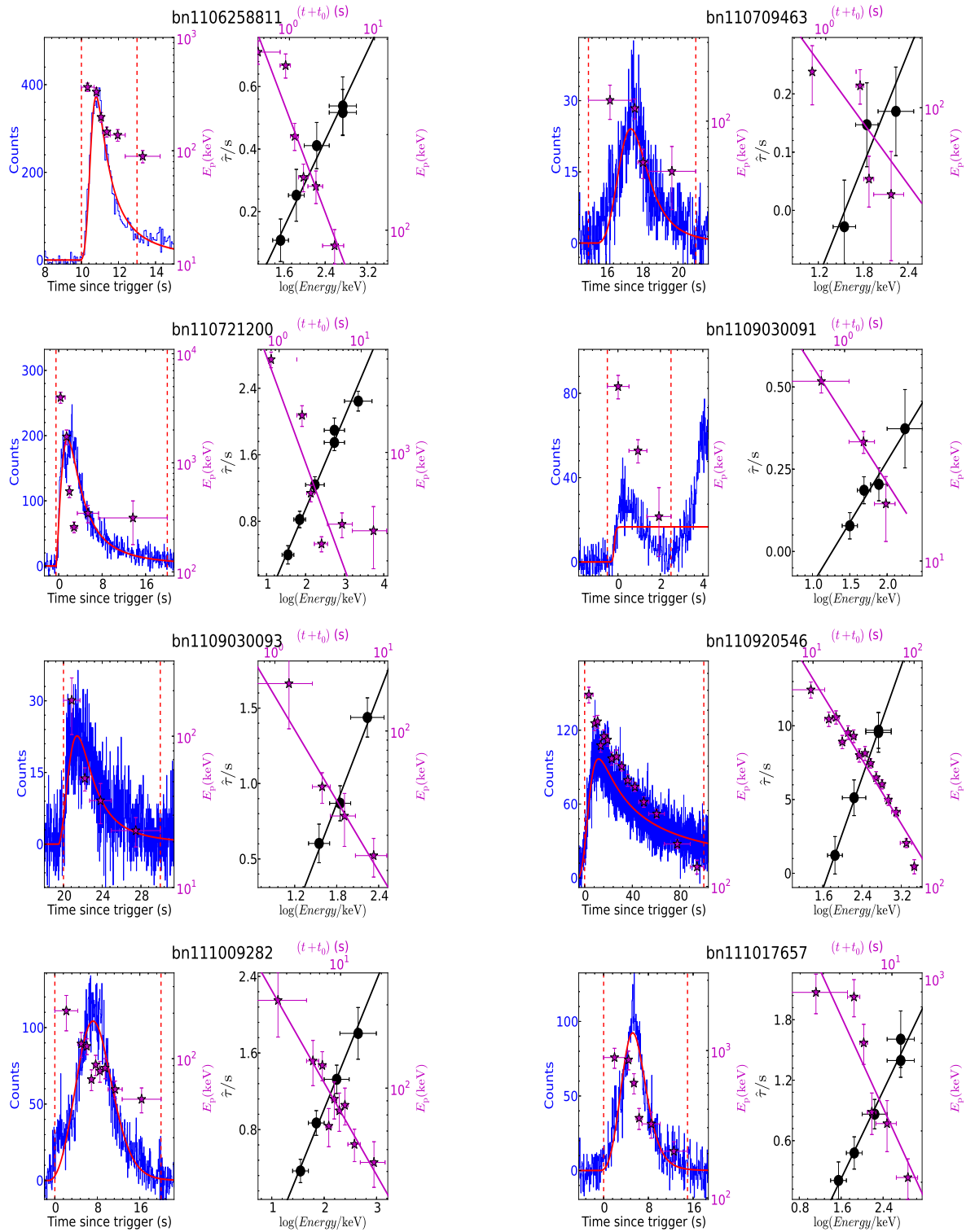


Fig. 1—Continued.

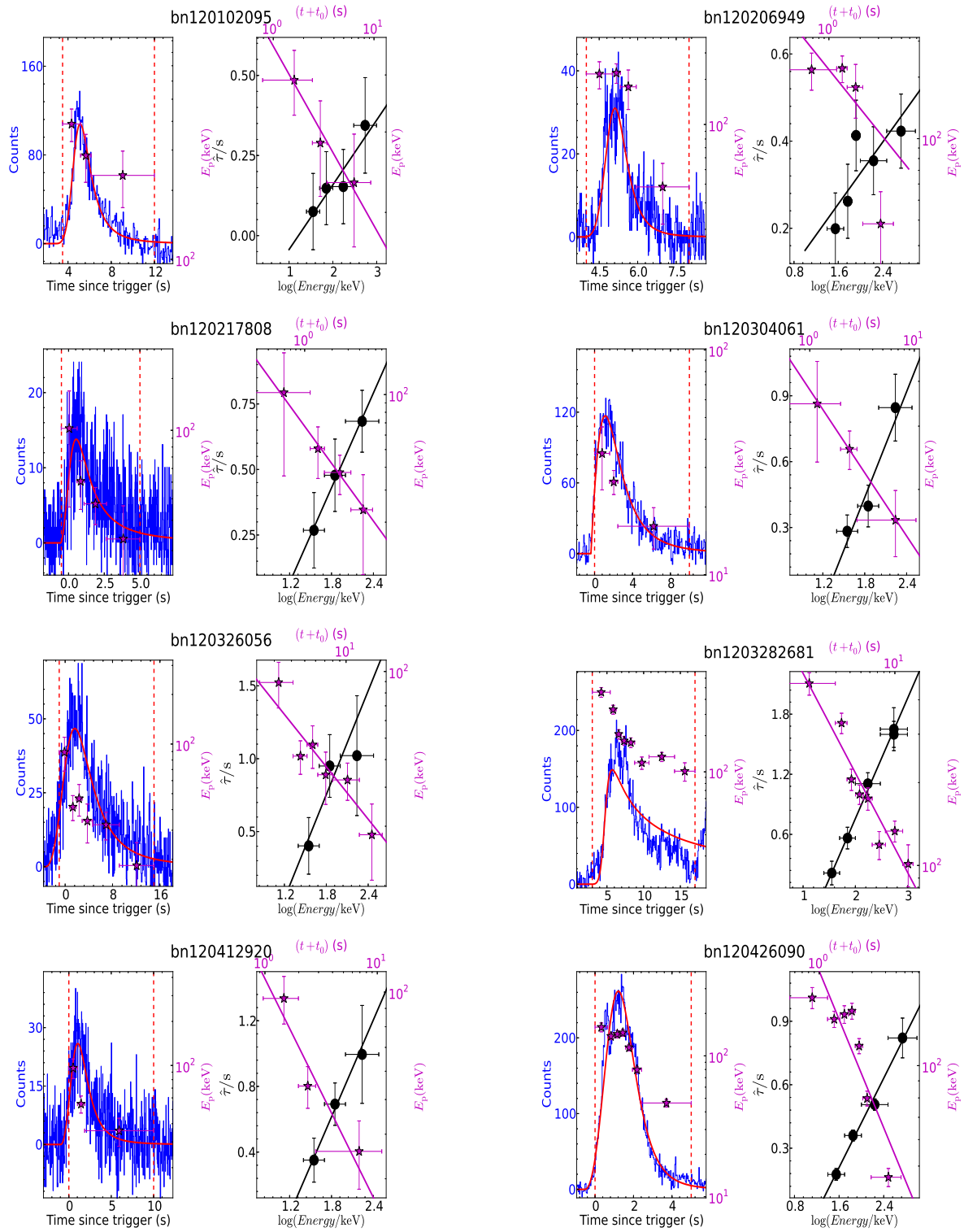


Fig. 1—Continued.

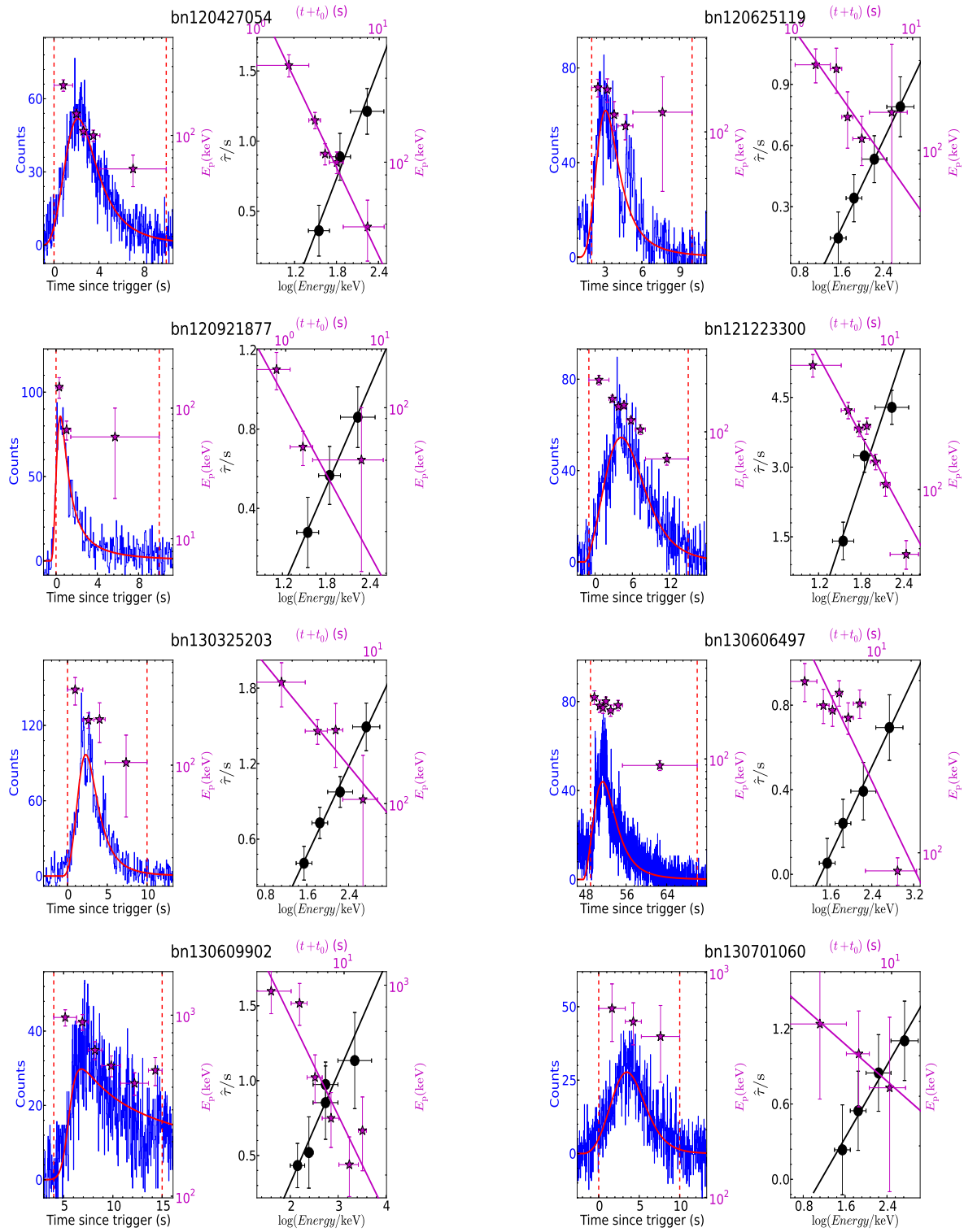


Fig. 1—Continued.

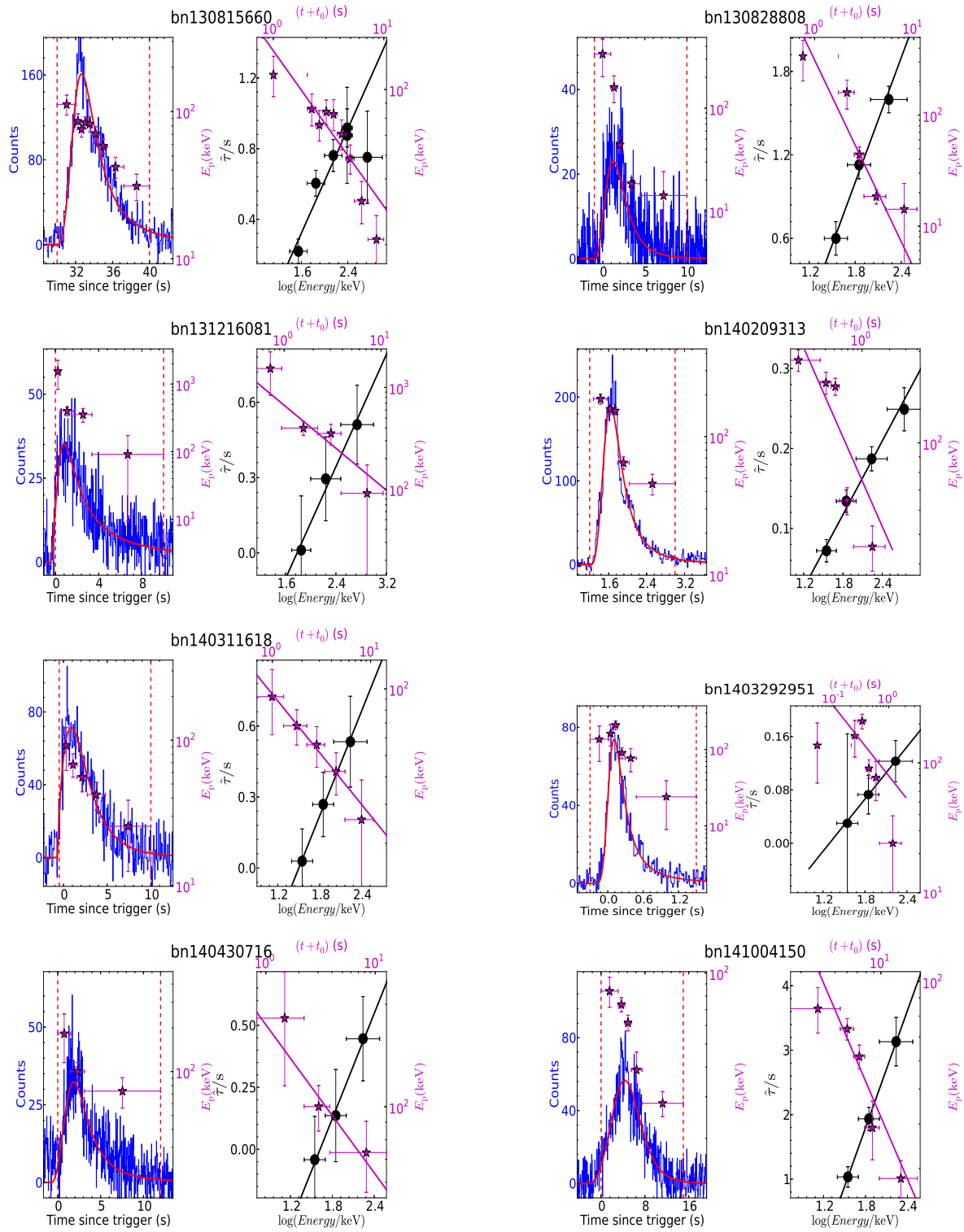


Fig. 1—Continued.

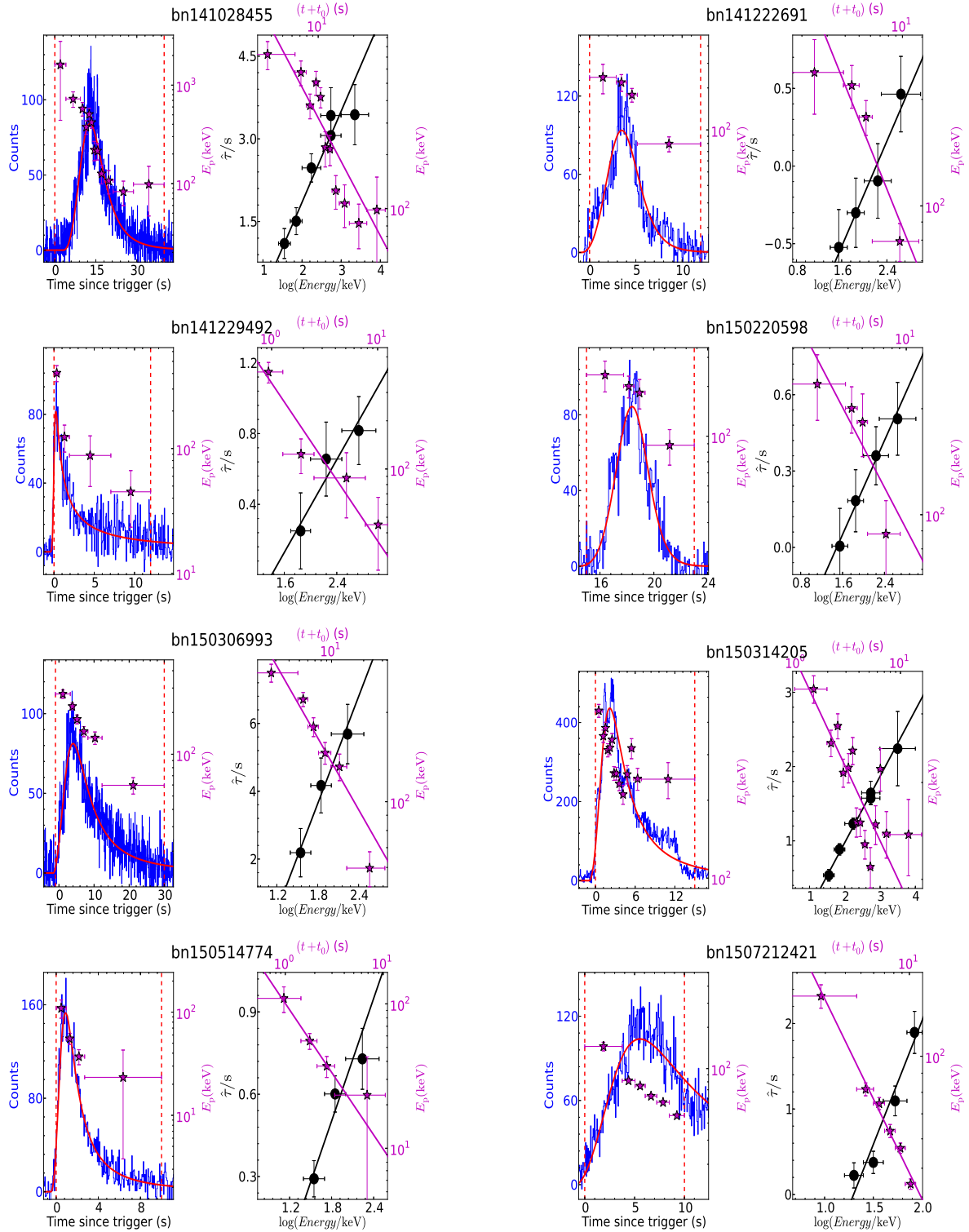


Fig. 1—Continued.

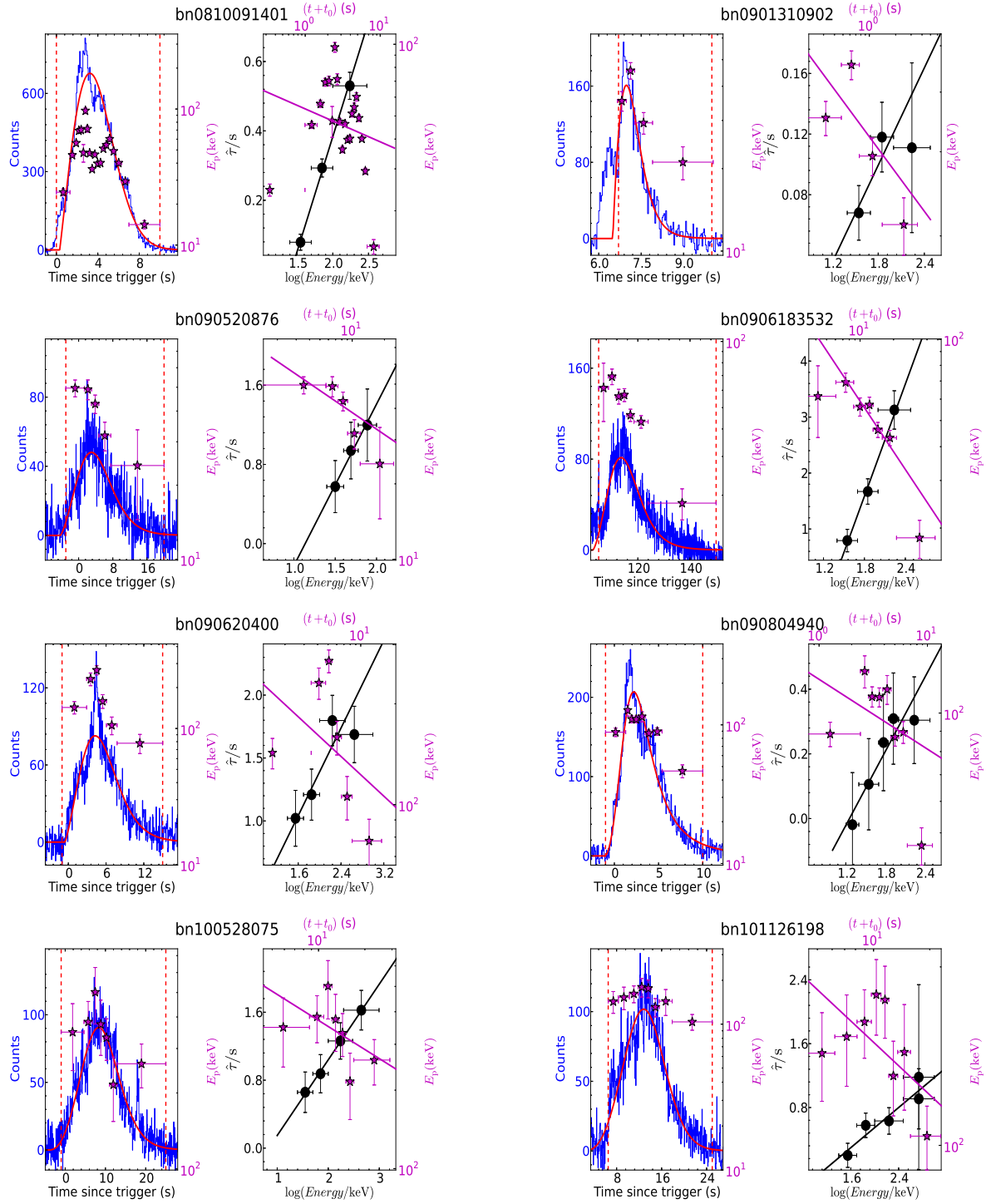


Fig. 2.— Our selected pulses with tracking spectral evolution. The meanings of the symbols and lines are the same as those in Figure 1.

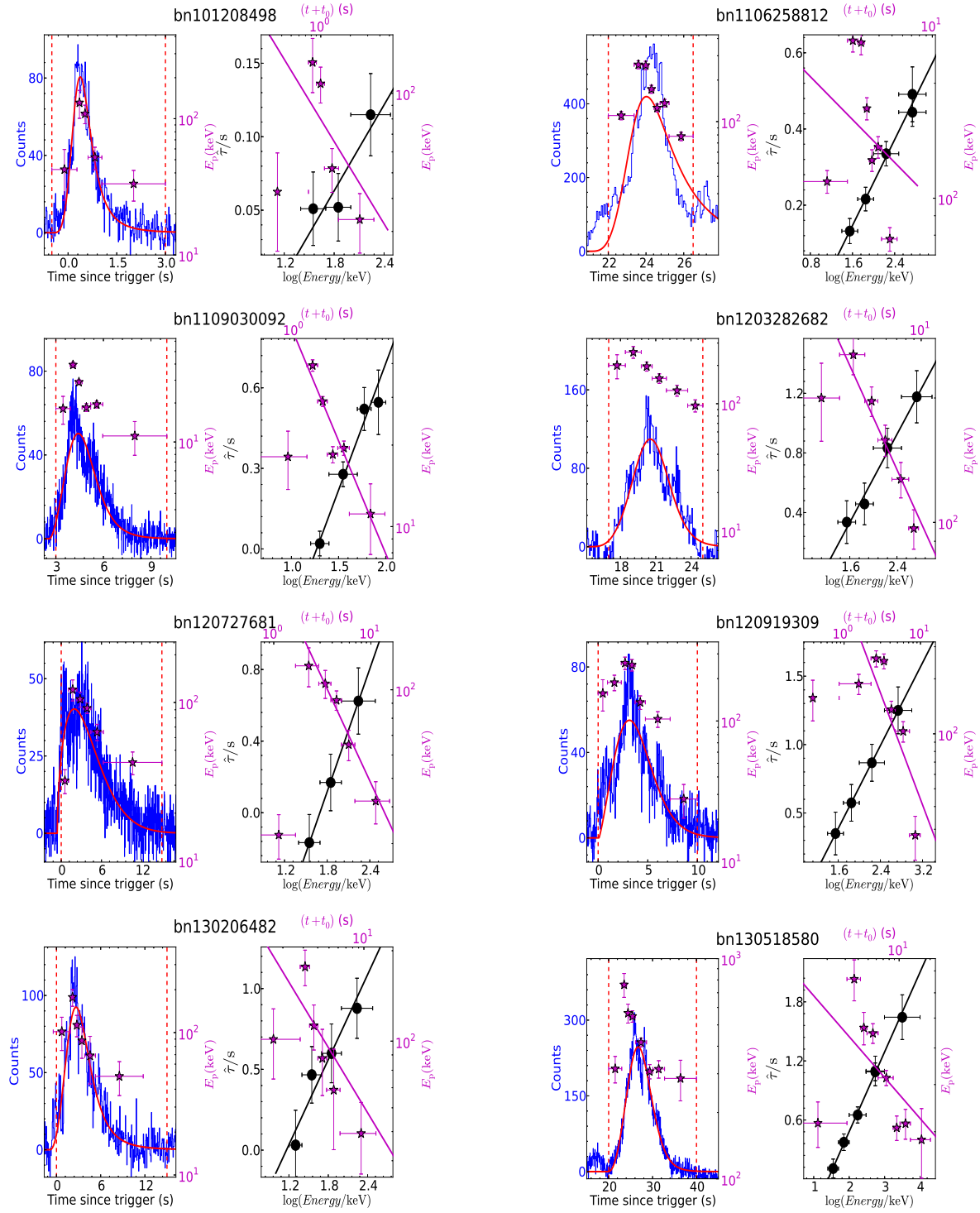


Fig. 2—Continued.

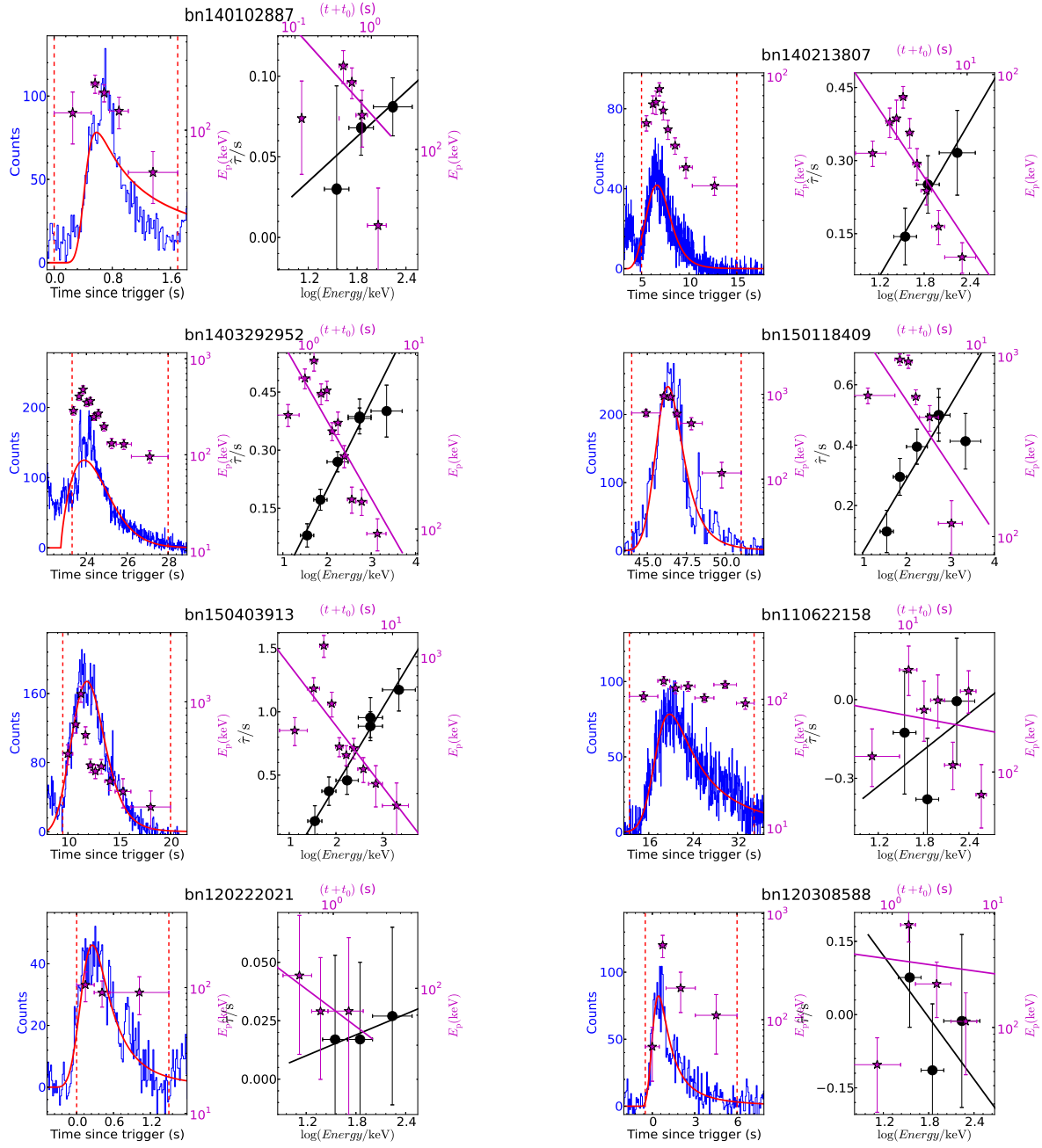


Fig. 2—Continued.

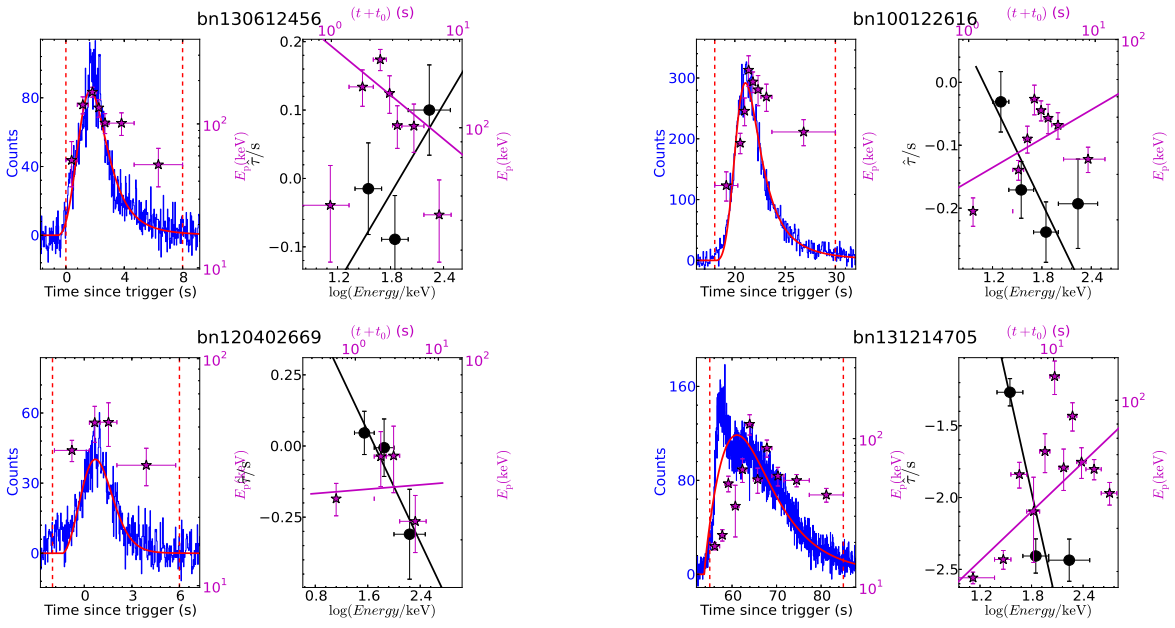


Fig. 2—Continued.

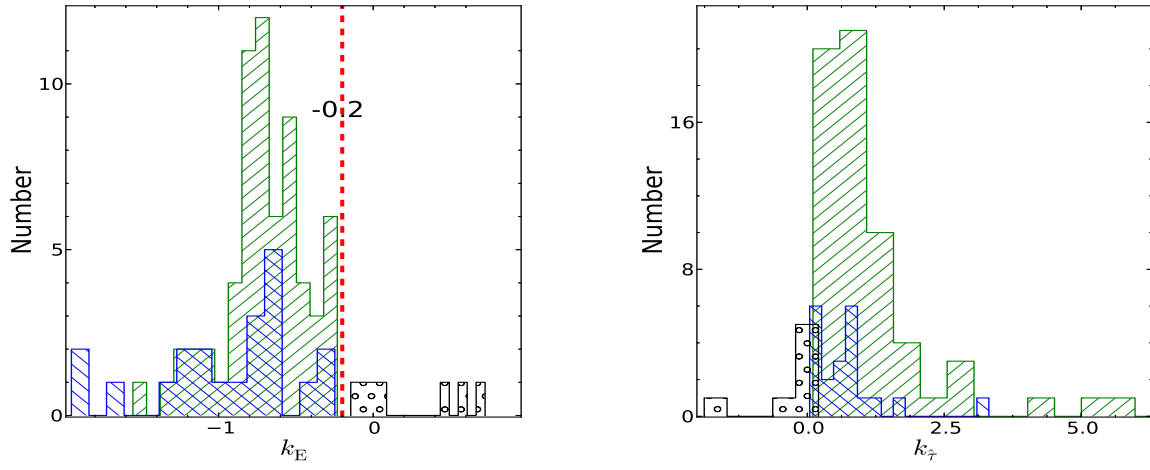


Fig. 3.— Left panel: k_E distribution, where the red vertical dashed line marks $k_E = -0.2$. Right panel: k_{τ} distribution, where the green “/”, blue “\”, and black “o” hatches represent the data from the H2S pulses, H2S-dominated-tracking pulses, and tracking spectral evolution pulses.

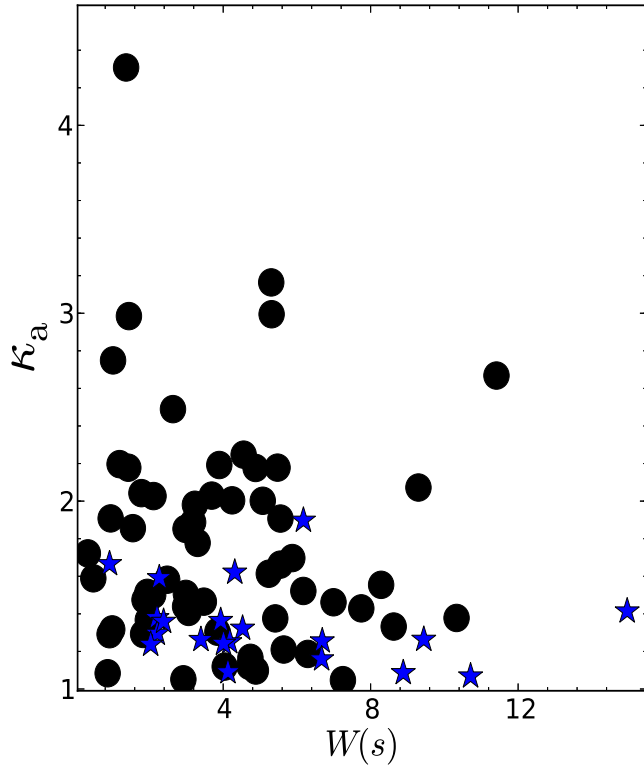


Fig. 4.— Relationship between the pulse asymmetry κ_a and its width W for the H2S pulses (black solid circles) and the tracking pulses (blue stars) in our sample.

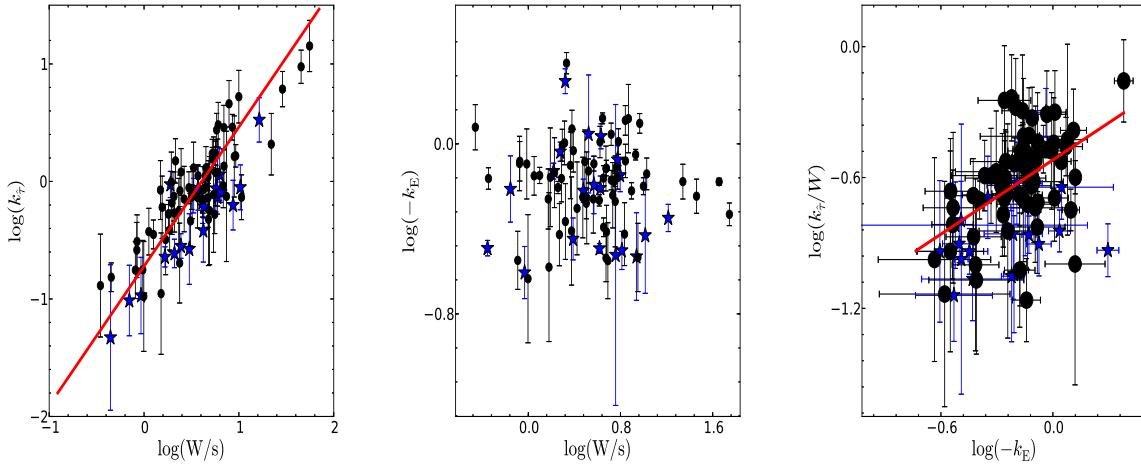


Fig. 5.— Relations of k_{τ} - W (left panel), k_E - W (middle panel), and k_{τ}/W - k_E (right panel) for H2S pulses (black “•”) and H2S-dominated-tracking pulses (blue “★”). The red solid lines in the left and right panels represent the best fitting for the data of the H2S pulses and H2S-dominated-tracking pulses.

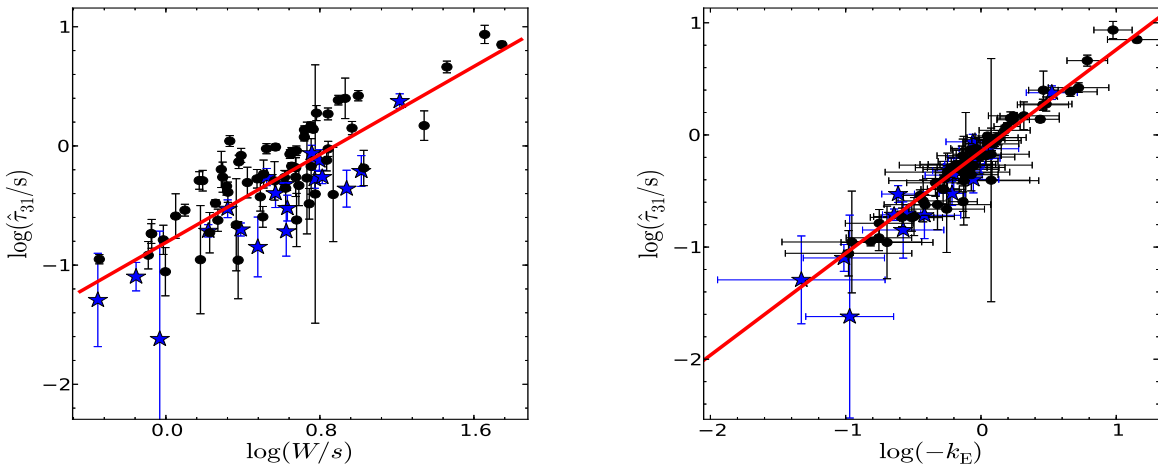


Fig. 6.— Relations of $\hat{\tau}_{31}$ - W and $\hat{\tau}_{31}$ - k_E for the H2S pulses (black “•”) and the H2S-dominated-tracking pulses (blue “★”). The red solid lines represent the best fitting to the H2S pulses and H2S-dominated-tracking pulses.

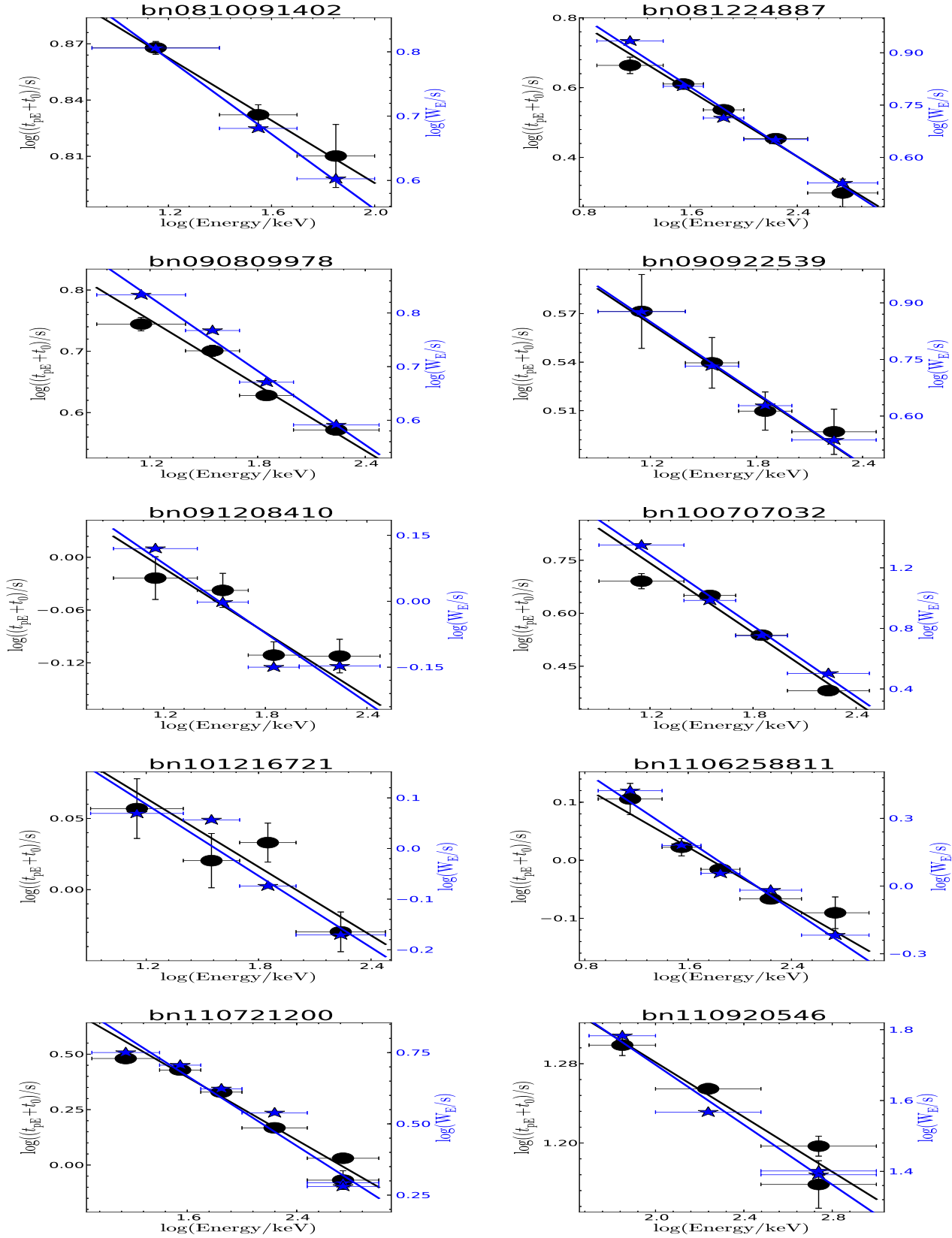


Fig. 7.— Relations of $t_{\text{pe}}-E$ (black “•”, left y -axis) and W_E-E (blue “★”, right y -axis) for 30 pulses in our sample. The two solid lines are the best linear fittings in logarithmic scale.

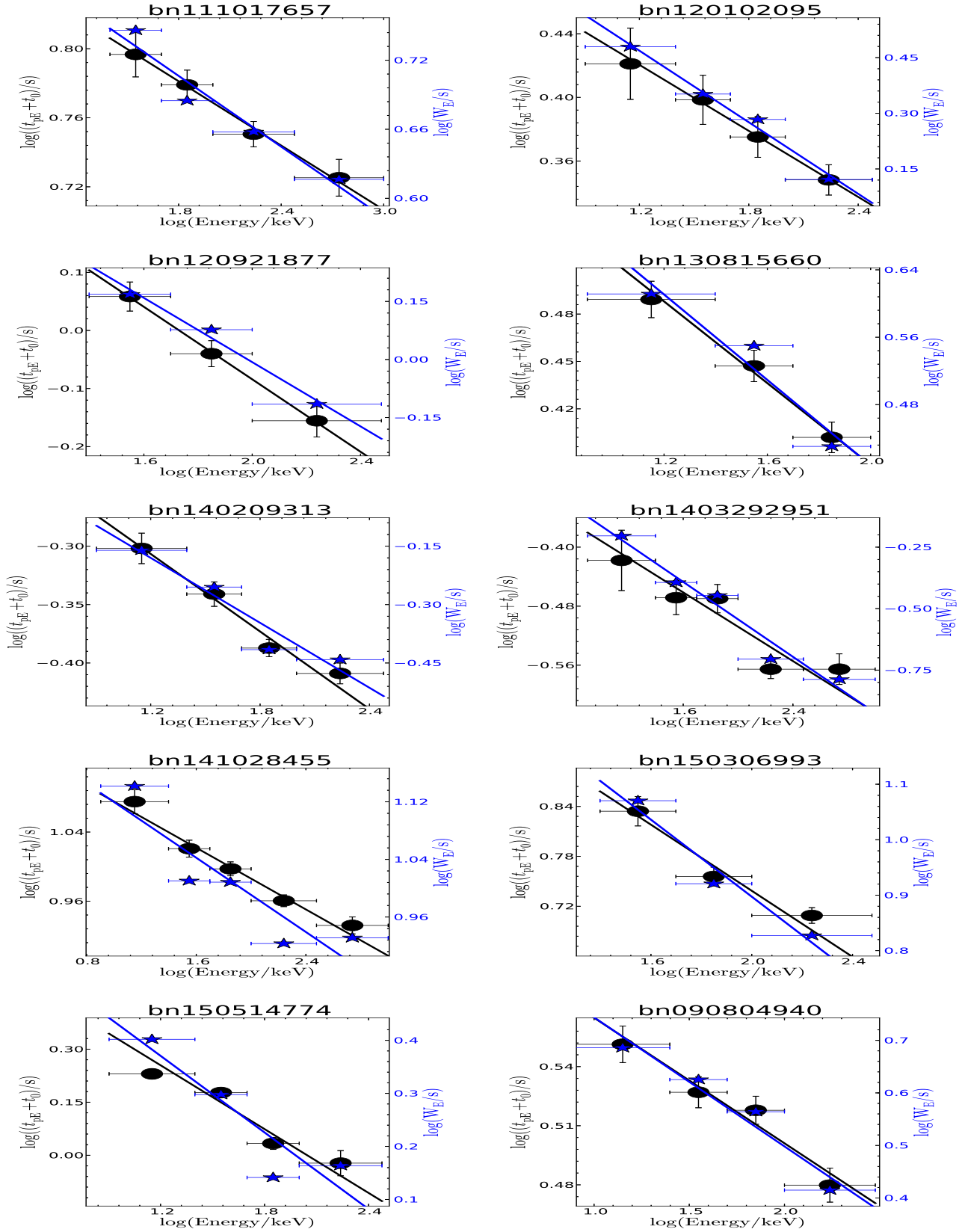


Fig. 7—Continued.

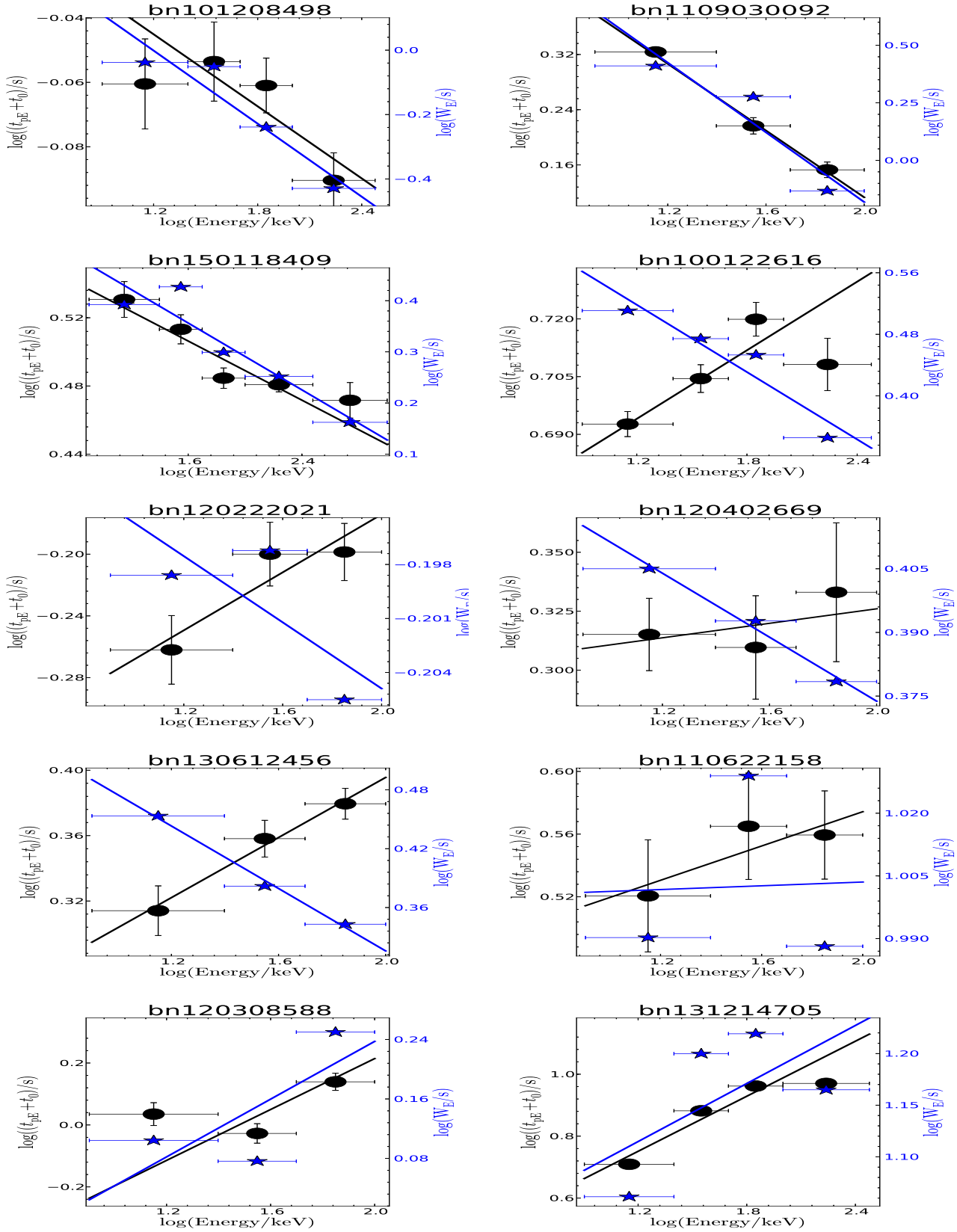


Fig. 7—Continued.

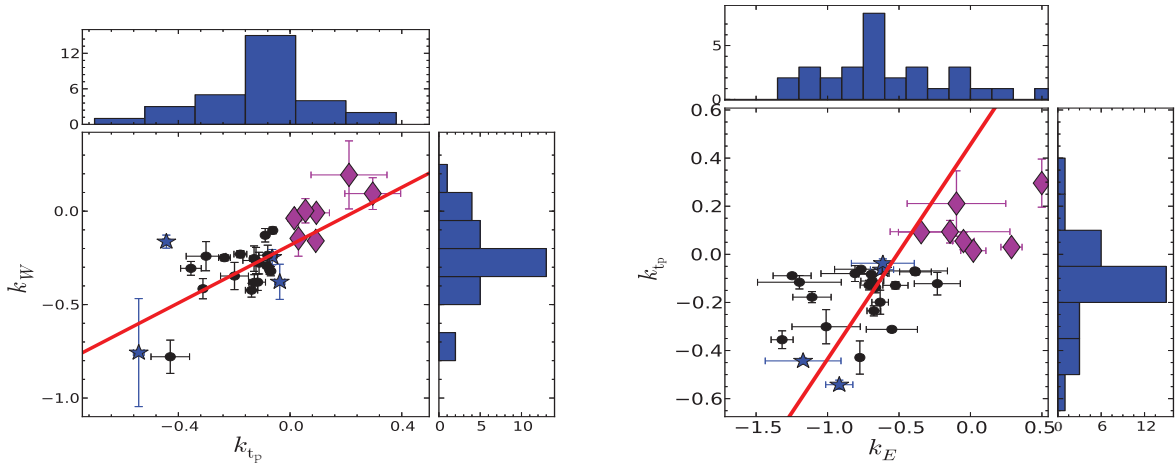


Fig. 8.— Relations of $k_W - k_{t_p}$ and $k_{t_p} - k_E$ together with k_W , k_{t_p} , and k_E distributions, where the circles, stars and diamonds stand for the H2S pulses, H2S-dominated-tracking pulses, and the tracking pulses, respectively. The red solid lines are the tentative correlations for H2S, H2S-dominated-tracking pulses and tracking pulses.

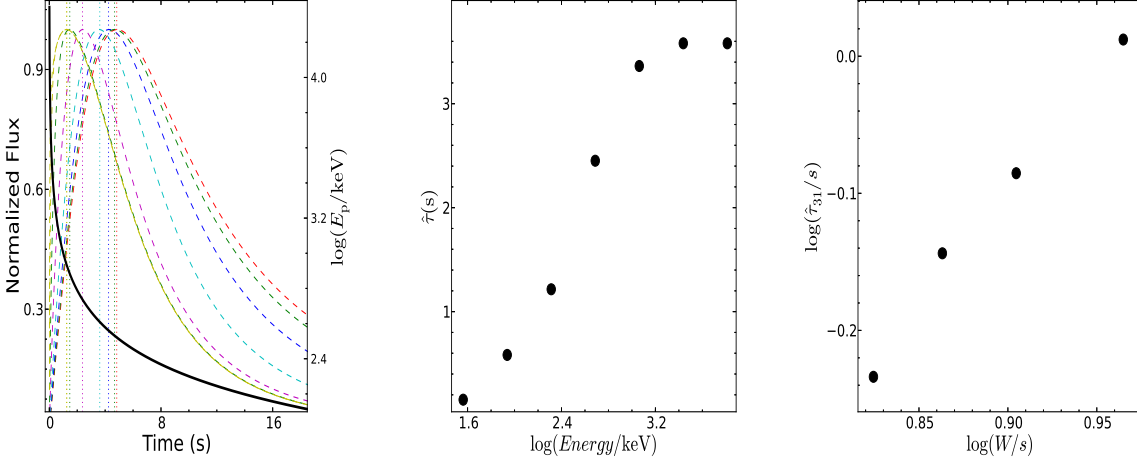


Fig. 9.— Left panel: Simulated light curves of the pulse (dashed lines, left y -axis) in different energy bands along with H2S’s E_p evolution (thick solid line, right y -axis), where the vertical dotted lines mark the peak times of each pulses. Middle panel: the relation between the spectral lag ($\hat{\tau}$) and photon energy. Right panel: the relation of the spectral lag ($\hat{\tau}_{31}$) and the pulse width W . Simulations with Equation (3) and the parameters of $F_m = 1$, $t_m = 5$, $r = 1$, $d = 2$, $t_0 = 0$, $\alpha = -1$, $\beta = -2.3$, $k = -1$ are adopted.

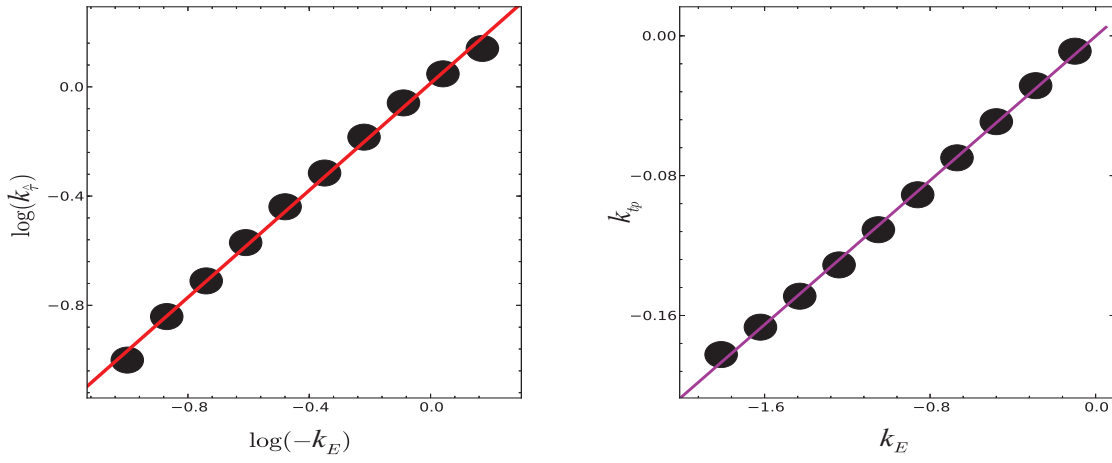


Fig. 10.— Relations of $k_{\hat{\tau}}-k_E$ and $k_{t_p}-k_E$ from our numerical simulations with Case (I).

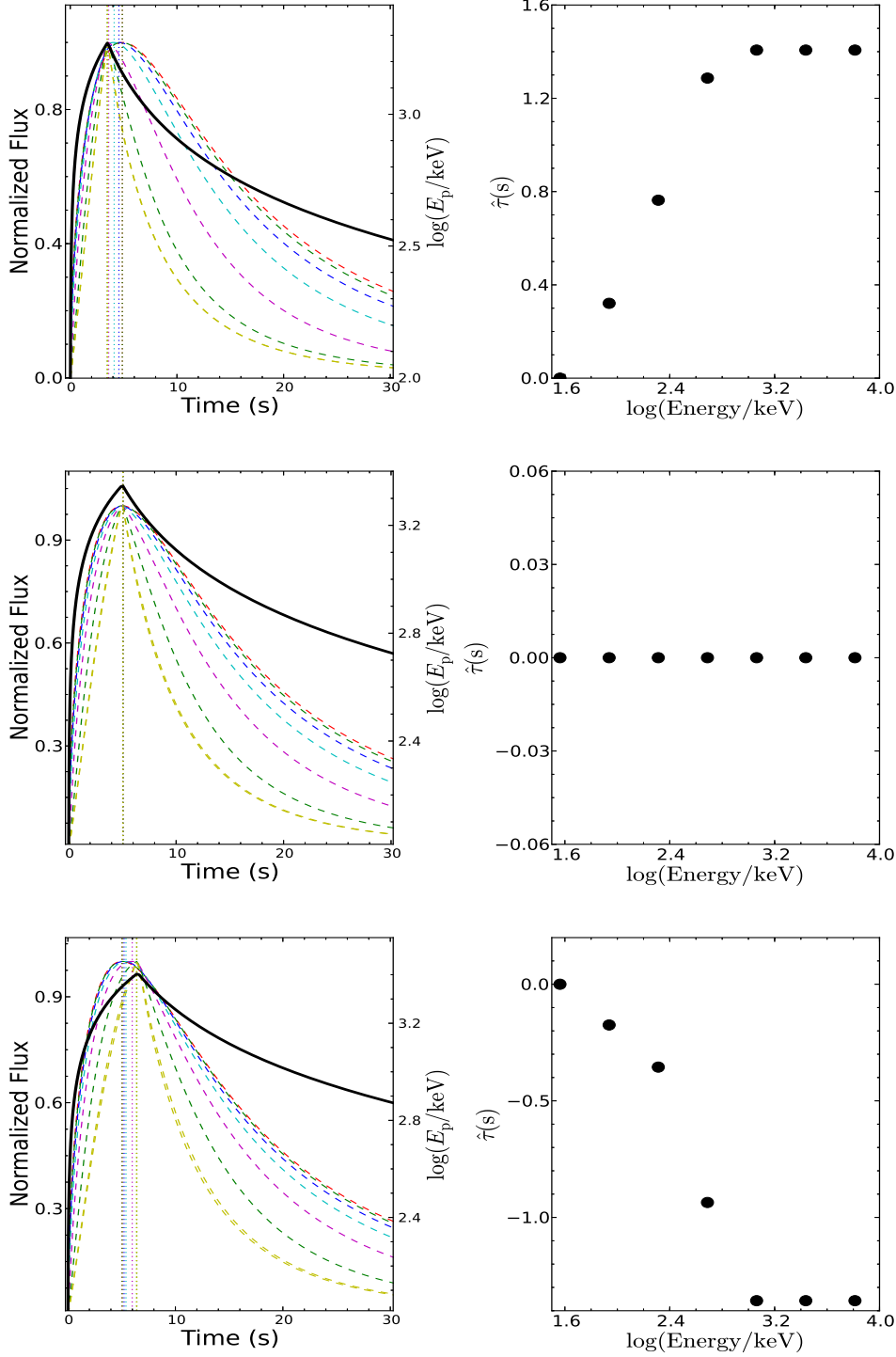


Fig. 11.— Simulated light curves (left panels) and the obtained $\hat{\tau}$ - E relations (right panels) for Case (II), where the upper, middle, and lower sub-figures are the results from the simulations with $\xi=0, -1.5$, and 1.5 , respectively.

Table 1. Results of light curve fitting with Equation (1) for 92 pulses.

GRB (Energy bin)	I_m	t_m	r	d	t_0	χ_r^2
bn080906212						
NaI ^a	156.04 ± 4.25	0.93 ± 0.03	1.12 ± 0.08	9.29 ± 3.20	0.23	1.17
bn0810091402						
NaI	157.84 ± 2.31	42.23 ± 0.05	3.09 ± 0.10	6.69 ± 0.53	-35.06	1.34
N1	107.40 ± 1.70	42.43 ± 0.06	2.32 ± 0.08	8.01 ± 0.86	-35.97	1.27
N2	46.13 ± 1.35	41.85 ± 0.08	3.44 ± 0.22	7.33 ± 1.14	-35.56	1.00
N3	8.66 ± 0.88	41.52 ± 0.25	4.11 ± 1.14	3.93 ± 1.44	-36.59	0.84
bn081125496						
NaI	120.36 ± 2.61	3.16 ± 0.07	1.47 ± 0.07	7.92 ± 1.76	0.81	1.41
bn081222204						
NaI	82.56 ± 2.02	3.27 ± 0.09	1.02 ± 0.06	14.91 ± 8.53	0.91	1.19
bn081224887						
NaI	157.30 ± 2.57	2.47 ± 0.05	1.55 ± 0.07	2.47 ± 0.13	0.82	1.26
N1	17.40 ± 0.93	3.79 ± 0.25	2.81 ± 0.43	2.16 ± 0.34	2.81	1.18
N2	31.57 ± 1.12	3.26 ± 0.12	2.74 ± 0.26	2.15 ± 0.20	1.57	1.15
N3	47.33 ± 1.28	2.62 ± 0.08	2.30 ± 0.15	2.62 ± 0.20	1.25	0.92
N4	64.52 ± 1.57	2.02 ± 0.06	1.15 ± 0.07	3.61 ± 0.39	0.41	0.78
N5	10.69 ± 1.01	1.17 ± 0.18	2.16 ± 0.59	2.51 ± 0.81	1.23	0.70
bn0901310901						
NaI	82.64 ± 3.24	3.27 ± 0.02	2.36 ± 0.21	17.49 ± 10.75	-2.30	1.46
bn0901310903						
NaI	137.96 ± 3.88	23.02 ± 0.01	2.49 ± 0.21	1.33 ± 0.06	-22.47	1.45
bn0905243461						
NaI	60.49 ± 2.60	5.71 ± 0.09	2.96 ± 0.35	1.86 ± 0.22	-2.86	1.08
bn0905243462						
NaI	39.22 ± 1.93	44.46 ± 0.15	2.67 ± 0.39	1.86 ± 0.25	-40.66	1.03
bn090530760						
NaI	141.51 ± 4.91	7.76 ± 0.28	2.17 ± 0.21	0.63 ± 0.04	3.05	1.03
bn0906183531						
NaI	38.27 ± 0.96	11.46 ± 0.28	1.18 ± 0.06	51523.54 ± 7402829.25	4.65	1.46
bn090626189						
NaI	211.12 ± 3.29	3.08 ± 0.04	1.99 ± 0.07	7.02 ± 0.79	0.33	1.86
bn090719063						
NaI	216.59 ± 3.89	5.25 ± 0.03	0.58 ± 0.03	31760.16 ± 3813718.24	-4.00	1.28
bn090809978						
NaI	163.23 ± 2.67	3.62 ± 0.05	2.31 ± 0.09	3.31 ± 0.19	0.78	1.34
N1	35.04 ± 1.17	4.77 ± 0.14	3.58 ± 0.31	3.39 ± 0.38	2.53	0.96
N2	41.14 ± 1.24	4.24 ± 0.10	3.37 ± 0.24	4.15 ± 0.45	2.27	1.17
N3	50.93 ± 1.35	3.47 ± 0.07	3.10 ± 0.18	3.57 ± 0.28	1.24	1.09
N4	47.10 ± 1.48	2.95 ± 0.07	3.31 ± 0.23	3.73 ± 0.36	1.19	1.10
bn090922539						
NaI	100.83 ± 2.34	2.26 ± 0.07	1.85 ± 0.12	2.40 ± 0.18	1.13	1.41
N1	20.69 ± 0.96	2.60 ± 0.20	2.63 ± 0.35	2.03 ± 0.27	2.82	1.06
N2	27.20 ± 1.14	2.33 ± 0.12	2.75 ± 0.31	2.23 ± 0.24	1.83	1.16
N3	32.89 ± 1.28	2.10 ± 0.09	2.63 ± 0.26	2.32 ± 0.22	1.16	1.05
N4	24.25 ± 1.29	2.01 ± 0.10	2.78 ± 0.37	2.38 ± 0.32	0.75	1.02
bn091020900						
NaI	33.61 ± 2.09	2.89 ± 0.24	1.03 ± 0.14	8.33 ± 6.95	1.87	1.10
bn091208410						
NaI	86.91 ± 3.31	8.49 ± 0.02	3.18 ± 0.31	2.61 ± 0.23	-7.64	1.19
N1	21.52 ± 1.49	8.59 ± 0.05	2.81 ± 0.50	3.23 ± 0.70	-7.39	1.14
N2	22.57 ± 1.66	8.56 ± 0.04	3.02 ± 0.57	3.16 ± 0.64	-7.62	0.96
N3	26.96 ± 1.91	8.42 ± 0.03	3.85 ± 0.71	1.98 ± 0.23	-7.81	0.74
N4	18.70 ± 1.66	8.42 ± 0.03	2.45 ± 0.58	2.48 ± 0.55	-7.87	0.71
bn100612726						
NaI	128.58 ± 2.41	3.86 ± 0.05	2.15 ± 0.09	11.80 ± 2.43	0.91	1.36
bn100707032						
NaI	352.33 ± 3.74	1.90 ± 0.03	2.64 ± 0.08	1.19 ± 0.02	0.81	1.41
N1	36.02 ± 1.04	4.09 ± 0.24	4.54 ± 0.57	0.59 ± 0.05	2.64	1.26
N2	55.10 ± 1.18	3.66 ± 0.11	3.34 ± 0.23	1.25 ± 0.06	2.08	1.24
N3	96.77 ± 1.65	2.64 ± 0.05	2.99 ± 0.12	1.70 ± 0.05	1.29	1.21
N4	187.42 ± 2.91	1.59 ± 0.03	2.90 ± 0.10	1.97 ± 0.04	0.78	1.19
bn101216721						
NaI	45.31 ± 1.58	0.50 ± 0.02	2.85 ± 0.24	5.30 ± 0.81	0.52	1.05
N1	10.97 ± 0.84	0.62 ± 0.06	3.83 ± 0.76	4.75 ± 1.45	0.86	0.82
N2	11.18 ± 0.74	0.53 ± 0.05	2.74 ± 0.51	3.62 ± 0.93	0.54	0.55
N3	13.17 ± 0.80	0.56 ± 0.03	3.62 ± 0.53	19.35 ± 16.72	0.77	0.40

Table 1—Continued

GRB (Energy bin)	I_m	t_m	r	d	t_0	χ_r^2
N4	12.46 ± 0.89	0.41 ± 0.03	2.94 ± 0.53	8.19 ± 4.10	0.40	0.37
bn110318552						
NaI	66.04 ± 1.99	5.33 ± 0.11	2.54 ± 0.19	3.80 ± 0.50	0.27	1.42
bn110505203						
NaI	80.51 ± 3.84	0.40 ± 0.04	2.96 ± 0.38	2.46 ± 0.32	0.91	1.05
bn110521478						
NaI	19.37 ± 3.33	0.37 ± 0.13	3.41 ± 2.00	1.25 ± 0.43	0.50	1.00
bn110605183						
NaI	51.97 ± 2.02	3.77 ± 0.19	1.96 ± 0.22	1.38 ± 0.15	1.95	1.14
bn1106258811						
NaI	371.53 ± 7.53	10.83 ± 0.01	2.71 ± 0.14	2.23 ± 0.09	-9.91	1.45
N1	43.35 ± 2.42	11.18 ± 0.08	1.58 ± 0.29	1.53 ± 0.23	-9.92	1.37
N2	70.04 ± 3.12	10.96 ± 0.04	2.80 ± 0.33	1.86 ± 0.15	-9.88	1.50
N3	113.51 ± 3.91	10.87 ± 0.02	2.54 ± 0.20	2.69 ± 0.19	-9.96	1.43
N4	149.92 ± 4.67	10.77 ± 0.02	2.23 ± 0.14	3.75 ± 0.31	-9.97	1.44
N5	17.18 ± 2.47	10.72 ± 0.05	4.32 ± 1.61	3.63 ± 1.44	-9.97	0.96
bn110709463						
NaI	23.90 ± 0.88	17.39 ± 0.04	2.53 ± 0.23	5.14 ± 0.94	-15.46	1.08
bn110721200						
NaI	194.81 ± 3.05	1.63 ± 0.04	1.12 ± 0.05	2.09 ± 0.10	0.46	1.43
N1	35.21 ± 1.27	2.57 ± 0.11	2.23 ± 0.22	2.18 ± 0.22	1.28	1.07
N2	42.78 ± 1.35	2.23 ± 0.09	2.05 ± 0.17	2.29 ± 0.20	1.16	1.15
N3	51.31 ± 1.50	1.68 ± 0.06	1.39 ± 0.10	2.15 ± 0.18	0.51	0.94
N4	65.03 ± 1.92	1.01 ± 0.05	0.53 ± 0.06	2.42 ± 0.28	0.03	0.98
N5	19.65 ± 1.65	0.40 ± 0.08	0.28 ± 0.11	2.40 ± 1.06	-0.01	0.69
B1	101.11 ± 3.37	0.62 ± 0.03	2.45 ± 0.22	1.42 ± 0.07	0.46	1.04
bn1109030091						
NaI	15.78 ± 0.58	1.00 ± 27492.79	12.02 ± 6.80	0.00 ± 0.05	0.58	1.46
bn1109030093						
NaI	23.24 ± 0.78	21.37 ± 0.06	1.57 ± 0.14	2.34 ± 0.28	-19.51	1.19
bn110920546						
NaI	96.62 ± 1.58	11.74 ± 0.24	2.33 ± 0.11	0.84 ± 0.03	6.00	1.05
N3	23.32 ± 0.63	13.89 ± 0.48	2.78 ± 0.23	0.76 ± 0.04	7.45	1.08
N4	45.53 ± 0.68	11.97 ± 0.22	2.57 ± 0.10	1.28 ± 0.05	7.96	1.08
N5	7.30 ± 0.50	8.39 ± 0.79	1.67 ± 0.28	1.83 ± 0.46	4.82	0.87
B1	37.46 ± 1.07	9.73 ± 0.36	1.19 ± 0.09	2.94 ± 0.47	3.55	1.09
bn111009282						
NaI	101.88 ± 1.99	7.32 ± 0.09	2.50 ± 0.11	21.68 ± 8.14	1.29	1.30
bn111017657						
NaI	92.22 ± 2.15	5.19 ± 0.07	2.61 ± 0.14	9.55 ± 1.93	0.69	1.27
N2	17.98 ± 0.99	5.57 ± 0.19	3.19 ± 0.42	8.35 ± 3.23	1.54	0.95
N3	25.10 ± 1.02	5.32 ± 0.12	3.59 ± 0.32	11.21 ± 3.54	1.75	0.92
N4	31.18 ± 1.08	4.94 ± 0.10	3.81 ± 0.28	11.82 ± 3.08	2.05	0.90
B1	32.04 ± 1.58	4.62 ± 0.13	3.59 ± 0.42	44.98 ± 70.78	2.22	1.11
bn120102095						
NaI	108.65 ± 3.63	5.14 ± 0.04	3.48 ± 0.29	3.75 ± 0.41	-2.71	1.33
N1	22.19 ± 1.64	5.35 ± 0.14	2.46 ± 0.46	5.63 ± 2.48	-2.38	1.44
N2	27.03 ± 1.80	5.22 ± 0.09	3.28 ± 0.55	4.41 ± 1.14	-2.71	1.50
N3	28.32 ± 1.80	5.09 ± 0.07	3.23 ± 0.49	3.93 ± 0.82	-3.05	1.40
N4	32.17 ± 2.28	4.94 ± 0.05	2.43 ± 0.43	2.54 ± 0.44	-3.93	1.16
bn120206949						
NaI	31.11 ± 1.28	5.11 ± 0.03	3.76 ± 0.36	5.48 ± 0.95	-3.83	1.19
bn120217808						
NaI	13.51 ± 0.89	0.53 ± 0.06	1.82 ± 0.35	2.12 ± 0.44	0.55	1.02
bn120304061						
NaI	114.95 ± 3.35	1.14 ± 0.05	0.91 ± 0.07	4.03 ± 0.80	0.38	0.99
bn120326056						
NaI	47.17 ± 2.55	1.57 ± 0.15	2.57 ± 0.29	2.94 ± 0.68	3.35	1.16
bn1203282681						
NaI	163.75 ± 3.45	6.30 ± 0.05	3.71 ± 0.22	2.22 ± 0.12	-2.48	1.42
bn120412920						
NaI	26.11 ± 1.44	1.03 ± 0.08	2.16 ± 0.32	3.56 ± 0.90	0.96	1.20
bn120426090						
NaI	261.05 ± 3.14	1.22 ± 0.01	2.25 ± 0.05	6.63 ± 0.42	0.54	1.47
bn120427054						
NaI	51.70 ± 1.44	2.16 ± 0.06	2.40 ± 0.16	4.25 ± 0.56	0.99	1.02
bn120625119						

Table 1—Continued

GRB (Energy bin)	I_m	t_m	r	d	t_0	χ_r^2
NaI	61.62 ± 1.90	3.10 ± 0.04	2.93 ± 0.21	3.87 ± 0.47	-1.00	1.46
bn120921877						
NaI	87.60 ± 4.22	0.40 ± 0.04	2.31 ± 0.31	1.84 ± 0.19	0.49	1.01
N2	27.70 ± 2.19	0.65 ± 0.07	3.21 ± 0.67	2.40 ± 0.43	0.63	0.98
N3	32.02 ± 2.26	0.42 ± 0.05	2.89 ± 0.49	2.87 ± 0.50	0.64	0.81
N4	24.65 ± 2.52	0.21 ± 0.04	4.16 ± 1.08	2.37 ± 0.45	0.55	0.68
bn121223300						
NaI	55.25 ± 2.17	4.13 ± 0.15	1.63 ± 0.15	5.75 ± 1.57	1.69	0.96
bn130325203						
NaI	95.66 ± 2.92	2.32 ± 0.06	2.59 ± 0.19	4.66 ± 0.69	0.66	1.27
bn130606497						
NaI	45.44 ± 0.77	51.32 ± 0.05	1.64 ± 0.07	3.48 ± 0.29	-47.58	1.60
bn130609902						
NaI	32.30 ± 1.29	7.01 ± 0.12	8.23 ± 1.18	1.64 ± 0.15	-1.46	1.00
bn130701060						
NaI	27.10 ± 1.13	3.50 ± 0.12	2.72 ± 0.26	11.25 ± 4.79	2.11	0.99
bn130815660						
NaI	160.79 ± 3.24	32.65 ± 0.04	2.37 ± 0.12	2.78 ± 0.16	-30.03	1.45
N1	46.70 ± 1.61	33.11 ± 0.08	2.63 ± 0.23	2.96 ± 0.31	-29.64	1.19
N2	51.11 ± 1.65	32.83 ± 0.06	2.85 ± 0.22	3.00 ± 0.26	-29.65	1.08
N3	44.88 ± 1.69	32.55 ± 0.06	3.19 ± 0.27	3.80 ± 0.42	-29.74	0.92
bn130828808						
NaI	22.64 ± 1.24	1.29 ± 0.10	1.43 ± 0.21	6.55 ± 3.35	0.79	0.96
bn131216081						
NaI	34.18 ± 1.60	0.81 ± 0.06	1.68 ± 0.23	1.55 ± 0.19	0.50	1.17
bn140209313						
NaI	189.57 ± 3.82	1.64 ± 0.01	2.58 ± 0.11	3.13 ± 0.12	-1.23	1.36
N1	34.52 ± 1.45	1.72 ± 0.01	2.85 ± 0.29	2.40 ± 0.20	-1.16	0.78
N2	47.73 ± 1.78	1.68 ± 0.01	3.12 ± 0.25	3.41 ± 0.29	-1.13	0.67
N3	62.78 ± 2.33	1.64 ± 0.01	3.82 ± 0.29	3.94 ± 0.32	-1.18	0.49
N4	58.20 ± 2.23	1.61 ± 0.01	3.76 ± 0.28	6.85 ± 0.99	-1.12	0.47
bn140311618						
NaI	71.29 ± 2.95	0.86 ± 0.07	0.72 ± 0.09	4.54 ± 1.62	0.69	1.19
bn1403292951						
NaI	74.36 ± 3.07	0.11 ± 0.01	3.06 ± 0.28	2.90 ± 0.24	0.19	1.00
N1	10.58 ± 1.00	0.19 ± 0.04	3.63 ± 0.98	3.02 ± 0.84	0.45	0.58
N2	17.60 ± 1.36	0.15 ± 0.02	3.00 ± 0.60	3.12 ± 0.68	0.23	0.51
N3	20.43 ± 1.43	0.15 ± 0.01	3.27 ± 0.55	5.34 ± 1.56	0.27	0.36
N4	31.13 ± 2.33	0.08 ± 0.01	3.88 ± 0.68	3.44 ± 0.58	0.14	0.33
B1	16.06 ± 2.29	0.08 ± 0.01	4.30 ± 1.60	3.22 ± 1.12	0.11	0.71
bn140430716						
NaI	31.22 ± 1.31	1.88 ± 0.07	2.35 ± 0.25	3.96 ± 0.78	0.74	1.20
bn141004150						
NaI	56.68 ± 1.85	4.32 ± 0.12	2.37 ± 0.17	9.44 ± 2.89	2.30	1.00
bn141028455						
NaI	84.73 ± 1.51	12.81 ± 0.11	2.35 ± 0.10	4.70 ± 0.42	-2.98	1.63
N1	15.20 ± 0.70	14.87 ± 0.38	3.13 ± 0.37	4.60 ± 0.98	0.32	1.23
N2	19.25 ± 0.74	13.46 ± 0.24	3.36 ± 0.32	4.91 ± 0.83	-1.49	1.09
N3	22.55 ± 0.69	12.92 ± 0.18	3.21 ± 0.23	4.60 ± 0.58	-1.56	0.93
N4	27.55 ± 0.78	12.11 ± 0.14	3.42 ± 0.22	6.26 ± 0.85	-1.55	1.07
B1	27.54 ± 1.00	11.53 ± 0.19	3.07 ± 0.28	6.24 ± 1.29	-1.54	1.22
bn141222691						
NaI	93.59 ± 2.55	3.53 ± 0.07	2.45 ± 0.16	12.84 ± 4.25	1.00	1.71
bn141229492						
NaI	80.15 ± 4.57	0.21 ± 0.04	6.01 ± 1.29	0.97 ± 0.08	0.59	0.96
bn150220598						
NaI	86.27 ± 2.91	18.36 ± 0.06	3.68 ± 0.28	13.25 ± 4.28	-13.91	0.97
bn150306993						
NaI	81.57 ± 1.90	4.01 ± 0.11	1.82 ± 0.12	2.28 ± 0.18	1.61	1.07
N2	18.34 ± 0.79	5.22 ± 0.28	3.21 ± 0.39	2.13 ± 0.26	4.41	1.06
N3	26.72 ± 0.83	4.09 ± 0.15	3.24 ± 0.25	2.54 ± 0.22	3.38	0.97
N4	30.64 ± 0.90	3.51 ± 0.11	2.89 ± 0.20	3.73 ± 0.39	3.05	0.91
bn150314205						
NaI	441.11 ± 3.91	2.10 ± 0.02	2.21 ± 0.05	1.86 ± 0.04	0.97	1.42
bn150514774						
NaI	152.90 ± 4.10	0.90 ± 0.03	2.14 ± 0.15	2.08 ± 0.13	0.49	1.13
N1	55.39 ± 2.19	1.21 ± 0.06	2.90 ± 0.30	2.19 ± 0.20	0.78	0.99

Table 1—Continued

GRB (Energy bin)	I_m	t_m	r	d	t_0	χ_r^2
N2	52.02 ± 2.23	1.01 ± 0.05	2.68 ± 0.28	2.71 ± 0.29	0.63	1.26
N3	41.26 ± 2.40	0.59 ± 0.04	2.69 ± 0.39	1.86 ± 0.19	0.38	0.79
N4	18.81 ± 1.80	0.46 ± 0.08	3.41 ± 0.89	2.10 ± 0.42	0.76	0.82
bn150721242						
NaI	105.53 ± 2.25	5.96 ± 0.13	1.68 ± 0.12	7.67 ± 3.31	0.94	1.02
bn0810091401						
NaI	676.59 ± 4.23	3.24 ± 0.01	1.05 ± 0.01	24486.30 ± 2042493.86	-0.32	1.49
bn0901310902						
NaI	164.08 ± 4.18	6.98 ± 0.01	0.91 ± 0.06	7.38 ± 1.89	-6.50	1.48
bn090520876						
NaI	47.62 ± 1.80	3.05 ± 0.19	1.50 ± 0.13	13.96 ± 9.42	4.35	0.96
bn0906183532						
NaI	83.35 ± 1.54	113.45 ± 0.15	1.47 ± 0.06	6.84 ± 1.20	-102.70	1.50
bn090620400						
NaI	80.53 ± 2.04	4.37 ± 0.09	1.32 ± 0.08	28.44 ± 26.32	0.58	1.49
bn090804940						
NaI	208.18 ± 3.13	2.19 ± 0.04	2.07 ± 0.07	3.60 ± 0.20	1.12	1.50
N1	59.89 ± 1.57	2.44 ± 0.08	3.29 ± 0.21	3.06 ± 0.23	2.32	1.25
N2	64.54 ± 1.59	2.24 ± 0.06	3.21 ± 0.18	3.42 ± 0.23	2.02	1.27
N3	61.29 ± 1.59	2.17 ± 0.05	2.96 ± 0.16	4.76 ± 0.43	1.75	1.22
N4	39.45 ± 1.72	1.90 ± 0.06	2.40 ± 0.24	3.38 ± 0.46	0.30	1.17
bn100528075						
NaI	88.93 ± 1.71	8.41 ± 0.12	2.47 ± 0.10	18.21 ± 5.68	4.06	1.30
bn101126198						
NaI	104.28 ± 2.07	12.70 ± 0.10	2.62 ± 0.11	14.53 ± 3.53	-2.11	1.35
bn101208498						
NaI	79.99 ± 2.25	0.38 ± 0.01	3.55 ± 0.23	4.52 ± 0.39	0.47	1.14
N1	21.48 ± 1.10	0.40 ± 0.03	3.47 ± 0.43	4.06 ± 0.67	0.63	0.85
N2	21.66 ± 1.00	0.41 ± 0.03	3.64 ± 0.40	5.95 ± 1.24	0.74	0.61
N3	22.90 ± 1.23	0.39 ± 0.02	3.23 ± 0.41	5.51 ± 1.22	0.28	0.42
N4	19.77 ± 1.48	0.34 ± 0.02	3.13 ± 0.58	4.91 ± 1.49	0.08	0.45
bn1106258812						
NaI	447.31 ± 6.17	24.13 ± 0.02	4.45 ± 0.15	4.93 ± 0.24	-21.05	1.30
bn1109030092						
NaI	50.23 ± 1.07	4.42 ± 0.03	1.70 ± 0.08	8.46 ± 1.60	-2.59	1.38
N1	28.78 ± 0.69	4.70 ± 0.04	2.26 ± 0.12	16.24 ± 5.58	-1.92	1.41
N2	15.52 ± 0.64	4.24 ± 0.04	2.16 ± 0.23	5.88 ± 1.51	-2.51	0.97
N3	10.59 ± 0.86	4.01 ± 0.04	3.58 ± 0.80	3.73 ± 1.00	-3.19	0.50
bn1203282682						
NaI	118.35 ± 3.23	20.51 ± 0.07	2.82 ± 0.18	12.98 ± 3.84	-15.38	1.50
bn120727681						
NaI	39.69 ± 0.90	1.95 ± 0.09	0.56 ± 0.03	31960.03 ± 4939224.04	0.58	1.08
bn120919309						
NaI	53.49 ± 1.41	3.21 ± 0.06	1.35 ± 0.09	25.86 ± 22.45	-0.08	1.50
bn130206482						
NaI	91.85 ± 2.47	2.66 ± 0.06	2.22 ± 0.14	5.47 ± 0.86	0.93	1.48
bn130518580						
NaI	248.54 ± 2.69	26.69 ± 0.04	2.20 ± 0.05	11.84 ± 1.38	-19.86	1.48
bn140102887						
NaI	42.67 ± 0.68	1.70 ± 22.86	4.05 ± 0.90	0.00 ± 0.03	-0.04	1.45
bn140213807						
NaI	42.24 ± 0.84	6.62 ± 0.04	2.06 ± 0.09	7.93 ± 1.28	-3.47	1.48
bn1403292952						
NaI	124.27 ± 1.60	23.90 ± 0.01	0.77 ± 0.03	48.98 ± 46.36	-22.75	1.31
bn150118409						
NaI	240.63 ± 4.55	46.32 ± 0.02	4.30 ± 0.18	6.13 ± 0.46	-43.24	1.33
N1	39.36 ± 2.22	46.64 ± 0.08	2.94 ± 0.42	4.48 ± 1.08	-44.06	1.06
N2	42.65 ± 1.75	46.51 ± 0.06	3.58 ± 0.33	6.46 ± 1.24	-43.01	1.15
N3	58.70 ± 2.12	46.30 ± 0.04	3.73 ± 0.28	7.49 ± 1.25	-43.52	1.30
N4	92.43 ± 2.62	46.27 ± 0.03	3.12 ± 0.17	18.91 ± 6.03	-43.78	1.49
N5	19.52 ± 1.56	46.21 ± 0.07	3.24 ± 0.57	44.09 ± 111.02	-44.00	0.89
bn150403913						
NaI	179.60 ± 3.32	11.79 ± 0.04	2.60 ± 0.10	7.18 ± 0.92	-7.48	1.43
bn100122616						
NaI	296.53 ± 4.04	21.06 ± 0.03	6.57 ± 0.20	4.16 ± 0.13	-16.00	1.03
N1	129.08 ± 2.46	20.93 ± 0.04	8.74 ± 0.37	4.37 ± 0.17	-14.54	0.98
N2	96.21 ± 2.24	21.06 ± 0.04	11.57 ± 0.61	4.80 ± 0.21	-13.93	1.08

Table 1—Continued

GRB (Energy bin)	I_m	t_m	r	d	t_0	χ_r^2
N3	58.33 ± 1.75	21.25 ± 0.05	11.18 ± 0.71	6.44 ± 0.44	-13.62	0.82
N4	28.11 ± 1.58	21.11 ± 0.08	13.95 ± 1.96	5.69 ± 0.70	-14.76	0.89
bn110622158						
NaI	71.00 ± 2.04	19.59 ± 0.14	0.54 ± 0.06	4.58 ± 1.43	-16.27	1.29
N1	21.67 ± 1.09	19.58 ± 0.27	1.71 ± 0.28	2.01 ± 0.36	-14.03	1.09
N2	20.46 ± 0.93	19.94 ± 0.29	3.33 ± 0.47	2.11 ± 0.29	-11.06	0.90
N3	21.21 ± 0.89	19.89 ± 0.23	3.00 ± 0.39	1.94 ± 0.23	-12.57	1.13
bn120402669						
NaI	40.17 ± 1.48	0.71 ± 0.05	1.73 ± 0.16	14.50 ± 8.81	1.36	1.22
N1	18.78 ± 0.89	0.70 ± 0.07	3.65 ± 0.40	7.51 ± 2.00	2.79	0.92
N2	11.57 ± 0.77	0.68 ± 0.10	4.12 ± 0.68	7.59 ± 2.89	3.02	0.80
N3	7.21 ± 0.65	0.79 ± 0.15	4.00 ± 0.93	18.61 ± 23.24	3.25	0.60
bn131214705						
NaI	119.01 ± 0.94	61.08 ± 0.06	0.84 ± 0.02	5.33 ± 0.35	-53.77	1.45
N1	67.14 ± 0.77	58.89 ± 0.07	1.44 ± 0.04	1.71 ± 0.05	-53.38	1.40
N2	34.10 ± 0.51	61.39 ± 0.12	1.18 ± 0.04	3.12 ± 0.23	-52.94	1.28
N3	22.71 ± 0.44	62.92 ± 0.15	3.46 ± 0.17	3.24 ± 0.21	-45.82	0.90
N4	12.25 ± 0.40	63.11 ± 0.19	0.93 ± 0.05	16916.82 ± 5971108.06	-54.47	0.67
bn130612456						
NaI	84.32 ± 1.94	1.68 ± 0.03	2.41 ± 0.14	4.76 ± 0.50	0.59	1.28
N1	23.47 ± 1.10	1.47 ± 0.07	1.86 ± 0.24	2.42 ± 0.35	0.36	0.93
N2	23.43 ± 0.99	1.69 ± 0.06	2.56 ± 0.26	4.85 ± 0.94	0.66	0.86
N3	23.35 ± 0.95	1.81 ± 0.05	3.29 ± 0.31	5.53 ± 1.00	0.82	0.69
bn120308588						
NaI	83.40 ± 4.02	0.44 ± 0.04	2.66 ± 0.34	2.39 ± 0.29	0.72	1.04
N1	18.36 ± 2.33	0.37 ± 0.09	3.01 ± 1.07	2.42 ± 0.79	0.70	1.07
N2	21.46 ± 2.44	0.22 ± 0.07	2.46 ± 0.82	1.55 ± 0.31	0.49	0.95
N3	18.57 ± 1.54	0.66 ± 0.09	2.86 ± 0.59	4.38 ± 1.46	1.15	0.87
bn120222021						
NaI	45.80 ± 1.94	0.25 ± 0.01	3.58 ± 0.36	3.23 ± 0.33	0.35	1.15
N1	12.74 ± 1.14	0.19 ± 0.03	2.21 ± 0.63	1.40 ± 0.21	0.15	0.61
N2	12.82 ± 0.98	0.28 ± 0.03	2.73 ± 0.57	4.10 ± 1.28	0.34	0.49
N3	13.14 ± 0.93	0.28 ± 0.03	3.03 ± 0.56	4.54 ± 1.30	0.39	0.41
bn140102887						
NaI	42.91 ± 0.90	0.68 ± 0.00	15.93 ± 2.79	0.02 ± 0.02	0.50	1.37
bn1109030091						
NaI	17.95 ± 0.36	0.31 ± 0.00	46.65 ± 18.87	0.00 ± 0.00	2.00	1.50

^aNaI: 8-1000 keV; N1: 8-25 keV; N2: 25-50 keV (Ⓐ); N3: 50-100 keV (Ⓑ); N4: 100-300 keV (Ⓒ); N5: 300-1000 keV (Ⓓ); B1: 300-1000 keV (Ⓔ); B2: 1000-5000 keV (Ⓕ).

Table 2. Results of the time-resolved spectral analysis for 92 pulses.

Timebin (s)	Amplitude	E_p (keV)	α	β	Flux (erg/s.cm ²)	χ_r^2
GRB 080906B (bn080906212)						
-0.26 -0.59	0.06 ± 0.01	267.40 ± 46.36	-0.53 ± 0.13	-2.05 ± 0.18	2.50E-06 ± 1.08E-07	1.07
0.59 -0.94	0.21 ± 0.06	160.72 ± 25.85	-0.43 ± 0.16	-1.98 ± 0.11	4.46E-06 ± 1.80E-07	1.06
0.94 -1.37	0.16 ± 0.05	158.20 ± 26.18	-0.47 ± 0.17	-2.05 ± 0.13	3.44E-06 ± 1.58E-07	0.96
1.37 -1.81	0.15 ± 0.04	171.11 ± 24.73	-0.46 ± 0.15	-2.27 ± 0.22	3.21E-06 ± 1.62E-07	0.87
1.81 -5.82	0.04 ± 0.03	82.30 ± 28.90	-0.65 ± 0.39	-1.87 ± 0.11	4.86E-07 ± 3.59E-08	0.92
GRB 081009A (1st pulse bn0810091401)						
-0.64 -1.31	1.37 ± 1.18	24.47 ± 1.42	-0.39 ± 0.32	-2.48 ± 0.05	1.18E-06 ± 3.45E-08	0.93
1.31 -1.76	0.66 ± 0.13	45.84 ± 1.49	-0.93 ± 0.09	-3.58 ± 0.38	3.52E-06 ± 9.65E-08	1.23
1.76 -2.06	0.78 ± 0.13	56.24 ± 2.01	-0.95 ± 0.08	-3.59 ± 0.45	5.59E-06 ± 1.64E-07	0.98
2.06 -2.28	0.99 ± 0.14	69.30 ± 2.63	-0.87 ± 0.07	-3.60 ± 0.51	8.02E-06 ± 2.48E-07	1.02
2.28 -2.50	0.97 ± 0.15	70.20 ± 3.24	-0.88 ± 0.08	-3.10 ± 0.27	8.48E-06 ± 2.70E-07	0.92
2.50 -2.71	1.73 ± 0.99	47.75 ± 7.07	-0.69 ± 0.24	-1.87 ± 0.00	1.38E-05 ± 2.55E-07	1.65
2.71 -2.90	0.87 ± 0.10	97.17 ± 4.56	-0.90 ± 0.06	-3.65 ± 0.82	1.11E-05 ± 4.10E-07	1.00
2.90 -3.10	1.08 ± 0.19	71.42 ± 3.75	-0.84 ± 0.09	-2.89 ± 0.20	9.46E-06 ± 3.08E-07	0.95
3.10 -3.32	1.98 ± 0.42	47.33 ± 1.43	-0.67 ± 0.10	-3.59 ± 0.28	6.65E-06 ± 1.61E-07	0.95
3.32 -3.58	3.55 ± 1.14	36.17 ± 1.10	-0.48 ± 0.14	-3.30 ± 0.15	5.38E-06 ± 1.23E-07	1.00
3.58 -3.85	1.19 ± 0.20	46.27 ± 1.21	-0.86 ± 0.08	-4.64 ± 1.24	5.42E-06 ± 1.31E-07	1.16
3.85 -4.12	3.27 ± 0.85	39.70 ± 1.03	-0.46 ± 0.12	-3.73 ± 0.25	5.34E-06 ± 1.16E-07	0.90
4.12 -4.40	2.10 ± 0.59	40.14 ± 1.34	-0.63 ± 0.12	-3.21 ± 0.16	5.36E-06 ± 1.30E-07	1.19
4.40 -4.67	1.13 ± 0.21	51.15 ± 1.63	-0.82 ± 0.09	-3.69 ± 0.41	5.64E-06 ± 1.49E-07	0.93
4.67 -4.97	0.74 ± 0.13	54.44 ± 2.18	-0.98 ± 0.09	-3.28 ± 0.30	5.58E-06 ± 1.67E-07	1.09
4.97 -5.32	0.56 ± 0.09	60.17 ± 2.42	-1.02 ± 0.08	-3.44 ± 0.44	5.04E-06 ± 1.63E-07	1.04
5.32 -5.74	1.40 ± 0.31	48.99 ± 1.54	-0.54 ± 0.11	-3.46 ± 0.25	3.92E-06 ± 1.01E-07	1.03
5.74 -6.30	1.81 ± 0.39	40.12 ± 0.84	-0.42 ± 0.10	-4.93 ± 1.06	2.63E-06 ± 5.62E-08	0.95
6.30 -7.01	0.95 ± 0.28	29.35 ± 0.82	-0.81 ± 0.12	-3.81 ± 0.31	2.06E-06 ± 4.58E-08	1.17
7.01 -10.81	0.87 ± 0.90	14.15 ± 0.99	-0.64 ± 0.37	-3.62 ± 0.23	3.36E-07 ± 1.09E-08	0.97
GRB 081009A (2nd pulse bn0810091402)						
36.22 -40.65	0.45 ± 0.30	16.74 ± 0.89	-0.76 ± 0.25	-3.85 ± 0.35	3.45E-07 ± 1.05E-08	1.09
40.65 -41.64	0.47 ± 0.24	16.20 ± 1.26	-1.14 ± 0.20	-3.69 ± 0.28	1.08E-06 ± 2.83E-08	1.01
41.64 -42.48	0.91 ± 0.48	17.42 ± 0.99	-0.92 ± 0.20	-3.90 ± 0.33	1.18E-06 ± 2.96E-08	1.10
42.48 -43.46	3.39 ± 2.60	17.19 ± 0.68	-0.43 ± 0.29	-3.65 ± 0.19	1.06E-06 ± 2.62E-08	1.14
43.46 -44.63	3.60 ± 4.37	13.55 ± 0.92	-0.52 ± 0.43	-3.42 ± 0.13	9.02E-07 ± 2.33E-08	1.17
44.63 -47.30	1.33 ± 1.92	9.21 ± 1.64	-0.88 ± 0.50	-3.72 ± 0.17	4.66E-07 ± 1.21E-08	0.98
47.30 -52.42	0.89 ± 0.16	7.72 ± 0.64	-0.76 ± 0.00	-3.54 ± 0.21	1.40E-07 ± 7.02E-09	1.16
GRB 081125A (bn081125496)						
-1.66 -2.14	0.04 ± 0.01	327.61 ± 40.31	-0.45 ± 0.11	-2.32 ± 0.26	1.86E-06 ± 7.27E-08	1.02
2.14 -2.87	0.21 ± 0.02	250.51 ± 15.71	-0.16 ± 0.09	-3.17 ± 0.58	5.82E-06 ± 2.16E-07	1.02
2.87 -3.85	0.31 ± 0.08	142.74 ± 12.78	0.00 ± 0.16	-2.32 ± 0.14	3.55E-06 ± 1.44E-07	1.00
3.85 -5.25	0.20 ± 0.04	135.43 ± 10.31	-0.28 ± 0.13	-2.92 ± 0.42	2.14E-06 ± 1.20E-07	1.14
5.25 -6.86	0.20 ± 0.05	117.09 ± 9.75	-0.28 ± 0.15	-2.77 ± 0.31	1.81E-06 ± 1.02E-07	1.07
6.86 -15.62	0.05 ± 0.07	48.05 ± 14.33	-0.63 ± 0.64	-2.26 ± 0.23	2.37E-07 ± 3.04E-08	1.19
GRB 081222A (bn081222204)						
-0.77 -2.28	0.04 ± 0.01	171.10 ± 31.69	-0.61 ± 0.14	-1.79 ± 0.07	1.26E-06 ± 4.40E-08	1.07
2.28 -3.78	0.05 ± 0.01	191.23 ± 30.21	-0.85 ± 0.10	-2.26 ± 0.24	1.62E-06 ± 7.68E-08	1.07
3.78 -5.01	0.07 ± 0.01	167.94 ± 27.29	-0.75 ± 0.12	-2.09 ± 0.15	1.80E-06 ± 8.16E-08	0.98
5.01 -6.40	0.08 ± 0.02	121.59 ± 15.01	-0.75 ± 0.12	-2.41 ± 0.24	1.31E-06 ± 7.91E-08	0.91
6.40 -20.03	0.01 ± 0.01	109.61 ± 35.47	-0.86 ± 0.26	-1.99 ± 0.20	2.36E-07 ± 2.27E-08	1.08
GRB 081224A (bn081224887)						
-0.90 -1.18	0.02 ± 0.00	793.94 ± 76.93	-0.23 ± 0.08	-2.56 ± 0.26	3.41E-06 ± 9.99E-08	1.16
1.18 -1.91	0.07 ± 0.00	547.59 ± 39.05	-0.17 ± 0.07	-2.99 ± 0.51	6.82E-06 ± 2.23E-07	0.90
1.91 -2.44	0.11 ± 0.01	397.39 ± 26.83	-0.22 ± 0.08	-2.56 ± 0.00	6.90E-06 ± 2.05E-07	0.95
2.44 -2.92	0.11 ± 0.01	430.57 ± 32.52	-0.39 ± 0.07	-2.56 ± 0.00	7.03E-06 ± 2.17E-07	0.96
2.92 -3.42	0.11 ± 0.01	372.98 ± 35.37	-0.48 ± 0.07	-2.54 ± 0.30	6.16E-06 ± 1.99E-07	0.97
3.42 -3.97	0.10 ± 0.01	383.78 ± 37.44	-0.60 ± 0.07	-2.86 ± 0.62	5.36E-06 ± 1.92E-07	1.03
3.97 -4.66	0.13 ± 0.02	227.34 ± 24.69	-0.41 ± 0.10	-2.15 ± 0.13	3.89E-06 ± 1.24E-07	0.97
4.66 -5.65	0.07 ± 0.01	279.85 ± 35.83	-0.76 ± 0.08	-2.39 ± 0.31	2.70E-06 ± 1.00E-07	1.00
5.65 -7.02	0.08 ± 0.02	170.43 ± 24.59	-0.50 ± 0.13	-1.99 ± 0.10	1.95E-06 ± 7.09E-08	0.90
7.02 -9.78	0.04 ± 0.01	176.86 ± 20.15	-0.73 ± 0.10	-2.90 ± 0.81	9.11E-07 ± 6.11E-08	1.04
9.78 -20.35	0.01 ± 0.00	155.71 ± 26.56	-1.06 ± 0.12	-2.56 ± 0.00	2.84E-07 ± 1.70E-08	0.90
GRB 090131A (1st pulse bn0901310901)						
1.92 -3.20	0.10 ± 0.05	71.61 ± 13.68	-0.83 ± 0.23	-2.33 ± 0.26	1.10E-06 ± 1.12E-07	1.13
3.20 -3.68	0.79 ± 0.51	56.18 ± 6.58	-0.25 ± 0.30	-2.53 ± 0.21	2.09E-06 ± 1.62E-07	1.17
3.68 -6.37	0.50 ± 1.29	28.19 ± 8.02	-0.25 ± 0.95	-2.03 ± 0.09	6.36E-07 ± 5.23E-08	1.15
GRB 090131A (2nd pulse bn0901310902)						
6.37 -6.78	21.49 ± 36.93	34.85 ± 4.24	0.97 ± 0.69	-2.21 ± 0.10	2.47E-06 ± 1.73E-07	1.02
6.78 -6.97	7.83 ± 7.49	39.88 ± 3.48	0.28 ± 0.41	-2.73 ± 0.18	3.59E-06 ± 2.23E-07	0.80

Table 2—Continued

Timebin (s)	Amplitude	E_p (keV)	α	β	Flux (erg/s.cm ²)	χ_r^2
6.97 -7.17	4.16 ± 3.22	45.15 ± 3.89	0.08 ± 0.34	-2.82 ± 0.22	3.59E-06 ± 2.27E-07	0.99
7.17 -7.44	20.85 ± 28.58	33.66 ± 3.13	0.72 ± 0.55	-2.54 ± 0.13	2.77E-06 ± 1.77E-07	1.09
7.44 -8.13	8.19 ± 17.39	23.98 ± 2.52	0.32 ± 0.78	-2.54 ± 0.12	1.13E-06 ± 7.60E-08	1.15
GRB 090131A (3rd pulse bn0901310901)						
21.95 -23.06	0.05 ± 0.01	169.10 ± 41.43	-1.03 ± 0.13	-2.16 ± 0.24	1.72E-06 ± 9.57E-08	0.97
23.06 -23.34	0.71 ± 0.54	69.32 ± 14.89	-0.36 ± 0.34	-1.94 ± 0.07	4.92E-06 ± 2.18E-07	1.00
23.34 -23.73	0.16 ± 0.07	91.47 ± 25.29	-1.04 ± 0.21	-2.07 ± 0.12	3.24E-06 ± 1.69E-07	0.96
23.73 -24.83	0.16 ± 0.18	46.26 ± 15.47	-0.82 ± 0.46	-1.97 ± 0.08	1.34E-06 ± 7.97E-08	1.15
GRB 090520A (bn090520876)						
-4.42 -1.34	0.06 ± 0.03	45.60 ± 3.89	-0.74 ± 0.28	-3.02 ± 0.00	2.16E-07 ± 1.08E-08	0.94
1.34 -3.01	0.48 ± 0.37	49.00 ± 4.52	-0.01 ± 0.35	-2.73 ± 0.24	5.95E-07 ± 4.53E-08	1.00
3.01 -4.72	0.25 ± 0.18	42.78 ± 3.67	-0.42 ± 0.31	-3.01 ± 0.38	4.76E-07 ± 3.72E-08	0.90
4.72 -7.53	0.18 ± 0.22	31.79 ± 4.25	-0.56 ± 0.49	-2.51 ± 0.18	3.53E-07 ± 2.95E-08	1.05
7.53 -20.48	0.01 ± 0.01	24.04 ± 9.54	-1.69 ± 0.50	-2.45 ± 0.46	1.04E-07 ± 1.81E-08	0.95
GRB 090524A (1st pulse bn0905243461)						
-0.77 -4.47	0.30 ± 0.45	63.98 ± 14.88	0.52 ± 0.72	-1.84 ± 0.11	5.53E-07 ± 4.88E-08	0.99
4.47 -6.65	0.13 ± 0.02	130.83 ± 10.27	-0.37 ± 0.11	-2.71 ± 0.39	1.47E-06 ± 1.05E-07	0.81
6.65 -10.56	0.06 ± 0.02	98.39 ± 10.98	-0.70 ± 0.14	-2.51 ± 0.32	7.49E-07 ± 6.35E-08	1.13
10.56 -14.85	0.02 ± 0.01	112.35 ± 23.39	-0.99 ± 0.18	-2.61 ± 0.90	4.24E-07 ± 6.95E-08	1.04
14.85 -26.40	0.02 ± 0.01	68.60 ± 20.53	-0.93 ± 0.40	-2.18 ± 0.00	1.90E-07 ± 1.40E-08	1.13
GRB 090524A (2nd pulse bn0905243462)						
26.40 -42.50	0.00 ± 0.00	55.90 ± 0.00	-1.21 ± 0.64	-2.09 ± 0.56	5.61E-08 ± 2.24E-08	0.94
42.50 -44.80	0.02 ± 0.01	79.43 ± 20.81	-1.34 ± 0.19	-2.39 ± 0.48	5.52E-07 ± 7.17E-08	1.04
44.80 -47.50	0.06 ± 0.04	51.50 ± 10.52	-0.95 ± 0.32	-2.32 ± 0.21	4.89E-07 ± 4.67E-08	1.15
47.50 -61.18	0.02 ± 0.00	32.34 ± 6.19	-1.06 ± 0.00	-2.18 ± 0.00	1.35E-07 ± 8.70E-09	1.05
GRB 090530B (bn090530760)						
-1.54 -6.37	0.14 ± 0.06	126.05 ± 13.44	0.43 ± 0.24	-1.96 ± 0.12	1.10E-06 ± 6.35E-08	1.11
6.37 -9.77	0.30 ± 0.10	103.64 ± 8.63	0.29 ± 0.20	-2.25 ± 0.14	1.45E-06 ± 8.51E-08	0.95
9.77 -13.31	0.32 ± 0.10	92.71 ± 6.19	0.22 ± 0.18	-2.64 ± 0.23	1.11E-06 ± 7.02E-08	1.08
13.31 -17.39	0.80 ± 0.36	70.46 ± 4.18	0.58 ± 0.23	-2.68 ± 0.17	8.81E-07 ± 4.95E-08	1.26
17.39 -22.53	0.53 ± 0.24	65.96 ± 4.17	0.35 ± 0.23	-2.72 ± 0.19	6.84E-07 ± 4.08E-08	1.01
22.53 -29.21	0.29 ± 0.16	61.73 ± 6.03	0.05 ± 0.27	-2.30 ± 0.12	6.50E-07 ± 4.03E-08	1.03
29.21 -37.71	0.33 ± 0.20	59.69 ± 5.75	0.18 ± 0.30	-2.30 ± 0.12	5.51E-07 ± 3.48E-08	1.06
37.71 -47.08	0.39 ± 0.36	49.87 ± 6.54	0.19 ± 0.40	-2.05 ± 0.08	5.67E-07 ± 3.38E-08	1.04
47.08 -58.62	0.05 ± 0.02	66.15 ± 8.13	-0.74 ± 0.19	-2.45 ± 0.23	3.91E-07 ± 3.18E-08	0.98
58.62 -68.81	0.08 ± 0.03	57.00 ± 3.67	-0.64 ± 0.16	-3.37 ± 0.75	3.26E-07 ± 2.53E-08	1.12
68.81 -76.26	0.16 ± 0.06	45.85 ± 2.54	-0.49 ± 0.18	-3.31 ± 0.45	3.67E-07 ± 2.17E-08	0.97
76.26 -84.07	0.09 ± 0.04	42.78 ± 2.46	-0.78 ± 0.17	-3.37 ± 0.58	3.40E-07 ± 2.13E-08	1.01
84.07 -94.58	0.07 ± 0.03	36.05 ± 1.82	-0.87 ± 0.17	-3.91 ± 1.22	2.51E-07 ± 1.54E-08	1.27
94.58 -111.35	0.05 ± 0.16	20.97 ± 10.04	-1.09 ± 1.18	-2.00 ± 0.00	3.23E-07 ± 9.48E-09	2.00
111.35 -135.69	0.31 ± 0.11	13.61 ± 3.32	-0.50 ± 0.00	-2.00 ± 0.00	2.52E-07 ± 7.05E-09	1.90
135.69 -156.86	0.01 ± 0.00	14.78 ± 10.17	-1.78 ± 0.32	-2.81 ± 0.67	9.66E-08 ± 1.32E-08	1.14
GRB 090618A (1st pulse bn0906183531)						
-3.46 -3.00	0.01 ± 0.00	511.85 ± 113.66	-0.72 ± 0.12	-2.11 ± 0.21	1.07E-06 ± 5.66E-08	1.11
3.00 -9.46	0.12 ± 0.03	137.94 ± 13.33	-0.01 ± 0.18	-1.98 ± 0.06	1.52E-06 ± 4.13E-08	1.32
9.46 -16.18	0.07 ± 0.02	140.39 ± 14.94	-0.55 ± 0.13	-2.12 ± 0.09	1.32E-06 ± 4.24E-08	1.22
16.18 -26.38	0.08 ± 0.02	99.76 ± 10.60	-0.56 ± 0.16	-2.22 ± 0.10	8.93E-07 ± 3.34E-08	1.07
26.38 -41.61	0.04 ± 0.02	69.59 ± 7.69	-0.75 ± 0.23	-3.12 ± 0.73	2.55E-07 ± 2.27E-08	1.11
41.61 -49.23	0.02 ± 0.03	49.22 ± 16.17	-0.92 ± 0.77	-2.89 ± 1.11	1.10E-07 ± 2.33E-08	1.05
49.23 -53.03	0.07 ± 0.03	87.78 ± 18.23	-0.87 ± 0.22	-2.10 ± 0.11	1.04E-06 ± 4.78E-08	1.17
GRB 090618A (2nd pulse bn0906183532)						
95.11 -100.11	0.13 ± 0.04	60.93 ± 5.34	-0.80 ± 0.17	-2.58 ± 0.14	9.34E-07 ± 3.60E-08	1.04
100.11 -104.43	0.05 ± 0.01	59.44 ± 5.24	-1.17 ± 0.16	-3.33 ± 1.02	5.48E-07 ± 4.06E-08	1.09
104.43 -108.75	0.05 ± 0.02	61.48 ± 7.10	-1.21 ± 0.16	-2.73 ± 0.33	6.92E-07 ± 4.08E-08	0.96
108.75 -111.45	0.10 ± 0.02	69.26 ± 5.63	-1.14 ± 0.12	-2.79 ± 0.27	1.34E-06 ± 5.80E-08	1.12
111.45 -113.91	0.12 ± 0.03	56.26 ± 4.34	-1.16 ± 0.13	-2.83 ± 0.24	1.35E-06 ± 5.36E-08	0.93
113.91 -115.79	0.10 ± 0.02	57.15 ± 3.85	-1.33 ± 0.11	-3.08 ± 0.45	1.57E-06 ± 6.90E-08	0.97
115.79 -118.53	0.07 ± 0.01	46.24 ± 2.97	-1.46 ± 0.10	-3.68 ± 1.40	1.10E-06 ± 5.55E-08	0.95
118.53 -123.96	0.05 ± 0.01	43.16 ± 2.83	-1.44 ± 0.11	-3.48 ± 0.98	7.07E-07 ± 3.57E-08	1.17
123.96 -149.57	0.06 ± 0.18	18.40 ± 2.97	-1.12 ± 1.00	-2.22 ± 0.00	3.19E-07 ± 8.85E-09	1.34
GRB 090620A (bn090620400)						
-1.22 -2.91	0.10 ± 0.04	142.76 ± 14.87	0.33 ± 0.24	-2.29 ± 0.17	9.09E-07 ± 5.00E-08	0.99
2.91 -4.17	0.08 ± 0.01	231.00 ± 24.74	-0.31 ± 0.13	-2.40 ± 0.24	2.42E-06 ± 1.04E-07	0.99
4.17 -4.85	0.13 ± 0.02	268.59 ± 20.95	-0.14 ± 0.11	-3.00 ± 0.50	4.19E-06 ± 1.69E-07	0.96
4.85 -6.06	0.13 ± 0.03	158.93 ± 18.28	-0.25 ± 0.16	-2.31 ± 0.19	2.04E-06 ± 1.00E-07	0.98
6.06 -7.76	0.14 ± 0.06	105.66 ± 15.67	-0.24 ± 0.23	-2.12 ± 0.12	1.35E-06 ± 7.33E-08	0.90
7.76 -15.81	0.03 ± 0.02	77.92 ± 12.50	-0.63 ± 0.27	-2.69 ± 0.48	2.43E-07 ± 2.84E-08	1.03

Table 2—Continued

Timebin (s)	Amplitude	E_p (keV)	α	β	Flux (erg/s.cm ²)	χ_r^2
GRB 090626A (bn090626189)						
-0.83 -1.90	0.05 ± 0.01	281.23 ± 29.58	-0.58 ± 0.08	-2.11 ± 0.12	2.30E-06 ± 6.13E-08	1.06
1.90 -2.59	0.18 ± 0.02	253.67 ± 21.11	-0.48 ± 0.07	-2.21 ± 0.11	6.50E-06 ± 1.55E-07	0.92
2.59 -3.28	0.25 ± 0.04	168.67 ± 16.98	-0.43 ± 0.10	-1.97 ± 0.06	5.86E-06 ± 1.37E-07	0.91
3.28 -3.75	0.63 ± 0.14	113.47 ± 8.90	-0.20 ± 0.12	-2.20 ± 0.07	6.14E-06 ± 1.74E-07	1.09
3.75 -4.43	0.43 ± 0.11	96.22 ± 8.82	-0.42 ± 0.13	-2.14 ± 0.07	4.20E-06 ± 1.27E-07	0.96
4.43 -5.50	0.24 ± 0.06	82.54 ± 7.18	-0.66 ± 0.13	-2.36 ± 0.11	2.35E-06 ± 8.79E-08	0.91
5.50 -12.12	0.06 ± 0.05	37.70 ± 6.82	-1.01 ± 0.30	-2.14 ± 0.07	5.28E-07 ± 2.50E-08	1.15
12.12 -14.34	0.00 ± 0.00	500.00 ± 0.00	-0.50 ± 0.00	-1.86 ± 0.44	3.18E-07 ± 3.96E-08	1.21
GRB 090719A (bn090719063)						
-0.26 -1.51	0.08 ± 0.01	359.92 ± 23.02	-0.08 ± 0.08	-2.58 ± 0.22	4.08E-06 ± 9.70E-08	1.00
1.51 -2.55	0.30 ± 0.04	178.35 ± 8.68	0.23 ± 0.10	-2.74 ± 0.19	3.91E-06 ± 1.16E-07	1.05
2.55 -3.46	0.18 ± 0.02	219.48 ± 14.55	-0.21 ± 0.08	-2.52 ± 0.19	4.39E-06 ± 1.23E-07	0.91
3.46 -4.24	0.13 ± 0.01	334.14 ± 24.79	-0.42 ± 0.06	-2.58 ± 0.25	6.05E-06 ± 1.54E-07	0.92
4.24 -4.78	0.18 ± 0.01	347.32 ± 23.59	-0.35 ± 0.06	-2.54 ± 0.20	8.92E-06 ± 2.12E-07	0.93
4.78 -5.25	0.26 ± 0.02	271.09 ± 17.36	-0.29 ± 0.07	-2.53 ± 0.17	9.04E-06 ± 2.12E-07	1.11
5.25 -5.72	0.25 ± 0.02	254.76 ± 18.15	-0.36 ± 0.07	-2.42 ± 0.15	8.19E-06 ± 2.00E-07	0.93
5.72 -6.26	0.24 ± 0.02	238.99 ± 13.78	-0.39 ± 0.06	-3.03 ± 0.39	6.74E-06 ± 1.85E-07	0.93
6.26 -6.78	0.30 ± 0.04	184.70 ± 13.26	-0.34 ± 0.08	-2.33 ± 0.12	6.50E-06 ± 1.69E-07	1.03
6.78 -7.52	0.24 ± 0.03	174.57 ± 11.31	-0.38 ± 0.08	-2.60 ± 0.19	4.50E-06 ± 1.36E-07	1.01
7.52 -9.04	0.14 ± 0.02	124.03 ± 8.51	-0.65 ± 0.08	-2.79 ± 0.29	1.92E-06 ± 7.90E-08	1.10
9.04 -11.66	0.13 ± 0.03	70.52 ± 6.08	-0.74 ± 0.13	-2.42 ± 0.12	1.09E-06 ± 4.42E-08	1.00
GRB 090804A (bn090804940)						
-0.77 -1.28	0.23 ± 0.07	88.58 ± 6.25	-0.15 ± 0.16	-2.63 ± 0.18	1.12E-06 ± 5.42E-08	0.97
1.28 -1.74	0.33 ± 0.07	127.42 ± 11.82	-0.46 ± 0.12	-2.36 ± 0.14	4.52E-06 ± 1.62E-07	1.07
1.74 -2.19	0.53 ± 0.10	109.95 ± 6.42	-0.24 ± 0.12	-3.03 ± 0.29	3.81E-06 ± 1.50E-07	1.19
2.19 -2.76	0.33 ± 0.05	109.61 ± 6.03	-0.47 ± 0.10	-3.60 ± 0.75	2.86E-06 ± 1.27E-07	1.03
2.76 -3.49	0.21 ± 0.04	114.68 ± 9.55	-0.60 ± 0.11	-2.68 ± 0.24	2.58E-06 ± 1.14E-07	0.98
3.49 -4.31	0.36 ± 0.08	87.09 ± 4.53	-0.34 ± 0.12	-3.38 ± 0.47	1.86E-06 ± 8.52E-08	1.09
4.31 -5.40	0.26 ± 0.06	89.52 ± 5.63	-0.40 ± 0.13	-2.94 ± 0.28	1.65E-06 ± 7.70E-08	0.98
5.40 -11.07	0.06 ± 0.04	46.46 ± 4.99	-0.80 ± 0.26	-2.64 ± 0.23	3.16E-07 ± 2.20E-08	1.01
GRB 090809B (bn090809978)						
-1.09 -0.91	0.01 ± 0.00	1390.47 ± 1025.72	-0.78 ± 0.20	-2.23 ± 0.68	8.37E-07 ± 7.77E-08	1.03
0.91 -2.91	0.06 ± 0.01	385.51 ± 42.17	-0.56 ± 0.07	-1.99 ± 0.09	3.70E-06 ± 9.75E-08	1.10
2.91 -3.89	0.15 ± 0.02	208.50 ± 24.11	-0.48 ± 0.10	-1.90 ± 0.06	4.69E-06 ± 1.16E-07	0.88
3.89 -5.13	0.23 ± 0.06	117.68 ± 13.51	-0.35 ± 0.14	-1.90 ± 0.05	3.34E-06 ± 9.24E-08	1.08
5.13 -7.21	0.08 ± 0.02	134.87 ± 17.68	-0.85 ± 0.10	-2.16 ± 0.14	1.84E-06 ± 7.46E-08	1.07
7.21 -16.13	0.02 ± 0.01	83.41 ± 18.78	-1.10 ± 0.18	-2.14 ± 0.17	4.42E-07 ± 3.20E-08	1.01
GRB 090922A (bn090922539)						
-1.22 -1.89	0.06 ± 0.02	130.45 ± 23.74	-0.56 ± 0.20	-2.12 ± 0.14	1.06E-06 ± 5.16E-08	1.12
1.89 -3.01	0.19 ± 0.07	128.20 ± 17.77	-0.25 ± 0.21	-2.11 ± 0.10	2.48E-06 ± 9.44E-08	1.00
3.01 -4.88	0.09 ± 0.04	110.80 ± 25.64	-0.68 ± 0.23	-1.94 ± 0.08	1.58E-06 ± 6.43E-08	1.18
4.88 -8.43	0.18 ± 0.18	65.37 ± 15.86	-0.21 ± 0.48	-1.86 ± 0.06	9.58E-07 ± 4.29E-08	1.05
8.43 -16.64	0.02 ± 0.01	60.95 ± 11.48	-1.03 ± 0.36	-2.83 ± 0.00	1.69E-07 ± 1.51E-08	1.01
GRB 091020A (bn091020900)						
-0.51 -2.72	0.02 ± 0.00	328.51 ± 211.99	-1.14 ± 0.15	-1.82 ± 0.43	9.25E-07 ± 6.93E-08	0.93
2.72 -5.13	0.03 ± 0.01	192.48 ± 117.13	-0.94 ± 0.24	-1.63 ± 0.14	1.11E-06 ± 7.23E-08	1.06
5.13 -13.79	0.20 ± 0.66	44.97 ± 20.72	0.23 ± 1.34	-1.69 ± 0.08	3.68E-07 ± 2.98E-08	0.99
13.79 -15.55	0.02 ± 0.01	72.34 ± 0.00	0.04 ± 0.00	-1.07 ± 0.21	2.47E-07 ± 4.84E-08	1.04
GRB 091208B (bn091208410)						
7.17 -8.63	0.05 ± 0.01	142.68 ± 40.84	-1.00 ± 0.15	-1.85 ± 0.09	1.58E-06 ± 7.14E-08	0.90
8.63 -9.58	0.06 ± 0.01	123.86 ± 22.21	-1.12 ± 0.11	-2.41 ± 0.35	1.55E-06 ± 1.07E-07	0.96
9.58 -13.25	0.02 ± 0.02	56.87 ± 21.98	-1.19 ± 0.38	-2.22 ± 0.28	2.81E-07 ± 3.68E-08	1.09
GRB 100122A (bn100122616)						
18.30 -20.29	2.46 ± 5.47	21.60 ± 2.72	-0.05 ± 0.79	-2.22 ± 0.05	9.25E-07 ± 3.99E-08	1.03
20.29 -20.78	43.47 ± 106.87	23.22 ± 2.75	0.73 ± 0.88	-2.10 ± 0.04	3.26E-06 ± 1.15E-07	0.98
20.78 -21.17	1.30 ± 0.93	41.22 ± 4.93	-0.45 ± 0.29	-2.16 ± 0.06	3.97E-06 ± 1.47E-07	1.02
21.17 -21.58	0.30 ± 0.11	58.82 ± 7.75	-1.05 ± 0.16	-2.28 ± 0.09	3.73E-06 ± 1.49E-07	0.90
21.58 -22.02	0.55 ± 0.22	53.11 ± 4.74	-0.71 ± 0.18	-2.47 ± 0.11	3.11E-06 ± 1.27E-07	1.04
22.02 -22.60	0.39 ± 0.20	49.62 ± 6.45	-0.81 ± 0.22	-2.21 ± 0.08	2.82E-06 ± 1.13E-07	1.02
22.60 -23.69	0.27 ± 0.14	46.57 ± 5.48	-0.77 ± 0.22	-2.28 ± 0.09	1.60E-06 ± 7.06E-08	1.12
23.69 -30.59	0.23 ± 0.21	34.38 ± 3.87	-0.36 ± 0.36	-2.33 ± 0.10	3.72E-07 ± 2.13E-08	1.16
GRB 100528A (bn100528075)						
-1.79 -4.68	0.02 ± 0.00	348.44 ± 103.17	-1.15 ± 0.09	-1.93 ± 0.14	9.24E-07 ± 3.42E-08	0.92
4.68 -6.75	0.04 ± 0.00	382.39 ± 78.34	-1.06 ± 0.07	-2.13 ± 0.19	2.00E-06 ± 7.28E-08	0.99
6.75 -8.18	0.04 ± 0.00	501.69 ± 126.54	-1.08 ± 0.07	-1.93 ± 0.11	2.82E-06 ± 1.00E-07	1.01
8.18 -9.49	0.05 ± 0.01	374.12 ± 92.39	-1.03 ± 0.08	-1.88 ± 0.09	2.80E-06 ± 9.22E-08	0.92

Table 2—Continued

Timebin (s)	Amplitude	E_p (keV)	α	β	Flux (erg/s.cm ²)	χ_r^2
9.49 -11.02	0.05 ± 0.01	331.38 ± 62.09	-1.01 ± 0.08	-2.15 ± 0.18	2.39E-06 ± 8.35E-08	1.00
11.02 -12.89	0.04 ± 0.01	215.79 ± 61.58	-1.11 ± 0.11	-1.91 ± 0.10	1.77E-06 ± 6.18E-08	1.06
12.89 -25.73	0.01 ± 0.00	390.99 ± 0.00	-1.58 ± 0.05	-1.94 ± 0.25	3.83E-07 ± 1.95E-08	0.95
GRB 100612A (bn100612726)						
-0.77 -2.71	0.08 ± 0.02	155.74 ± 17.72	-0.34 ± 0.13	-1.94 ± 0.08	1.52E-06 ± 5.21E-08	1.04
2.71 -3.64	0.29 ± 0.06	122.09 ± 8.95	-0.21 ± 0.12	-2.46 ± 0.15	2.86E-06 ± 1.21E-07	1.04
3.64 -4.34	0.34 ± 0.09	107.74 ± 10.50	-0.32 ± 0.14	-2.17 ± 0.09	3.52E-06 ± 1.39E-07	1.00
4.34 -5.04	0.46 ± 0.14	88.71 ± 7.39	-0.25 ± 0.16	-2.36 ± 0.12	2.90E-06 ± 1.28E-07	1.09
5.04 -6.48	0.20 ± 0.06	73.15 ± 6.56	-0.61 ± 0.15	-2.47 ± 0.15	1.42E-06 ± 7.29E-08	1.07
6.48 -12.16	0.07 ± 0.06	46.44 ± 6.80	-0.65 ± 0.34	-2.48 ± 0.22	2.91E-07 ± 2.66E-08	0.92
GRB 100707A (bn100707032)						
-0.58 -1.33	0.07 ± 0.00	525.70 ± 23.96	0.54 ± 0.08	-2.25 ± 0.06	9.54E-06 ± 1.65E-07	1.10
1.33 -1.70	0.23 ± 0.02	445.71 ± 25.31	0.37 ± 0.09	-2.26 ± 0.08	2.09E-05 ± 4.52E-07	1.01
1.70 -2.09	0.36 ± 0.03	323.81 ± 16.64	0.60 ± 0.11	-2.28 ± 0.08	1.76E-05 ± 3.56E-07	1.02
2.09 -2.49	0.29 ± 0.02	338.33 ± 19.38	0.24 ± 0.09	-2.33 ± 0.10	1.50E-05 ± 3.28E-07	0.94
2.49 -2.96	0.39 ± 0.04	253.59 ± 14.14	0.35 ± 0.10	-2.31 ± 0.10	1.12E-05 ± 2.51E-07	1.08
2.96 -3.46	0.59 ± 0.09	186.44 ± 11.10	0.45 ± 0.12	-2.22 ± 0.09	8.87E-06 ± 2.15E-07	0.89
3.46 -3.99	0.60 ± 0.11	165.76 ± 10.61	0.30 ± 0.12	-2.19 ± 0.08	7.83E-06 ± 1.98E-07	1.09
3.99 -4.57	0.67 ± 0.14	142.40 ± 9.41	0.28 ± 0.13	-2.17 ± 0.08	6.52E-06 ± 1.76E-07	0.96
4.57 -5.28	0.61 ± 0.14	123.80 ± 8.41	0.14 ± 0.13	-2.19 ± 0.08	5.07E-06 ± 1.47E-07	1.02
5.28 -6.53	0.31 ± 0.05	138.27 ± 9.11	-0.09 ± 0.11	-2.29 ± 0.10	3.54E-06 ± 1.06E-07	1.02
6.53 -8.86	0.23 ± 0.03	132.50 ± 7.20	-0.15 ± 0.09	-2.51 ± 0.14	2.37E-06 ± 7.51E-08	1.13
8.86 -30.40	0.05 ± 0.01	93.23 ± 5.36	-0.74 ± 0.07	-2.47 ± 0.13	6.45E-07 ± 2.27E-08	1.34
GRB 101126A (bn101126198)						
-0.26 -8.31	0.02 ± 0.00	143.03 ± 24.37	-1.34 ± 0.08	-2.58 ± 0.63	5.22E-07 ± 3.56E-08	1.12
8.31 -10.27	0.05 ± 0.01	152.56 ± 26.79	-1.07 ± 0.09	-2.00 ± 0.10	1.76E-06 ± 5.99E-08	0.95
10.27 -11.85	0.06 ± 0.01	161.61 ± 21.35	-1.07 ± 0.08	-2.23 ± 0.16	1.98E-06 ± 7.30E-08	1.05
11.85 -13.07	0.07 ± 0.01	179.58 ± 26.16	-1.10 ± 0.07	-2.15 ± 0.14	2.50E-06 ± 8.33E-08	0.97
13.07 -14.18	0.09 ± 0.01	176.05 ± 24.46	-1.01 ± 0.08	-2.08 ± 0.10	2.92E-06 ± 8.82E-08	1.09
14.18 -15.58	0.08 ± 0.02	130.98 ± 18.87	-0.99 ± 0.10	-2.07 ± 0.09	2.18E-06 ± 7.36E-08	1.17
15.58 -17.88	0.04 ± 0.01	143.70 ± 29.06	-1.29 ± 0.09	-2.10 ± 0.13	1.40E-06 ± 5.52E-08	1.12
17.88 -27.14	0.02 ± 0.00	103.65 ± 12.79	-1.37 ± 0.08	-2.97 ± 1.08	4.26E-07 ± 3.34E-08	1.12
27.14 -40.83	0.00 ± 0.00	99.63 ± 36.07	-1.57 ± 0.18	-2.55 ± 0.00	1.42E-07 ± 1.36E-08	1.05
GRB 101208A (bn101208498)						
-1.47 -0.28	0.16 ± 0.28	42.35 ± 17.11	-0.63 ± 0.72	-1.93 ± 0.10	9.10E-07 ± 7.81E-08	1.13
0.28 -0.43	0.42 ± 0.17	130.94 ± 30.36	-0.57 ± 0.23	-2.00 ± 0.13	7.74E-06 ± 4.16E-07	1.03
0.43 -0.62	0.41 ± 0.15	108.72 ± 16.86	-0.59 ± 0.20	-2.56 ± 0.32	4.84E-06 ± 3.52E-07	1.02
0.62 -1.04	0.63 ± 0.64	51.95 ± 9.79	-0.34 ± 0.45	-2.24 ± 0.15	2.08E-06 ± 1.71E-07	1.00
1.04 -2.56	0.03 ± 0.05	33.27 ± 8.44	-1.24 ± 0.62	-2.88 ± 1.11	2.48E-07 ± 5.77E-08	0.94
GRB 101216A (bn101216721)						
-0.51 -0.38	0.04 ± 0.01	238.75 ± 54.38	-0.78 ± 0.15	-2.22 ± 0.33	1.53E-06 ± 9.09E-08	0.87
0.38 -0.58	0.21 ± 0.06	165.03 ± 29.08	-0.47 ± 0.19	-2.21 ± 0.20	4.39E-06 ± 2.37E-07	1.04
0.58 -0.80	0.26 ± 0.11	112.60 ± 20.19	-0.46 ± 0.25	-2.24 ± 0.19	3.15E-06 ± 2.01E-07	0.99
0.80 -1.56	0.08 ± 0.05	79.73 ± 19.80	-0.87 ± 0.29	-2.19 ± 0.18	1.08E-06 ± 8.37E-08	1.02
1.56 -3.26	0.00 ± 0.00	234.38 ± 0.00	-1.90 ± 0.27	-1.93 ± 0.35	1.87E-07 ± 4.50E-08	1.09
GRB 110318A (bn110318552)						
0.00 -4.79	0.02 ± 0.01	198.49 ± 49.72	-0.82 ± 0.16	-2.00 ± 0.00	7.80E-07 ± 4.79E-08	1.06
4.79 -6.45	0.10 ± 0.04	111.86 ± 19.13	-0.51 ± 0.21	-2.30 ± 0.33	1.28E-06 ± 1.34E-07	1.17
6.45 -9.09	0.36 ± 0.41	57.01 ± 10.94	0.07 ± 0.51	-2.05 ± 0.13	8.33E-07 ± 6.90E-08	0.85
9.09 -20.03	0.03 ± 0.06	40.66 ± 18.12	-0.82 ± 0.81	-2.00 ± 0.00	2.09E-07 ± 1.37E-08	1.20
GRB 110505A (bn110505203)						
-1.02 -0.36	0.46 ± 0.12	37.88 ± 6.42	0.19 ± 0.00	-1.69 ± 0.09	6.52E-07 ± 6.21E-08	1.07
0.36 -0.69	1.85 ± 3.72	44.76 ± 10.86	0.46 ± 0.84	-1.93 ± 0.11	1.52E-06 ± 1.43E-07	0.84
0.69 -1.17	1.25 ± 0.36	31.22 ± 5.79	0.19 ± 0.00	-1.66 ± 0.07	1.34E-06 ± 1.16E-07	0.73
1.17 -2.51	1.35 ± 0.64	20.41 ± 5.53	0.19 ± 0.00	-1.76 ± 0.07	5.42E-07 ± 5.28E-08	0.98
GRB 110521A (bn110521478)						
-0.45 -0.67	0.03 ± 0.01	409.53 ± 188.90	-0.99 ± 0.15	-1.77 ± 0.11	1.77E-06 ± 1.05E-07	0.94
0.67 -1.11	1.76 ± 3.09	52.63 ± 11.96	0.41 ± 0.78	-2.03 ± 0.10	2.01E-06 ± 1.47E-07	0.88
1.11 -1.72	3.92 ± 8.25	40.94 ± 7.45	0.68 ± 0.89	-2.21 ± 0.13	1.24E-06 ± 1.06E-07	1.06
1.72 -3.46	1.73 ± 4.47	31.18 ± 5.90	0.36 ± 1.02	-2.38 ± 0.17	4.72E-07 ± 4.84E-08	1.11
3.46 -10.24	2.85 ± 4.64	12.53 ± 8.92	0.34 ± 0.00	-2.05 ± 0.13	1.42E-07 ± 2.37E-08	1.06
GRB 110605A (bn110605183)						
-0.83 -3.68	0.02 ± 0.00	326.72 ± 54.68	-0.55 ± 0.12	-1.93 ± 0.12	1.24E-06 ± 4.28E-08	0.97
3.68 -5.68	0.07 ± 0.02	186.22 ± 25.03	-0.28 ± 0.16	-2.11 ± 0.15	1.53E-06 ± 6.18E-08	0.95
5.68 -9.11	0.06 ± 0.02	151.78 ± 18.31	-0.32 ± 0.16	-2.31 ± 0.21	9.32E-07 ± 4.82E-08	0.95
9.11 -16.30	0.05 ± 0.02	103.45 ± 14.62	-0.29 ± 0.23	-2.15 ± 0.14	5.11E-07 ± 3.02E-08	1.06
GRB 110622A (bn110622158)						

Table 2—Continued

Timebin (s)	Amplitude	E_p (keV)	α	β	Flux (erg/s.cm ²)	χ_r^2
-0.26 -9.03	0.08 ± 0.06	72.58 ± 14.62	-0.21 ± 0.38	-1.90 ± 0.07	4.66E-07 ± 2.00E-08	1.11
9.03 -13.67	0.06 ± 0.02	88.34 ± 12.59	-0.69 ± 0.17	-2.08 ± 0.09	8.06E-07 ± 2.98E-08	1.13
13.67 -20.51	0.10 ± 0.01	113.40 ± 5.56	-0.72 ± 0.06	-2.47 ± 0.10	1.39E-06 ± 3.17E-08	1.28
20.51 -26.14	0.14 ± 0.02	102.64 ± 5.04	-0.61 ± 0.07	-2.36 ± 0.07	1.62E-06 ± 3.31E-08	1.27
26.14 -30.72	0.09 ± 0.01	111.31 ± 7.45	-0.70 ± 0.08	-2.39 ± 0.12	1.25E-06 ± 3.62E-08	1.30
30.72 -38.47	0.10 ± 0.02	93.41 ± 4.50	-0.51 ± 0.09	-2.73 ± 0.16	8.05E-07 ± 2.55E-08	1.28
38.47 -100.99	0.03 ± 0.01	56.02 ± 2.54	-0.98 ± 0.08	-2.91 ± 0.19	2.65E-07 ± 8.25E-09	1.09
GRB 110625A (1st pulse bn1106258811)						
-0.26 -2.49	0.45 ± 0.81	70.49 ± 16.77	0.89 ± 0.90	-1.80 ± 0.08	6.45E-07 ± 3.88E-08	0.95
2.49 -3.86	0.04 ± 0.01	254.67 ± 58.85	-0.57 ± 0.17	-1.86 ± 0.12	1.54E-06 ± 6.52E-08	1.06
3.86 -5.23	0.11 ± 0.02	249.68 ± 19.19	0.12 ± 0.13	-2.26 ± 0.13	3.23E-06 ± 8.64E-08	0.94
5.23 -7.97	0.03 ± 0.01	181.03 ± 46.11	-0.45 ± 0.25	-1.84 ± 0.12	8.39E-07 ± 4.11E-08	0.87
9.98 -10.68	0.12 ± 0.01	364.19 ± 30.78	-0.26 ± 0.09	-2.50 ± 0.20	6.42E-06 ± 2.10E-07	1.06
10.68 -10.93	0.29 ± 0.03	330.42 ± 28.86	-0.33 ± 0.09	-2.42 ± 0.15	1.39E-05 ± 4.55E-07	0.96
10.93 -11.19	0.51 ± 0.10	197.70 ± 19.39	-0.09 ± 0.13	-2.41 ± 0.15	1.04E-05 ± 3.79E-07	0.92
11.19 -11.56	0.57 ± 0.16	146.80 ± 14.71	0.07 ± 0.17	-2.25 ± 0.11	6.68E-06 ± 2.53E-07	1.03
11.56 -12.36	0.18 ± 0.04	137.46 ± 16.18	-0.53 ± 0.14	-2.51 ± 0.23	2.71E-06 ± 1.38E-07	1.08
12.36 -14.25	0.11 ± 0.04	89.32 ± 11.11	-0.68 ± 0.17	-2.48 ± 0.24	1.12E-06 ± 7.60E-08	1.12
GRB 110625A (2nd pulse bn1106258812)						
14.25 -15.04	0.10 ± 0.11	73.35 ± 27.86	-0.66 ± 0.47	-1.98 ± 0.15	1.14E-06 ± 1.04E-07	1.08
15.04 -22.28	0.06 ± 0.01	87.00 ± 6.55	-0.75 ± 0.10	-2.35 ± 0.10	7.43E-07 ± 2.39E-08	1.17
22.28 -23.37	0.40 ± 0.08	110.58 ± 7.54	-0.28 ± 0.11	-2.19 ± 0.06	4.03E-06 ± 9.32E-08	1.00
23.37 -23.82	0.29 ± 0.02	258.56 ± 17.22	-0.67 ± 0.05	-2.45 ± 0.14	1.05E-05 ± 2.13E-07	1.06
23.82 -24.15	0.39 ± 0.03	255.58 ± 18.30	-0.60 ± 0.06	-2.24 ± 0.08	1.45E-05 ± 2.81E-07	0.95
24.15 -24.43	0.66 ± 0.08	171.75 ± 11.41	-0.42 ± 0.07	-2.22 ± 0.07	1.39E-05 ± 2.79E-07	0.96
24.43 -24.75	0.90 ± 0.15	125.69 ± 8.20	-0.31 ± 0.09	-2.25 ± 0.07	1.11E-05 ± 2.39E-07	0.89
24.75 -25.22	0.44 ± 0.05	136.07 ± 8.80	-0.64 ± 0.07	-2.44 ± 0.11	7.45E-06 ± 1.75E-07	1.08
25.22 -26.55	0.39 ± 0.09	78.20 ± 5.53	-0.50 ± 0.11	-2.24 ± 0.06	3.05E-06 ± 7.44E-08	1.31
26.55 -28.32	0.09 ± 0.01	203.79 ± 14.54	-0.98 ± 0.05	-2.92 ± 0.47	2.82E-06 ± 7.78E-08	1.05
28.32 -29.59	0.16 ± 0.02	165.95 ± 14.76	-0.70 ± 0.07	-2.10 ± 0.07	3.94E-06 ± 8.63E-08	1.09
29.59 -34.18	0.06 ± 0.04	56.77 ± 12.53	-0.72 ± 0.35	-2.13 ± 0.12	4.28E-07 ± 2.83E-08	1.15
GRB 110709C (bn110709463)						
-0.32 -2.01	0.04 ± 0.04	74.32 ± 36.14	-0.80 ± 0.44	-1.80 ± 0.12	6.61E-07 ± 5.66E-08	0.93
2.01 -2.75	0.19 ± 0.10	65.45 ± 8.45	-0.50 ± 0.26	-2.56 ± 0.28	9.44E-07 ± 8.27E-08	0.98
2.75 -3.67	0.20 ± 0.38	37.58 ± 13.15	-0.53 ± 0.74	-1.99 ± 0.11	7.57E-07 ± 6.88E-08	0.99
3.67 -6.42	0.00 ± 0.00	75.93 ± 0.00	-1.95 ± 0.24	-2.01 ± 0.47	1.73E-07 ± 4.57E-08	1.06
6.42 -15.58	0.00 ± 0.00	75.93 ± 0.00	-0.82 ± 0.00	-1.46 ± 0.38	5.58E-08 ± 2.60E-08	1.16
15.58 -17.41	0.04 ± 0.01	133.76 ± 31.36	-0.83 ± 0.17	-1.99 ± 0.19	1.06E-06 ± 8.13E-08	0.97
17.41 -17.77	0.17 ± 0.06	119.50 ± 16.55	-0.50 ± 0.18	-2.59 ± 0.47	2.07E-06 ± 2.06E-07	0.77
17.77 -18.33	0.65 ± 0.73	56.19 ± 11.39	0.06 ± 0.50	-1.95 ± 0.10	1.64E-06 ± 1.18E-07	1.03
18.33 -21.12	0.06 ± 0.10	49.61 ± 20.58	-0.57 ± 0.67	-1.92 ± 0.13	4.03E-07 ± 4.10E-08	0.91
GRB 110721A (bn110721200)						
-0.77 -1.19	0.03 ± 0.00	3972.97 ± 458.76	-0.98 ± 0.02	-2.06 ± 0.11	4.91E-06 ± 8.80E-08	0.96
1.19 -1.71	0.06 ± 0.00	1734.53 ± 263.45	-0.98 ± 0.04	-2.48 ± 0.26	7.84E-06 ± 1.95E-07	1.01
1.71 -2.23	0.10 ± 0.01	547.02 ± 66.74	-0.85 ± 0.06	-2.30 ± 0.17	7.29E-06 ± 2.20E-07	0.98
2.23 -3.43	0.13 ± 0.01	257.30 ± 28.71	-0.79 ± 0.07	-1.90 ± 0.04	5.59E-06 ± 9.68E-08	1.14
3.43 -7.34	0.04 ± 0.00	344.71 ± 62.81	-1.15 ± 0.05	-1.87 ± 0.06	2.23E-06 ± 4.36E-08	1.09
7.34 -20.16	0.01 ± 0.00	312.69 ± 134.79	-1.16 ± 0.12	-1.81 ± 0.12	4.98E-07 ± 2.01E-08	1.03
GRB 110903B (1st pulse bn1109030091)						
-0.51 -0.52	0.09 ± 0.03	61.10 ± 6.77	-1.14 ± 0.17	-2.88 ± 0.57	1.04E-06 ± 9.19E-08	0.91
0.52 -1.37	0.11 ± 0.07	33.22 ± 3.65	-1.27 ± 0.27	-2.64 ± 0.22	1.07E-06 ± 7.03E-08	0.95
1.37 -2.56	0.05 ± 0.10	17.79 ± 5.61	-1.36 ± 0.78	-2.80 ± 0.41	3.03E-07 ± 3.74E-08	1.15
GRB 110903B (2nd pulse bn1109030092)						
2.56 -3.91	0.05 ± 0.02	18.11 ± 4.40	-1.69 ± 0.15	-3.36 ± 0.78	8.35E-07 ± 4.78E-08	1.19
3.91 -4.26	0.46 ± 0.15	39.39 ± 1.91	-1.06 ± 0.15	-3.55 ± 0.57	2.71E-06 ± 1.14E-07	1.15
4.26 -4.66	0.89 ± 0.41	29.00 ± 1.21	-0.85 ± 0.20	-3.35 ± 0.00	2.23E-06 ± 5.87E-08	1.16
4.66 -5.20	1.15 ± 1.11	18.46 ± 1.28	-0.86 ± 0.37	-3.14 ± 0.17	1.55E-06 ± 5.59E-08	1.12
5.20 -5.96	0.93 ± 0.65	19.51 ± 1.18	-0.84 ± 0.27	-3.64 ± 0.32	1.18E-06 ± 3.93E-08	1.19
5.96 -10.05	0.65 ± 2.77	11.14 ± 3.25	-0.72 ± 1.44	-3.09 ± 0.18	2.33E-07 ± 1.40E-08	0.94
19.83 -21.70	0.05 ± 0.02	172.78 ± 70.26	-0.94 ± 0.18	-1.65 ± 0.09	2.03E-06 ± 9.62E-08	0.93
GRB 110903B (3d pulse bn1109030093)						
21.70 -22.71	0.33 ± 0.28	52.55 ± 9.18	-0.45 ± 0.37	-2.14 ± 0.11	1.45E-06 ± 9.16E-08	1.06
22.71 -24.93	0.05 ± 0.05	37.49 ± 11.12	-1.23 ± 0.43	-2.17 ± 0.12	6.52E-07 ± 4.84E-08	1.05
24.93 -31.42	0.01 ± 0.01	53.73 ± 0.00	-1.37 ± 0.43	-1.81 ± 0.15	2.01E-07 ± 3.02E-08	1.04
GRB 1109030092.00						
-0.51 -0.52	0.09 ± 0.03	61.10 ± 6.77	-1.14 ± 0.17	-2.88 ± 0.57	1.04E-06 ± 9.19E-08	0.91
0.52 -1.37	0.11 ± 0.07	33.22 ± 3.65	-1.27 ± 0.27	-2.64 ± 0.22	1.07E-06 ± 7.03E-08	0.95

Table 2—Continued

Timebin (s)	Amplitude	E_p (keV)	α	β	Flux (erg/s.cm ²)	χ_r^2
1.37 -2.56	0.05 ± 0.10	17.79 ± 5.61	-1.36 ± 0.78	-2.80 ± 0.41	3.03E-07 ± 3.74E-08	1.15
2.50 -3.91	0.05 ± 0.02	18.11 ± 4.40	-1.69 ± 0.15	-3.36 ± 0.78	8.35E-07 ± 4.78E-08	1.19
3.91 -4.26	0.46 ± 0.15	39.39 ± 1.91	-1.06 ± 0.15	-3.55 ± 0.57	2.71E-06 ± 1.14E-07	1.15
4.26 -4.66	0.89 ± 0.41	29.00 ± 1.21	-0.85 ± 0.20	-3.35 ± 0.00	2.23E-06 ± 5.87E-08	1.16
4.66 -5.20	1.15 ± 1.11	18.46 ± 1.28	-0.86 ± 0.37	-3.14 ± 0.17	1.55E-06 ± 5.59E-08	1.12
5.20 -5.96	0.93 ± 0.65	19.51 ± 1.18	-0.84 ± 0.27	-3.64 ± 0.32	1.18E-06 ± 3.93E-08	1.19
5.96 -10.05	0.65 ± 2.77	11.14 ± 3.25	-0.72 ± 1.44	-3.09 ± 0.18	2.33E-07 ± 1.40E-08	0.94
19.83 -21.70	0.05 ± 0.02	172.78 ± 70.26	-0.94 ± 0.18	-1.65 ± 0.09	2.03E-06 ± 9.62E-08	0.93
21.70 -22.71	0.33 ± 0.28	52.55 ± 9.18	-0.45 ± 0.37	-2.14 ± 0.11	1.45E-06 ± 9.16E-08	1.06
22.71 -24.93	0.05 ± 0.05	37.49 ± 11.12	-1.23 ± 0.43	-2.17 ± 0.12	6.52E-07 ± 4.84E-08	1.05
24.93 -31.42	0.01 ± 0.01	53.73 ± 0.00	-1.37 ± 0.43	-1.81 ± 0.15	2.01E-07 ± 3.02E-08	1.04
GRB 110920B (bn110920546)						
-1.54 -7.04	0.02 ± 0.00	575.68 ± 41.18	0.10 ± 0.09	-2.45 ± 0.19	2.34E-06 ± 6.53E-08	1.30
7.04 -9.61	0.06 ± 0.00	443.60 ± 28.49	0.08 ± 0.08	-2.32 ± 0.12	4.37E-06 ± 1.02E-07	1.11
9.61 -12.14	0.06 ± 0.00	450.67 ± 26.45	0.02 ± 0.07	-2.68 ± 0.26	4.44E-06 ± 1.07E-07	1.08
12.14 -14.78	0.07 ± 0.01	362.15 ± 21.29	0.21 ± 0.09	-2.29 ± 0.11	4.06E-06 ± 8.69E-08	1.15
14.78 -17.58	0.06 ± 0.00	393.85 ± 23.73	0.06 ± 0.08	-2.56 ± 0.22	3.80E-06 ± 8.94E-08	1.11
17.58 -20.85	0.06 ± 0.00	381.23 ± 21.50	0.06 ± 0.08	-2.99 ± 0.46	3.28E-06 ± 8.27E-08	1.02
20.85 -24.51	0.06 ± 0.01	321.37 ± 18.69	0.12 ± 0.09	-2.50 ± 0.20	2.84E-06 ± 6.80E-08	1.14
24.51 -28.88	0.05 ± 0.00	327.32 ± 20.24	0.03 ± 0.09	-2.44 ± 0.19	2.52E-06 ± 6.08E-08	1.06
28.88 -33.41	0.06 ± 0.00	299.40 ± 12.34	0.15 ± 0.08	-3.82 ± 0.00	2.02E-06 ± 5.85E-08	1.01
33.41 -38.83	0.06 ± 0.01	263.68 ± 14.19	0.06 ± 0.09	-3.12 ± 0.56	1.67E-06 ± 5.96E-08	0.97
38.83 -45.47	0.06 ± 0.00	248.37 ± 10.03	0.07 ± 0.08	-3.82 ± 0.00	1.36E-06 ± 3.96E-08	1.14
45.47 -53.85	0.06 ± 0.01	216.27 ± 10.37	0.26 ± 0.11	-3.57 ± 0.96	1.02E-06 ± 5.10E-08	1.18
53.85 -66.94	0.05 ± 0.01	194.06 ± 7.83	0.09 ± 0.09	-3.82 ± 0.00	7.11E-07 ± 2.17E-08	1.19
66.94 -88.62	0.05 ± 0.01	147.31 ± 5.81	0.22 ± 0.11	-3.82 ± 0.00	4.08E-07 ± 1.27E-08	0.99
88.62 -99.07	0.07 ± 0.02	119.53 ± 7.55	0.46 ± 0.24	-3.82 ± 0.00	2.50E-07 ± 1.32E-08	1.14
GRB 111009A -111009282						
-0.64 -4.32	0.02 ± 0.00	207.55 ± 54.58	-0.95 ± 0.11	-1.89 ± 0.23	8.80E-07 ± 6.06E-08	1.16
4.32 -5.60	0.08 ± 0.02	125.42 ± 23.36	-0.71 ± 0.15	-1.94 ± 0.14	1.71E-06 ± 1.10E-07	0.87
5.60 -6.49	0.13 ± 0.03	120.92 ± 14.52	-0.58 ± 0.13	-2.29 ± 0.23	1.95E-06 ± 1.40E-07	1.04
6.49 -7.29	0.38 ± 0.22	72.92 ± 11.48	-0.18 ± 0.27	-1.87 ± 0.08	2.37E-06 ± 1.25E-07	1.13
7.29 -8.09	0.16 ± 0.06	91.33 ± 13.94	-0.61 ± 0.18	-2.08 ± 0.13	1.94E-06 ± 1.26E-07	0.85
8.09 -8.91	0.19 ± 0.08	82.89 ± 13.09	-0.58 ± 0.19	-2.02 ± 0.11	2.06E-06 ± 1.22E-07	1.05
8.91 -10.04	0.11 ± 0.03	86.83 ± 13.21	-0.80 ± 0.16	-2.17 ± 0.16	1.43E-06 ± 9.77E-08	1.15
10.04 -12.69	0.12 ± 0.06	62.69 ± 8.40	-0.55 ± 0.22	-2.18 ± 0.12	7.58E-07 ± 4.89E-08	0.96
12.69 -20.16	0.03 ± 0.03	53.92 ± 10.10	-0.66 ± 0.36	-2.46 ± 0.33	1.76E-07 ± 2.34E-08	0.94
GRB 111017A (bn111017657)						
-0.13 -3.90	0.02 ± 0.00	807.21 ± 139.22	-0.79 ± 0.07	-2.39 ± 0.31	1.52E-06 ± 5.47E-08	0.93
3.90 -5.00	0.04 ± 0.00	865.95 ± 126.15	-0.76 ± 0.06	-2.18 ± 0.14	4.26E-06 ± 1.24E-07	0.96
5.00 -5.82	0.05 ± 0.00	602.26 ± 94.61	-0.82 ± 0.06	-2.09 ± 0.13	4.38E-06 ± 1.50E-07	1.13
5.82 -6.87	0.05 ± 0.01	348.23 ± 56.59	-0.79 ± 0.08	-2.06 ± 0.14	2.79E-06 ± 9.09E-08	0.87
6.87 -10.11	0.02 ± 0.00	318.06 ± 63.39	-0.99 ± 0.08	-2.16 ± 0.25	1.11E-06 ± 4.24E-08	0.85
10.11 -15.04	0.01 ± 0.00	207.55 ± 0.00	-1.31 ± 0.13	-1.82 ± 0.23	2.37E-07 ± 2.52E-08	1.08
GRB 120102A (bn120102095)						
-2.18 -3.54	0.01 ± 0.00	414.60 ± 155.43	-1.33 ± 0.07	-2.26 ± 0.66	6.26E-07 ± 3.86E-08	1.04
3.54 -5.16	0.05 ± 0.00	389.72 ± 63.13	-1.01 ± 0.06	-2.05 ± 0.12	3.04E-06 ± 9.04E-08	1.43
5.16 -6.13	0.06 ± 0.01	283.92 ± 67.09	-1.03 ± 0.09	-1.81 ± 0.07	2.93E-06 ± 8.61E-08	0.89
6.13 -12.35	0.01 ± 0.00	232.48 ± 64.40	-1.26 ± 0.09	-2.18 ± 0.35	5.92E-07 ± 3.19E-08	1.00
GRB 120206A (bn120206949)						
4.22 -5.01	0.09 ± 0.04	217.26 ± 44.67	0.02 ± 0.30	-1.78 ± 0.07	2.71E-06 ± 1.19E-07	0.96
5.01 -5.33	0.20 ± 0.06	220.84 ± 32.84	0.06 ± 0.24	-2.08 ± 0.12	5.18E-06 ± 2.34E-07	0.95
5.33 -5.94	0.09 ± 0.04	178.31 ± 52.43	-0.47 ± 0.28	-1.79 ± 0.08	2.51E-06 ± 1.27E-07	1.04
5.94 -7.74	0.19 ± 0.12	38.34 ± 16.70	0.02 ± 0.00	-1.56 ± 0.08	5.00E-07 ± 5.14E-08	0.96
GRB 120217A (bn120217808)						
-0.51 -0.60	0.05 ± 0.07	102.56 ± 66.74	-0.48 ± 0.66	-1.59 ± 0.06	1.04E-06 ± 5.62E-08	1.01
0.60 -1.10	0.34 ± 0.59	50.60 ± 15.91	-0.23 ± 0.76	-2.05 ± 0.13	1.07E-06 ± 9.21E-08	0.98
1.10 -2.66	0.09 ± 0.14	37.43 ± 9.12	-0.72 ± 0.69	-2.50 ± 0.29	3.03E-07 ± 3.82E-08	0.97
2.66 -4.74	0.09 ± 0.06	23.37 ± 13.04	-0.55 ± 0.00	-1.96 ± 0.17	1.84E-07 ± 3.52E-08	1.07
GRB 120222A (bn120222021)						
-0.26 -0.29	0.16 ± 0.10	105.15 ± 27.95	-0.35 ± 0.35	-1.85 ± 0.10	2.04E-06 ± 1.27E-07	0.96
0.29 -0.54	0.46 ± 0.37	91.39 ± 21.40	-0.05 ± 0.42	-1.85 ± 0.09	3.47E-06 ± 2.03E-07	0.92
0.54 -1.00	0.14 ± 0.12	91.46 ± 30.52	-0.47 ± 0.43	-1.88 ± 0.13	1.70E-06 ± 1.36E-07	0.95
1.00 -1.46	0.02 ± 0.00	113.30 ± 0.00	-0.62 ± 0.00	-1.99 ± 0.55	3.67E-07 ± 1.26E-07	1.00
1.46 -2.37	0.01 ± 0.00	113.30 ± 0.00	-0.62 ± 0.00	-1.64 ± 0.26	2.70E-07 ± 6.89E-08	1.13
GRB 120304A (bn120304061)						
-0.43 -1.59	0.10 ± 0.11	34.63 ± 10.80	-1.10 ± 0.40	-1.98 ± 0.06	1.16E-06 ± 5.68E-08	1.14

Table 2—Continued

Timebin (s)	Amplitude	E_p (keV)	α	β	Flux (erg/s.cm ²)	χ_r^2
1.59 -2.45	0.10 ± 0.08	25.90 ± 3.18	-1.32 ± 0.31	-2.42 ± 0.12	9.67E-07 ± 5.57E-08	0.98
2.45 -4.22	0.17 ± 0.66	16.43 ± 3.43	-1.04 ± 1.35	-2.24 ± 0.07	5.83E-07 ± 3.62E-08	0.91
GRB 120308B (bn120308588)						
-0.32 -0.49	0.78 ± 2.55	55.65 ± 29.35	0.31 ± 1.45	-1.62 ± 0.04	2.05E-06 ± 1.10E-07	0.95
0.49 -0.97	0.06 ± 0.01	503.05 ± 119.44	-0.85 ± 0.13	-2.41 ± 0.42	4.01E-06 ± 2.62E-07	1.05
0.97 -3.04	0.03 ± 0.02	198.42 ± 81.55	-0.73 ± 0.31	-1.89 ± 0.14	1.10E-06 ± 7.39E-08	0.87
3.04 -6.02	0.00 ± 0.00	500.00 ± 0.00	-0.94 ± 0.35	-1.38 ± 0.10	3.23E-07 ± 5.41E-08	1.26
GRB 120326A (bn120326056)						
-1.09 -0.76	0.03 ± 0.01	89.22 ± 20.77	-1.07 ± 0.20	-2.49 ± 0.65	4.50E-07 ± 7.39E-08	0.85
0.76 -1.85	0.77 ± 1.08	41.47 ± 7.16	0.17 ± 0.58	-2.13 ± 0.12	7.37E-07 ± 6.62E-08	1.04
1.85 -2.87	0.19 ± 0.21	46.67 ± 10.16	-0.46 ± 0.46	-2.15 ± 0.15	7.16E-07 ± 7.00E-08	1.03
2.87 -4.65	0.22 ± 0.40	34.17 ± 9.08	-0.39 ± 0.70	-2.07 ± 0.12	4.88E-07 ± 4.75E-08	0.90
4.65 -9.15	0.07 ± 0.10	32.37 ± 6.19	-0.64 ± 0.57	-2.46 ± 0.25	1.79E-07 ± 2.24E-08	0.88
9.15 -13.70	0.40 ± 0.28	18.31 ± 6.90	0.11 ± 0.00	-2.08 ± 0.22	8.58E-08 ± 2.21E-08	0.97
GRB 1203282B (1st pulse bn1203282681)						
-0.06 -1.48	0.04 ± 0.03	164.90 ± 72.73	-0.13 ± 0.48	-1.47 ± 0.06	9.74E-07 ± 5.84E-08	1.12
1.48 -2.80	0.03 ± 0.01	277.93 ± 100.74	-0.58 ± 0.21	-1.64 ± 0.09	1.28E-06 ± 7.57E-08	0.95
2.80 -5.44	0.05 ± 0.00	458.67 ± 42.87	-0.63 ± 0.05	-2.02 ± 0.08	3.76E-06 ± 9.27E-08	1.08
5.44 -6.25	0.15 ± 0.01	329.36 ± 28.07	-0.46 ± 0.06	-1.93 ± 0.05	7.88E-06 ± 1.70E-07	1.04
6.25 -6.95	0.23 ± 0.03	205.48 ± 18.26	-0.45 ± 0.08	-1.89 ± 0.05	7.24E-06 ± 1.56E-07	1.14
6.95 -7.72	0.25 ± 0.03	181.23 ± 14.64	-0.38 ± 0.08	-1.99 ± 0.06	6.22E-06 ± 1.47E-07	0.91
7.72 -8.77	0.17 ± 0.02	175.03 ± 16.33	-0.62 ± 0.08	-2.03 ± 0.08	4.40E-06 ± 1.17E-07	0.98
8.77 -10.73	0.14 ± 0.03	118.89 ± 13.91	-0.65 ± 0.11	-1.87 ± 0.05	2.75E-06 ± 7.23E-08	1.04
GRB 1203282B (2nd pulse bn1203282682)						
10.73 -14.21	0.10 ± 0.02	133.29 ± 11.64	-0.60 ± 0.08	-2.06 ± 0.08	1.88E-06 ± 5.72E-08	0.91
14.21 -16.32	0.11 ± 0.04	101.23 ± 17.59	-0.52 ± 0.19	-1.80 ± 0.06	1.64E-06 ± 6.15E-08	0.94
16.32 -18.42	0.05 ± 0.01	199.96 ± 42.82	-0.87 ± 0.11	-1.76 ± 0.06	1.86E-06 ± 6.16E-08	1.03
18.42 -19.77	0.11 ± 0.01	254.57 ± 26.94	-0.66 ± 0.07	-1.84 ± 0.05	4.65E-06 ± 1.00E-07	0.98
19.77 -20.69	0.19 ± 0.02	196.54 ± 16.19	-0.53 ± 0.07	-2.04 ± 0.07	5.50E-06 ± 1.32E-07	1.04
20.69 -21.90	0.18 ± 0.02	158.16 ± 13.71	-0.57 ± 0.08	-2.06 ± 0.08	3.96E-06 ± 1.08E-07	1.08
21.90 -23.72	0.14 ± 0.02	127.13 ± 12.51	-0.64 ± 0.09	-2.02 ± 0.07	2.70E-06 ± 7.99E-08	1.04
23.72 -28.96	0.06 ± 0.01	96.68 ± 10.56	-0.92 ± 0.09	-2.15 ± 0.10	1.05E-06 ± 4.26E-08	1.11
28.96 -39.62	0.04 ± 0.01	84.06 ± 9.72	-0.93 ± 0.11	-2.18 ± 0.11	5.94E-07 ± 2.89E-08	1.05
GRB 120402B (bn120402669)						
-3.20 1.88	0.01 ± 0.00	35.22 ± 0.00	-0.86 ± 0.00	-1.39 ± 0.19	2.19E-07 ± 6.52E-08	0.83
-1.88 -0.33	0.14 ± 0.11	39.44 ± 4.24	-0.64 ± 0.33	-2.74 ± 0.27	4.07E-07 ± 3.33E-08	1.10
0.33 -1.00	0.09 ± 0.04	52.23 ± 9.44	-1.23 ± 0.22	-2.41 ± 0.23	1.22E-06 ± 9.96E-08	1.03
1.00 -2.06	0.06 ± 0.03	52.50 ± 11.44	-1.25 ± 0.24	-2.30 ± 0.19	9.39E-07 ± 7.75E-08	0.83
2.06 -5.76	0.08 ± 0.12	33.93 ± 6.37	-0.59 ± 0.66	-2.66 ± 0.38	1.59E-07 ± 2.29E-08	1.02
GRB 120412B (bn120412920)						
-0.83 -1.02	0.15 ± 0.11	96.01 ± 14.64	0.36 ± 0.40	-2.22 ± 0.25	5.72E-07 ± 6.70E-08	0.85
1.02 -1.86	0.37 ± 0.33	54.56 ± 7.29	-0.05 ± 0.40	-2.45 ± 0.21	7.01E-07 ± 6.57E-08	0.97
1.86 -5.12	0.85 ± 2.35	35.80 ± 7.76	0.64 ± 1.12	-2.19 ± 0.17	2.14E-07 ± 2.79E-08	1.13
GRB 120426A (bn120426090)						
-0.51 -0.65	0.22 ± 0.03	159.78 ± 11.59	-0.43 ± 0.08	-2.22 ± 0.09	4.30E-06 ± 1.01E-07	1.05
0.65 -1.01	0.70 ± 0.09	137.83 ± 7.70	-0.41 ± 0.08	-2.62 ± 0.13	9.39E-06 ± 2.36E-07	1.00
1.01 -1.30	0.72 ± 0.09	142.51 ± 8.67	-0.53 ± 0.07	-2.53 ± 0.12	1.16E-05 ± 2.77E-07	1.09
1.30 -1.59	0.70 ± 0.08	145.81 ± 8.08	-0.57 ± 0.07	-2.75 ± 0.17	1.14E-05 ± 2.85E-07	1.08
1.59 -1.95	0.79 ± 0.11	114.54 ± 5.95	-0.46 ± 0.08	-2.75 ± 0.15	8.24E-06 ± 2.15E-07	1.20
1.95 -2.42	1.05 ± 0.22	79.80 ± 4.09	-0.34 ± 0.11	-2.65 ± 0.10	5.58E-06 ± 1.50E-07	0.96
2.42 -6.53	0.13 ± 0.05	46.28 ± 2.90	-0.74 ± 0.17	-2.86 ± 0.20	5.67E-07 ± 2.56E-08	1.02
GRB 120427A (bn120427054)						
-0.77 -1.67	0.06 ± 0.01	222.39 ± 20.25	-0.04 ± 0.15	-2.46 ± 0.25	1.39E-06 ± 6.06E-08	0.95
1.67 -2.31	0.39 ± 0.10	141.31 ± 9.50	0.48 ± 0.19	-2.72 ± 0.23	2.59E-06 ± 1.22E-07	1.00
2.31 -2.92	0.54 ± 0.21	107.15 ± 9.33	0.37 ± 0.24	-2.40 ± 0.14	2.35E-06 ± 1.14E-07	1.00
2.92 -4.09	0.30 ± 0.12	99.88 ± 8.89	0.17 ± 0.23	-2.45 ± 0.16	1.38E-06 ± 7.33E-08	1.18
4.09 -9.34	0.07 ± 0.08	58.63 ± 14.44	-0.37 ± 0.53	-2.12 ± 0.15	3.21E-07 ± 2.86E-08	1.11
GRB 120625A (bn120625119)						
-1.92 -1.40	0.03 ± 0.03	131.95 ± 59.58	-0.40 ± 0.51	-1.72 ± 0.08	6.35E-07 ± 4.00E-08	1.02
1.40 -2.99	0.09 ± 0.02	193.60 ± 25.24	-0.22 ± 0.17	-2.14 ± 0.12	2.17E-06 ± 8.17E-08	0.84
2.99 -3.49	0.15 ± 0.04	187.76 ± 32.32	-0.35 ± 0.19	-2.08 ± 0.12	3.72E-06 ± 1.66E-07	0.89
3.49 -4.10	0.19 ± 0.09	129.34 ± 27.72	-0.30 ± 0.28	-1.90 ± 0.08	2.96E-06 ± 1.31E-07	1.00
4.10 -5.29	0.15 ± 0.08	109.37 ± 20.49	-0.26 ± 0.30	-2.06 ± 0.11	1.54E-06 ± 8.34E-08	0.93
5.29 -9.22	0.01 ± 0.01	134.09 ± 92.84	-1.06 ± 0.38	-1.90 ± 0.18	4.00E-07 ± 3.73E-08	1.10
GRB 120727B (bn120727681)						
-0.38 -1.10	7.48 ± 19.78	32.09 ± 5.53	0.76 ± 1.04	-1.95 ± 0.05	1.50E-06 ± 6.70E-08	1.15
1.10 -2.33	0.07 ± 0.02	120.61 ± 18.25	-1.01 ± 0.12	-2.49 ± 0.41	1.54E-06 ± 1.21E-07	1.01

Table 2—Continued

Timebin (s)	Amplitude	E_p (keV)	α	β	Flux (erg/s.cm ²)	χ_r^2
2.33 -3.30	0.14 ± 0.03	104.89 ± 11.47	-0.73 ± 0.14	-2.57 ± 0.32	1.80E-06 ± 1.25E-07	1.09
3.30 -4.41	0.18 ± 0.05	92.11 ± 6.97	-0.54 ± 0.14	-3.05 ± 0.54	1.40E-06 ± 9.96E-08	1.02
4.41 -6.27	0.14 ± 0.06	65.09 ± 7.70	-0.68 ± 0.22	-2.40 ± 0.16	1.01E-06 ± 6.04E-08	1.34
6.27 -17.53	0.02 ± 0.02	41.83 ± 6.85	-1.12 ± 0.39	-2.67 ± 0.41	1.59E-07 ± 1.76E-08	1.22
GRB 120919A (bn120919309)						
-0.45 -0.94	0.05 ± 0.02	157.08 ± 39.47	-0.51 ± 0.25	-1.83 ± 0.09	1.29E-06 ± 5.81E-08	0.90
0.94 -2.34	0.08 ± 0.02	187.91 ± 23.76	-0.51 ± 0.12	-2.05 ± 0.10	2.24E-06 ± 7.09E-08	1.01
2.34 -3.09	0.13 ± 0.01	258.47 ± 26.16	-0.53 ± 0.09	-2.08 ± 0.09	4.81E-06 ± 1.24E-07	0.99
3.09 -3.72	0.13 ± 0.01	250.12 ± 23.41	-0.67 ± 0.07	-2.37 ± 0.17	4.84E-06 ± 1.39E-07	0.85
3.72 -4.76	0.17 ± 0.04	135.83 ± 15.01	-0.50 ± 0.13	-2.07 ± 0.08	2.91E-06 ± 8.63E-08	1.13
4.76 -7.26	0.06 ± 0.01	103.28 ± 13.20	-0.96 ± 0.12	-2.28 ± 0.14	1.16E-06 ± 4.92E-08	0.94
7.26 -10.56	0.11 ± 0.04	27.85 ± 7.51	-0.53 ± 0.00	-1.96 ± 0.10	3.00E-07 ± 3.04E-08	0.95
GRB 120921A (bn120921877)						
-0.70 -0.62	0.12 ± 0.07	144.98 ± 26.00	0.25 ± 0.37	-2.08 ± 0.25	1.32E-06 ± 1.19E-07	0.98
0.62 -1.43	1.22 ± 1.65	68.30 ± 11.30	0.82 ± 0.69	-2.17 ± 0.16	1.20E-06 ± 1.08E-07	0.87
1.43 -7.10	0.01 ± 0.02	60.21 ± 39.86	-1.11 ± 0.80	-2.17 ± 0.38	1.78E-07 ± 3.33E-08	1.00
GRB 121223A (bn121223300)						
-1.66 -2.24	0.03 ± 0.01	211.21 ± 14.42	0.07 ± 0.16	100.00 ± 0.00	5.27E-07 ± 2.87E-08	1.05
2.24 -3.34	0.11 ± 0.02	161.05 ± 7.98	0.23 ± 0.15	100.00 ± 0.00	9.90E-07 ± 4.16E-08	1.02
3.34 -4.21	0.15 ± 0.03	144.22 ± 6.58	0.11 ± 0.13	100.00 ± 0.00	1.15E-06 ± 4.39E-08	1.14
4.21 -5.09	0.14 ± 0.03	146.65 ± 7.15	0.14 ± 0.14	100.00 ± 0.00	1.07E-06 ± 4.36E-08	1.01
5.09 -6.48	0.12 ± 0.02	118.13 ± 5.54	-0.06 ± 0.13	100.00 ± 0.00	7.16E-07 ± 2.76E-08	0.99
6.48 -8.12	0.05 ± 0.01	103.30 ± 7.32	-0.64 ± 0.13	100.00 ± 0.00	4.86E-07 ± 2.37E-08	0.98
8.12 -12.88	0.02 ± 0.01	67.67 ± 5.81	-0.93 ± 0.17	100.00 ± 0.00	1.81E-07 ± 1.05E-08	1.05
12.88 -16.38	0.00 ± 0.00	211.36 ± 0.00	-1.64 ± 0.21	100.00 ± 0.00	8.98E-08 ± 1.32E-08	1.09
GRB 130206B (bn130206482)						
-0.44 -1.89	0.07 ± 0.05	101.42 ± 26.64	-0.30 ± 0.35	-1.74 ± 0.06	9.44E-07 ± 4.47E-08	1.03
1.89 -2.46	0.12 ± 0.03	176.84 ± 23.97	-0.42 ± 0.15	-2.34 ± 0.23	2.52E-06 ± 1.31E-07	0.97
2.46 -3.07	0.18 ± 0.08	112.68 ± 19.27	-0.30 ± 0.24	-2.00 ± 0.10	2.16E-06 ± 1.12E-07	1.04
3.07 -3.83	0.14 ± 0.09	87.70 ± 21.79	-0.51 ± 0.31	-1.88 ± 0.08	1.67E-06 ± 9.05E-08	0.98
3.83 -5.29	0.10 ± 0.10	68.78 ± 25.27	-0.53 ± 0.47	-1.76 ± 0.06	1.06E-06 ± 5.71E-08	1.01
5.29 -11.77	0.13 ± 0.26	49.30 ± 13.19	0.16 ± 0.88	-2.15 ± 0.20	1.76E-07 ± 2.33E-08	0.95
GRB 130325A (bn130325203)						
-0.62 -1.92	0.02 ± 0.00	372.27 ± 87.42	-0.68 ± 0.13	-1.89 ± 0.12	1.30E-06 ± 5.40E-08	0.93
1.92 -3.33	0.07 ± 0.01	219.33 ± 29.26	-0.68 ± 0.11	-2.16 ± 0.14	2.31E-06 ± 7.41E-08	1.07
3.33 -4.74	0.02 ± 0.01	221.94 ± 73.88	-1.16 ± 0.14	-2.22 ± 0.40	9.99E-07 ± 6.40E-08	0.91
4.74 -8.96	0.01 ± 0.01	104.68 ± 64.12	-0.95 ± 0.46	-1.97 ± 0.24	2.73E-07 ± 3.05E-08	1.02
GRB 130518A (bn130518580)						
11.26 -18.73	0.02 ± 0.00	290.15 ± 37.61	-0.68 ± 0.09	-2.13 ± 0.14	1.08E-06 ± 3.57E-08	0.91
18.73 -22.98	0.03 ± 0.00	316.10 ± 43.57	-0.68 ± 0.09	-1.96 ± 0.08	1.71E-06 ± 5.11E-08	1.06
22.98 -24.07	0.06 ± 0.00	761.13 ± 94.51	-0.84 ± 0.05	-2.19 ± 0.11	5.98E-06 ± 1.65E-07	0.96
24.07 -24.74	0.11 ± 0.01	565.41 ± 55.81	-0.71 ± 0.06	-2.30 ± 0.12	8.77E-06 ± 2.42E-07	0.98
24.74 -26.11	0.15 ± 0.01	546.97 ± 32.77	-0.74 ± 0.03	-2.25 ± 0.06	1.14E-05 ± 1.83E-07	1.08
26.11 -28.62	0.15 ± 0.01	416.58 ± 19.14	-0.78 ± 0.03	-2.37 ± 0.07	8.92E-06 ± 1.18E-07	1.07
28.62 -30.06	0.13 ± 0.01	307.20 ± 22.90	-0.67 ± 0.05	-2.22 ± 0.08	6.07E-06 ± 1.25E-07	0.98
30.06 -32.73	0.07 ± 0.01	315.16 ± 28.65	-0.88 ± 0.05	-2.27 ± 0.12	3.33E-06 ± 7.65E-08	0.99
32.73 -40.60	0.02 ± 0.00	285.62 ± 59.76	-1.06 ± 0.08	-2.08 ± 0.17	8.37E-07 ± 3.28E-08	0.90
40.60 -52.99	0.01 ± 0.00	280.58 ± 120.88	-1.30 ± 0.14	-2.25 ± 0.00	2.62E-07 ± 2.47E-08	1.11
GRB 130606B (bn130606497)						
-0.96 -8.65	0.04 ± 0.00	490.31 ± 34.91	-0.75 ± 0.04	-2.16 ± 0.07	2.48E-06 ± 4.05E-08	1.05
8.65 -9.17	0.12 ± 0.01	921.08 ± 134.11	-0.95 ± 0.04	-2.00 ± 0.08	1.14E-05 ± 2.70E-07	1.11
9.17 -9.49	0.14 ± 0.00	2889.70 ± 419.27	-1.06 ± 0.03	-2.11 ± 0.12	1.75E-05 ± 3.99E-07	1.07
9.49 -9.80	0.17 ± 0.01	919.77 ± 112.62	-0.88 ± 0.04	-2.11 ± 0.09	1.78E-05 ± 4.07E-07	1.03
9.80 -10.12	0.17 ± 0.01	924.39 ± 124.72	-0.92 ± 0.04	-2.04 ± 0.08	1.73E-05 ± 4.08E-07	0.89
10.12 -10.48	0.17 ± 0.01	660.94 ± 89.74	-0.84 ± 0.05	-1.93 ± 0.06	1.49E-05 ± 3.67E-07	1.17
10.48 -11.02	0.13 ± 0.01	539.31 ± 62.84	-0.86 ± 0.05	-2.16 ± 0.10	9.90E-06 ± 2.55E-07	1.00
11.02 -11.58	0.13 ± 0.01	490.94 ± 53.11	-0.82 ± 0.05	-2.24 ± 0.12	9.27E-06 ± 2.41E-07	0.79
11.58 -12.21	0.12 ± 0.01	519.56 ± 74.98	-0.89 ± 0.06	-1.95 ± 0.07	8.45E-06 ± 2.15E-07	1.10
12.21 -12.75	0.11 ± 0.01	936.43 ± 138.82	-0.97 ± 0.04	-2.03 ± 0.08	1.08E-05 ± 2.55E-07	1.10
12.75 -13.15	0.13 ± 0.01	1196.59 ± 206.43	-0.96 ± 0.04	-1.83 ± 0.06	1.47E-05 ± 3.32E-07	1.09
13.15 -13.51	0.15 ± 0.01	1057.93 ± 161.16	-0.96 ± 0.04	-1.97 ± 0.07	1.53E-05 ± 3.51E-07	0.90
13.51 -13.87	0.15 ± 0.01	1083.51 ± 200.77	-0.99 ± 0.04	-1.80 ± 0.05	1.54E-05 ± 3.65E-07	0.94
13.87 -14.22	0.15 ± 0.01	822.75 ± 218.44	-1.07 ± 0.05	-1.69 ± 0.04	1.33E-05 ± 3.49E-07	0.99
14.22 -14.50	0.16 ± 0.01	2294.92 ± 522.17	-1.17 ± 0.03	-1.91 ± 0.09	1.67E-05 ± 4.00E-07	1.05
14.50 -14.91	0.13 ± 0.01	859.92 ± 199.77	-1.11 ± 0.05	-1.81 ± 0.06	1.16E-05 ± 3.08E-07	0.87
14.91 -15.33	0.11 ± 0.00	2441.80 ± 519.77	-1.24 ± 0.03	-2.17 ± 0.18	1.12E-05 ± 2.73E-07	0.86
15.33 -15.90	0.09 ± 0.00	1390.13 ± 420.68	-1.30 ± 0.04	-1.96 ± 0.11	7.86E-06 ± 1.99E-07	1.16

Table 2—Continued

Timebin (s)	Amplitude	E_p (keV)	α	β	Flux (erg/s.cm ²)	χ_r^2
15.90 -16.57	0.08 ± 0.00	1201.37 ± 293.71	-1.32 ± 0.03	-2.35 ± 0.27	6.65E-06 ± 1.71E-07	0.99
16.57 -17.35	0.07 ± 0.00	628.79 ± 138.80	-1.36 ± 0.04	-2.39 ± 0.32	5.09E-06 ± 1.61E-07	0.89
17.35 -18.42	0.05 ± 0.00	711.67 ± 232.61	-1.47 ± 0.04	-2.20 ± 0.25	3.73E-06 ± 1.24E-07	1.06
18.42 -20.09	0.05 ± 0.01	257.60 ± 67.77	-1.42 ± 0.06	-2.10 ± 0.16	2.40E-06 ± 7.30E-08	0.97
20.09 -38.55	0.02 ± 0.00	401.73 ± 68.22	-1.54 ± 0.03	-2.46 ± 0.40	1.10E-06 ± 2.65E-08	1.18
38.55 -39.93	0.07 ± 0.01	434.20 ± 52.18	-0.90 ± 0.06	-2.19 ± 0.12	4.47E-06 ± 1.15E-07	1.10
39.93 -41.13	0.13 ± 0.02	212.77 ± 24.29	-0.63 ± 0.09	-2.01 ± 0.07	4.23E-06 ± 1.01E-07	0.97
41.13 -42.72	0.08 ± 0.01	231.31 ± 19.63	-0.94 ± 0.06	-3.07 ± 0.69	2.80E-06 ± 8.74E-08	0.82
42.72 -45.54	0.07 ± 0.01	185.69 ± 16.27	-0.90 ± 0.07	-2.66 ± 0.30	1.89E-06 ± 6.09E-08	0.97
45.54 -49.13	0.07 ± 0.01	171.48 ± 12.77	-0.87 ± 0.07	-2.88 ± 0.40	1.61E-06 ± 5.48E-08	1.23
49.13 -50.38	0.09 ± 0.01	298.33 ± 36.03	-0.88 ± 0.07	-2.20 ± 0.13	3.97E-06 ± 1.03E-07	1.09
50.38 -51.19	0.14 ± 0.02	255.91 ± 27.82	-0.75 ± 0.08	-2.19 ± 0.11	5.45E-06 ± 1.38E-07	1.03
51.19 -51.73	0.22 ± 0.03	248.13 ± 24.19	-0.58 ± 0.09	-2.18 ± 0.09	7.87E-06 ± 1.93E-07	1.06
51.73 -52.36	0.16 ± 0.01	277.14 ± 22.44	-0.72 ± 0.07	-2.76 ± 0.31	6.39E-06 ± 1.74E-07	0.98
52.36 -53.58	0.11 ± 0.01	236.50 ± 23.63	-0.74 ± 0.08	-2.30 ± 0.14	3.87E-06 ± 1.02E-07	1.01
53.58 -55.29	0.08 ± 0.01	258.98 ± 23.43	-0.84 ± 0.06	-2.69 ± 0.34	2.97E-06 ± 8.42E-08	0.87
55.29 -66.18	0.07 ± 0.02	89.11 ± 7.75	-0.68 ± 0.12	-2.37 ± 0.11	7.41E-07 ± 2.51E-08	0.96
GRB 130609B (bn130609902)						
-3.26 -1.53	0.01 ± 0.00	489.79 ± 75.49	0.67 ± 0.43	-5.92 ± 0.00	6.70E-07 ± 6.80E-08	0.89
1.53 -6.32	0.02 ± 0.00	771.60 ± 100.03	-0.45 ± 0.09	-2.67 ± 0.43	1.83E-06 ± 6.73E-08	1.03
6.32 -7.50	0.04 ± 0.00	916.18 ± 92.24	-0.48 ± 0.06	-2.73 ± 0.30	5.88E-06 ± 1.51E-07	1.01
7.50 -8.88	0.05 ± 0.00	640.75 ± 73.57	-0.52 ± 0.07	-2.21 ± 0.14	4.54E-06 ± 1.49E-07	1.20
8.88 -10.78	0.04 ± 0.00	526.20 ± 69.33	-0.59 ± 0.08	-2.41 ± 0.30	2.73E-06 ± 1.14E-07	1.09
10.78 -13.61	0.03 ± 0.00	420.62 ± 60.15	-0.53 ± 0.10	-2.08 ± 0.14	1.99E-06 ± 7.42E-08	1.02
13.61 -16.74	0.02 ± 0.00	495.72 ± 87.41	-0.77 ± 0.08	-2.15 ± 0.20	1.74E-06 ± 7.58E-08	1.00
16.74 -18.85	0.04 ± 0.01	344.59 ± 56.14	-0.65 ± 0.10	-1.93 ± 0.10	2.18E-06 ± 7.56E-08	1.05
18.85 -20.72	0.04 ± 0.01	343.62 ± 50.00	-0.67 ± 0.09	-2.14 ± 0.18	2.28E-06 ± 8.38E-08	0.97
20.72 -21.99	0.05 ± 0.01	400.86 ± 52.32	-0.53 ± 0.09	-2.22 ± 0.19	3.22E-06 ± 1.20E-07	1.08
21.99 -23.18	0.07 ± 0.01	277.71 ± 38.30	-0.43 ± 0.12	-1.95 ± 0.09	3.11E-06 ± 1.02E-07	1.02
23.18 -25.71	0.03 ± 0.00	366.73 ± 46.17	-0.88 ± 0.07	-5.92 ± 0.00	1.52E-06 ± 8.14E-08	0.97
25.71 -32.70	0.01 ± 0.00	215.46 ± 50.27	-0.87 ± 0.19	-5.92 ± 0.00	2.60E-07 ± 3.42E-08	0.90
GRB 130612B (bn130612456)						
0.04 -0.78	0.19 ± 0.23	55.98 ± 19.40	-0.49 ± 0.53	-1.81 ± 0.07	1.37E-06 ± 7.54E-08	0.90
0.78 -1.53	0.11 ± 0.02	135.79 ± 18.39	-0.86 ± 0.11	-2.23 ± 0.15	2.51E-06 ± 9.99E-08	1.13
1.53 -2.10	0.16 ± 0.02	166.52 ± 13.16	-0.82 ± 0.07	-2.93 ± 0.44	3.75E-06 ± 1.41E-07	0.91
2.10 -2.41	0.25 ± 0.07	129.45 ± 18.07	-0.52 ± 0.16	-2.15 ± 0.12	4.08E-06 ± 1.71E-07	0.89
2.41 -2.95	0.16 ± 0.05	101.78 ± 16.10	-0.68 ± 0.18	-2.16 ± 0.13	2.21E-06 ± 1.11E-07	1.02
2.95 -4.68	0.05 ± 0.01	101.27 ± 18.12	-0.95 ± 0.16	-2.29 ± 0.22	8.08E-07 ± 5.42E-08	0.87
4.68 -9.22	0.02 ± 0.02	52.11 ± 15.55	-1.07 ± 0.42	-2.38 ± 0.34	1.79E-07 ± 2.43E-08	0.98
GRB 130701B (bn130701060)						
-2.94 -3.28	0.01 ± 0.00	692.17 ± 198.36	-0.92 ± 0.11	-2.14 ± 0.29	9.42E-07 ± 5.07E-08	1.08
3.28 -5.26	0.03 ± 0.00	605.28 ± 128.37	-0.93 ± 0.09	-1.98 ± 0.00	2.28E-06 ± 7.83E-08	1.07
5.26 -11.97	0.01 ± 0.00	519.50 ± 194.00	-1.41 ± 0.17	-1.93 ± 0.43	4.01E-07 ± 2.65E-08	0.97
GRB 130815B (bn130815660)						
29.38 -32.06	0.07 ± 0.02	112.03 ± 17.39	-0.61 ± 0.17	-2.07 ± 0.12	1.01E-06 ± 5.22E-08	1.00
32.06 -32.45	0.67 ± 0.30	86.01 ± 10.59	-0.15 ± 0.22	-2.01 ± 0.07	4.46E-06 ± 1.70E-07	1.03
32.45 -32.82	0.75 ± 0.35	75.96 ± 8.93	-0.22 ± 0.23	-2.11 ± 0.08	4.13E-06 ± 1.70E-07	0.98
32.82 -33.27	0.39 ± 0.12	84.15 ± 8.01	-0.51 ± 0.16	-2.46 ± 0.15	3.00E-06 ± 1.42E-07	0.94
33.27 -33.81	0.23 ± 0.07	82.57 ± 9.88	-0.73 ± 0.16	-2.37 ± 0.15	2.41E-06 ± 1.25E-07	1.03
33.81 -34.55	0.17 ± 0.06	70.77 ± 8.19	-0.84 ± 0.17	-2.45 ± 0.17	1.72E-06 ± 9.50E-08	1.13
34.55 -35.44	0.18 ± 0.07	58.43 ± 6.54	-0.83 ± 0.20	-2.50 ± 0.17	1.34E-06 ± 7.76E-08	1.01
35.44 -37.22	0.20 ± 0.18	42.09 ± 6.84	-0.62 ± 0.36	-2.18 ± 0.09	8.66E-07 ± 4.99E-08	0.99
37.22 -44.48	0.01 ± 0.01	31.20 ± 6.35	-1.39 ± 0.42	-2.65 ± 0.49	1.33E-07 ± 1.92E-08	1.07
GRB 130828B (bn130828808)						
-2.05 -0.95	0.01 ± 0.01	337.04 ± 134.23	0.08 ± 0.41	-1.90 ± 0.72	7.40E-07 ± 7.14E-08	0.92
0.95 -1.72	0.05 ± 0.02	159.86 ± 46.60	-0.59 ± 0.25	-2.14 ± 0.46	1.15E-06 ± 1.48E-07	1.00
1.72 -2.36	1.40 ± 2.29	44.09 ± 7.51	0.42 ± 0.70	-2.26 ± 0.15	8.50E-07 ± 7.89E-08	0.90
2.36 -4.45	3.27 ± 1.06	18.51 ± 2.68	0.39 ± 0.00	-2.29 ± 0.12	2.50E-07 ± 2.76E-08	0.96
4.45 -7.55	1.20 ± 2.05	14.20 ± 10.03	0.39 ± 0.00	-2.33 ± 0.45	4.38E-08 ± 1.91E-08	1.13
GRB 131214A (bn131214705)						
53.95 -57.22	0.69 ± 0.73	18.86 ± 1.03	-0.78 ± 0.38	-2.55 ± 0.07	9.98E-07 ± 3.64E-08	1.41
57.22 -58.41	0.88 ± 0.83	22.40 ± 1.97	-0.91 ± 0.34	-2.31 ± 0.05	2.85E-06 ± 9.26E-08	1.08
58.41 -59.94	0.07 ± 0.01	49.82 ± 6.00	-1.76 ± 0.07	-2.55 ± 0.41	2.47E-06 ± 1.55E-07	1.18
59.94 -61.55	0.19 ± 0.18	35.15 ± 13.38	-1.23 ± 0.35	-1.90 ± 0.04	3.18E-06 ± 1.15E-07	1.22
61.55 -63.13	0.18 ± 0.06	61.86 ± 11.19	-1.15 ± 0.14	-2.02 ± 0.07	3.23E-06 ± 1.32E-07	1.06
63.13 -64.80	0.09 ± 0.01	125.17 ± 19.56	-1.36 ± 0.06	-2.30 ± 0.28	3.13E-06 ± 1.83E-07	1.04
64.80 -66.72	0.19 ± 0.08	53.04 ± 10.20	-1.07 ± 0.18	-1.97 ± 0.05	2.87E-06 ± 1.12E-07	1.09

Table 2—Continued

Timebin (s)	Amplitude	E_p (keV)	α	β	Flux (erg/s.cm ²)	χ_r^2
66.72 -68.94	0.09 ± 0.01	86.34 ± 11.42	-1.36 ± 0.08	-2.32 ± 0.19	2.23E-06 ± 1.22E-07	1.46
68.94 -71.67	0.14 ± 0.05	56.01 ± 8.02	-1.07 ± 0.15	-2.00 ± 0.00	2.16E-06 ± 4.64E-08	1.35
71.67 -77.35	0.09 ± 0.02	52.33 ± 4.96	-1.11 ± 0.12	-2.37 ± 0.12	1.01E-06 ± 4.78E-08	1.13
77.35 -85.06	0.04 ± 0.02	41.77 ± 4.43	-1.08 ± 0.20	-2.82 ± 0.41	3.04E-07 ± 2.81E-08	1.11
GRB 131216A (bn131216081)						
-0.83 -0.45	0.01 ± 0.00	1536.26 ± 701.37	-0.53 ± 0.20	-1.82 ± 0.18	1.25E-06 ± 8.80E-08	1.05
0.45 -1.72	0.04 ± 0.01	398.87 ± 60.12	-0.31 ± 0.13	-2.02 ± 0.12	2.57E-06 ± 9.81E-08	1.09
1.72 -3.37	0.03 ± 0.01	352.98 ± 81.71	-0.58 ± 0.15	-1.97 ± 0.16	1.44E-06 ± 6.98E-08	0.97
GRB 140102A (bn140102887)						
-0.01 -0.51	0.10 ± 0.05	131.22 ± 50.74	-0.79 ± 0.30	-1.86 ± 0.10	2.36E-06 ± 1.23E-07	1.01
0.51 -0.62	0.31 ± 0.07	207.86 ± 29.53	-0.60 ± 0.16	-2.87 ± 0.60	8.09E-06 ± 4.65E-07	0.97
0.62 -0.76	0.46 ± 0.10	179.94 ± 24.06	-0.53 ± 0.15	-2.28 ± 0.15	1.08E-05 ± 4.08E-07	0.94
0.76 -1.02	0.23 ± 0.08	135.03 ± 32.91	-0.87 ± 0.19	-2.03 ± 0.10	5.65E-06 ± 2.31E-07	1.00
1.02 -1.39	0.32 ± 0.50	51.49 ± 19.89	-0.58 ± 0.68	-2.00 ± 0.10	1.95E-06 ± 1.39E-07	0.88
1.96 -2.25	0.45 ± 0.08	174.56 ± 16.37	-0.33 ± 0.13	-2.38 ± 0.13	8.71E-06 ± 2.72E-07	0.92
2.25 -2.40	0.46 ± 0.09	201.81 ± 24.02	-0.42 ± 0.14	-2.35 ± 0.16	1.16E-05 ± 4.23E-07	1.08
2.40 -2.59	0.31 ± 0.07	210.01 ± 37.64	-0.57 ± 0.15	-1.94 ± 0.08	1.02E-05 ± 3.45E-07	0.86
2.59 -2.69	0.32 ± 0.12	201.00 ± 60.57	-0.56 ± 0.24	-1.80 ± 0.08	1.08E-05 ± 4.94E-07	0.89
2.69 -2.88	0.32 ± 0.06	242.22 ± 32.23	-0.43 ± 0.13	-2.15 ± 0.11	1.08E-05 ± 3.62E-07	1.01
2.88 -3.18	0.26 ± 0.06	183.04 ± 24.93	-0.54 ± 0.14	-2.28 ± 0.16	6.16E-06 ± 2.38E-07	1.03
3.18 -3.40	0.40 ± 0.10	149.21 ± 18.06	-0.46 ± 0.16	-2.46 ± 0.20	6.67E-06 ± 2.85E-07	0.97
3.40 -3.62	0.18 ± 0.10	120.38 ± 38.84	-0.77 ± 0.29	-2.03 ± 0.15	3.72E-06 ± 2.20E-07	1.03
3.62 -4.40	0.08 ± 0.06	100.50 ± 39.98	-0.78 ± 0.38	-1.95 ± 0.13	1.41E-06 ± 9.24E-08	1.11
4.40 -5.31	0.02 ± 0.00	133.46 ± 0.00	-0.80 ± 0.00	-1.65 ± 0.11	6.63E-07 ± 6.79E-08	1.07
GRB 140209A (bn140209313)						
1.28 -1.58	0.44 ± 0.07	187.09 ± 15.18	-0.14 ± 0.11	-2.11 ± 0.08	9.44E-06 ± 2.49E-07	1.06
1.58 -1.69	1.16 ± 0.20	157.63 ± 13.02	-0.25 ± 0.11	-2.16 ± 0.07	1.99E-05 ± 5.33E-07	0.96
1.69 -1.79	1.56 ± 0.25	153.28 ± 9.79	-0.06 ± 0.10	-2.42 ± 0.10	2.02E-05 ± 5.61E-07	1.01
1.79 -2.04	3.16 ± 1.84	64.57 ± 6.56	0.27 ± 0.27	-1.98 ± 0.05	7.32E-06 ± 2.28E-07	1.02
2.04 -3.01	0.45 ± 0.40	45.54 ± 7.73	-0.38 ± 0.37	-2.03 ± 0.06	1.59E-06 ± 7.70E-08	1.07
GRB 140213A (bn140213807)						
-0.96 -1.05	0.02 ± 0.00	195.22 ± 66.00	-1.38 ± 0.09	-2.05 ± 0.20	1.08E-06 ± 5.49E-08	0.98
1.05 -1.57	0.07 ± 0.01	326.99 ± 83.07	-1.25 ± 0.06	-2.03 ± 0.15	3.77E-06 ± 1.46E-07	1.02
1.57 -2.06	0.09 ± 0.01	301.60 ± 53.88	-1.09 ± 0.06	-2.15 ± 0.18	4.28E-06 ± 1.59E-07	0.96
2.06 -2.68	0.08 ± 0.01	260.50 ± 49.99	-1.00 ± 0.08	-1.94 ± 0.09	3.80E-06 ± 1.28E-07	0.95
2.68 -3.51	0.10 ± 0.02	137.38 ± 18.59	-0.86 ± 0.10	-2.19 ± 0.14	2.34E-06 ± 1.01E-07	1.02
3.51 -4.38	0.55 ± 0.30	62.10 ± 6.88	-0.10 ± 0.25	-2.10 ± 0.07	1.85E-06 ± 8.43E-08	1.07
4.38 -5.58	0.14 ± 0.04	62.03 ± 5.00	-0.82 ± 0.14	-2.71 ± 0.23	1.06E-06 ± 5.99E-08	1.00
5.58 -6.02	0.36 ± 0.13	58.99 ± 5.01	-0.71 ± 0.16	-2.61 ± 0.17	2.19E-06 ± 1.10E-07	0.91
6.02 -6.36	0.31 ± 0.09	72.66 ± 7.15	-0.84 ± 0.14	-2.52 ± 0.16	3.09E-06 ± 1.52E-07	1.02
6.36 -6.68	0.37 ± 0.12	74.50 ± 9.71	-0.78 ± 0.16	-2.18 ± 0.09	4.06E-06 ± 1.72E-07	1.07
6.68 -7.08	0.28 ± 0.06	86.03 ± 6.23	-0.80 ± 0.10	-2.95 ± 0.33	2.84E-06 ± 1.39E-07	1.03
7.08 -7.48	0.44 ± 0.16	67.74 ± 6.70	-0.58 ± 0.17	-2.37 ± 0.11	2.91E-06 ± 1.36E-07	0.94
7.48 -8.08	0.40 ± 0.18	55.01 ± 5.82	-0.56 ± 0.21	-2.33 ± 0.10	1.95E-06 ± 9.65E-08	0.94
8.08 -8.98	0.35 ± 0.18	45.88 ± 4.16	-0.58 ± 0.22	-2.47 ± 0.12	1.27E-06 ± 6.43E-08	1.00
8.98 -10.33	0.17 ± 0.11	36.04 ± 4.12	-0.87 ± 0.26	-2.39 ± 0.11	8.49E-07 ± 4.68E-08	0.89
10.33 -15.10	0.04 ± 0.03	29.38 ± 2.99	-1.10 ± 0.30	-2.76 ± 0.29	2.16E-07 ± 1.84E-08	0.94
GRB 140311C (bn140311618)						
-0.88 -0.61	0.03 ± 0.02	92.17 ± 30.18	-1.11 ± 0.22	-2.10 ± 0.26	7.30E-07 ± 8.25E-08	1.04
0.61 -1.56	0.13 ± 0.07	68.03 ± 12.36	-0.67 ± 0.26	-2.21 ± 0.18	1.05E-06 ± 9.13E-08	1.04
1.56 -2.72	0.12 ± 0.09	55.83 ± 11.66	-0.66 ± 0.34	-2.18 ± 0.16	7.77E-07 ± 7.16E-08	1.05
2.72 -4.80	0.10 ± 0.10	42.24 ± 9.14	-0.67 ± 0.45	-2.23 ± 0.17	4.27E-07 ± 4.30E-08	1.07
4.80 -13.38	0.02 ± 0.08	25.59 ± 13.07	-0.93 ± 1.44	-2.11 ± 0.00	1.04E-07 ± 7.91E-09	0.94
GRB 1403292A (1st pulse bn1403292951)						
-0.45 0.05	0.04 ± 0.03	117.90 ± 80.05	-0.06 ± 0.00	-1.49 ± 0.15	5.75E-07 ± 1.02E-07	0.85
-0.05 -0.01	0.37 ± 0.52	136.30 ± 66.39	0.14 ± 0.86	-1.72 ± 0.11	5.02E-06 ± 4.34E-07	0.84
0.01 -0.08	0.51 ± 0.36	161.51 ± 50.70	-0.06 ± 0.44	-1.74 ± 0.08	1.02E-05 ± 5.74E-07	0.76
0.08 -0.19	0.49 ± 0.13	209.59 ± 27.04	-0.11 ± 0.20	-2.34 ± 0.17	1.13E-05 ± 5.00E-07	0.88
0.19 -0.29	2.88 ± 3.05	90.63 ± 14.75	0.84 ± 0.60	-2.27 ± 0.16	5.39E-06 ± 3.63E-07	0.75
0.29 -0.48	0.48 ± 0.64	76.96 ± 25.84	-0.17 ± 0.65	-2.00 ± 0.13	2.80E-06 ± 2.17E-07	0.84
0.48 -1.54	0.49 ± 0.45	24.01 ± 15.05	-0.06 ± 0.00	-1.65 ± 0.08	6.03E-07 ± 6.41E-08	0.97
GRB 1403292A (2nd pulse bn1403292952)						
20.44 -21.09	0.18 ± 0.02	223.54 ± 22.80	-0.78 ± 0.08	-2.34 ± 0.14	5.90E-06 ± 1.66E-07	0.97
21.09 -21.43	0.33 ± 0.04	231.75 ± 21.27	-0.66 ± 0.08	-2.32 ± 0.11	1.10E-05 ± 2.86E-07	0.98
21.43 -21.78	0.34 ± 0.04	209.21 ± 19.69	-0.67 ± 0.09	-2.30 ± 0.11	1.01E-05 ± 2.69E-07	1.01
21.78 -22.08	0.31 ± 0.03	256.32 ± 22.90	-0.83 ± 0.07	-2.57 ± 0.19	1.18E-05 ± 3.19E-07	0.95
22.08 -22.42	0.46 ± 0.09	155.23 ± 15.90	-0.57 ± 0.11	-2.19 ± 0.08	9.50E-06 ± 2.61E-07	0.85

Table 2—Continued

Timebin (s)	Amplitude	E_p (keV)	α	β	Flux (erg/s.cm ²)	χ_r^2
22.42 -22.86	0.23 ± 0.03	228.36 ± 25.41	-0.86 ± 0.08	-2.27 ± 0.12	8.15E-06 ± 2.23E-07	0.93
22.86 -23.20	0.30 ± 0.03	261.02 ± 24.25	-0.74 ± 0.07	-2.38 ± 0.13	1.13E-05 ± 2.94E-07	1.12
23.20 -23.54	0.28 ± 0.03	287.91 ± 29.25	-0.78 ± 0.07	-2.28 ± 0.11	1.20E-05 ± 3.07E-07	1.12
23.54 -23.75	0.38 ± 0.03	404.20 ± 36.93	-0.72 ± 0.06	-2.28 ± 0.09	2.27E-05 ± 5.57E-07	0.92
23.75 -23.93	0.40 ± 0.02	477.02 ± 44.48	-0.76 ± 0.05	-2.30 ± 0.10	2.76E-05 ± 6.92E-07	0.91
23.93 -24.11	0.45 ± 0.04	350.43 ± 33.67	-0.74 ± 0.06	-2.25 ± 0.09	2.37E-05 ± 5.80E-07	0.96
24.11 -24.27	0.50 ± 0.04	361.58 ± 32.41	-0.76 ± 0.06	-2.38 ± 0.11	2.69E-05 ± 6.73E-07	1.07
24.27 -24.46	0.57 ± 0.06	247.52 ± 20.56	-0.61 ± 0.08	-2.38 ± 0.11	1.99E-05 ± 4.95E-07	1.00
24.46 -24.71	0.33 ± 0.03	268.01 ± 27.83	-0.95 ± 0.07	-2.46 ± 0.16	1.37E-05 ± 3.73E-07	1.00
24.71 -25.01	0.40 ± 0.06	196.75 ± 20.04	-0.67 ± 0.09	-2.21 ± 0.09	1.14E-05 ± 3.02E-07	0.94
25.01 -25.46	0.36 ± 0.08	131.72 ± 15.81	-0.67 ± 0.13	-2.16 ± 0.08	6.79E-06 ± 1.98E-07	0.95
25.46 -26.20	0.22 ± 0.05	128.80 ± 15.31	-0.77 ± 0.12	-2.27 ± 0.11	4.15E-06 ± 1.35E-07	0.86
26.20 -27.66	0.14 ± 0.05	95.87 ± 14.13	-0.79 ± 0.16	-2.18 ± 0.10	2.15E-06 ± 8.05E-08	0.96
GRB 140430B (bn140430716)						
-0.11 -1.50	0.03 ± 0.01	182.19 ± 66.98	-0.63 ± 0.24	-1.62 ± 0.07	1.24E-06 ± 5.62E-08	0.89
1.50 -3.11	0.16 ± 0.07	100.15 ± 15.31	-0.16 ± 0.23	-1.85 ± 0.06	1.62E-06 ± 6.40E-08	0.98
3.11 -9.79	0.09 ± 0.09	73.34 ± 17.32	0.03 ± 0.47	-1.79 ± 0.08	4.65E-07 ± 2.73E-08	1.15
GRB 141004B (bn141004150)						
-1.22 -3.11	0.21 ± 0.17	83.92 ± 12.19	0.63 ± 0.44	-2.00 ± 0.15	5.15E-07 ± 4.75E-08	1.13
3.11 -4.32	0.64 ± 0.32	73.68 ± 5.08	0.50 ± 0.26	-2.95 ± 0.34	8.01E-07 ± 6.39E-08	0.93
4.32 -5.52	0.48 ± 0.26	61.68 ± 4.72	0.14 ± 0.26	-2.93 ± 0.33	6.96E-07 ± 5.58E-08	1.03
5.52 -7.47	0.27 ± 0.36	38.99 ± 7.28	-0.28 ± 0.53	-2.01 ± 0.00	6.39E-07 ± 2.56E-08	1.16
7.47 -13.95	0.80 ± 1.85	28.14 ± 3.41	0.52 ± 0.92	-3.05 ± 0.52	7.86E-08 ± 1.13E-08	1.11
GRB 141028A (bn141028455)						
-1.22 -4.06	0.00 ± 0.00	1612.93 ± 1173.84	-1.09 ± 0.14	-4.87 ± 0.00	2.77E-07 ± 2.49E-08	0.93
4.06 -9.33	0.01 ± 0.00	724.81 ± 129.76	-0.83 ± 0.06	-2.02 ± 0.16	1.22E-06 ± 4.49E-08	1.12
9.33 -10.89	0.03 ± 0.00	575.32 ± 90.58	-0.75 ± 0.07	-1.92 ± 0.10	2.81E-06 ± 8.91E-08	1.04
10.89 -12.10	0.05 ± 0.01	375.94 ± 59.19	-0.71 ± 0.08	-1.83 ± 0.07	3.18E-06 ± 8.33E-08	1.25
12.10 -13.02	0.05 ± 0.00	505.61 ± 77.30	-0.79 ± 0.06	-1.97 ± 0.11	3.92E-06 ± 1.20E-07	1.09
13.02 -13.88	0.06 ± 0.01	418.38 ± 54.06	-0.75 ± 0.07	-2.15 ± 0.15	3.94E-06 ± 1.18E-07	0.99
13.88 -15.06	0.06 ± 0.01	219.42 ± 48.72	-0.81 ± 0.12	-1.72 ± 0.05	2.51E-06 ± 6.28E-08	1.15
15.06 -16.09	0.07 ± 0.01	214.65 ± 41.12	-0.72 ± 0.12	-1.74 ± 0.05	2.94E-06 ± 7.04E-08	1.31
16.09 -18.08	0.06 ± 0.02	125.93 ± 26.78	-0.69 ± 0.18	-1.77 ± 0.05	1.51E-06 ± 4.31E-08	0.99
18.08 -21.36	0.05 ± 0.02	107.00 ± 28.61	-0.76 ± 0.22	-1.75 ± 0.05	1.02E-06 ± 3.09E-08	1.11
21.36 -28.78	0.04 ± 0.03	82.80 ± 23.06	-0.54 ± 0.33	-1.76 ± 0.06	5.24E-07 ± 1.92E-08	1.14
28.78 -41.22	0.01 ± 0.02	98.35 ± 51.51	-0.48 ± 0.64	-1.80 ± 0.15	1.68E-07 ± 1.46E-08	1.06
GRB 141222B (bn141222691)						
-0.45 -2.89	0.03 ± 0.00	238.24 ± 56.70	-1.03 ± 0.09	-1.76 ± 0.06	1.34E-06 ± 3.41E-08	0.90
2.89 -4.00	0.08 ± 0.01	218.98 ± 30.21	-0.74 ± 0.09	-1.86 ± 0.06	3.11E-06 ± 7.20E-08	1.07
4.00 -5.17	0.10 ± 0.02	178.22 ± 20.11	-0.58 ± 0.10	-2.01 ± 0.09	2.60E-06 ± 7.13E-08	1.13
5.17 -9.43	0.11 ± 0.05	79.41 ± 9.75	-0.28 ± 0.22	-2.05 ± 0.08	7.36E-07 ± 2.95E-08	1.12
9.43 -17.04	0.04 ± 0.01	80.94 ± 9.24	-0.86 ± 0.14	-2.35 ± 0.15	4.53E-07 ± 2.24E-08	1.02
17.04 -19.55	0.06 ± 0.01	107.51 ± 10.06	-0.91 ± 0.10	-2.60 ± 0.27	9.34E-07 ± 4.52E-08	1.06
19.55 -21.62	0.26 ± 0.16	48.81 ± 5.80	-0.43 ± 0.27	-2.13 ± 0.06	1.01E-06 ± 3.72E-08	0.96
21.62 -28.64	0.10 ± 0.07	35.19 ± 3.50	-0.72 ± 0.28	-2.41 ± 0.09	3.39E-07 ± 1.56E-08	0.94
28.64 -39.23	0.06 ± 0.06	32.33 ± 5.74	-0.84 ± 0.41	-2.19 ± 0.07	2.69E-07 ± 1.37E-08	1.05
GRB 141229A (bn141229492)						
-0.51 -0.68	0.04 ± 0.01	402.86 ± 59.13	0.28 ± 0.25	-2.07 ± 0.13	2.64E-06 ± 1.13E-07	1.12
0.68 -1.92	0.14 ± 0.11	123.79 ± 30.21	0.29 ± 0.51	-1.78 ± 0.08	1.33E-06 ± 6.81E-08	1.08
1.92 -7.06	0.03 ± 0.03	87.93 ± 38.38	-0.46 ± 0.59	-1.91 ± 0.16	3.13E-07 ± 2.98E-08	0.98
7.06 -17.22	0.01 ± 0.01	44.96 ± 21.57	-0.74 ± 0.00	-1.86 ± 0.00	8.75E-08 ± 1.32E-08	1.07
GRB 150118B (bn150118409)						
43.97 -45.84	0.04 ± 0.00	602.45 ± 59.75	-0.65 ± 0.06	-2.00 ± 0.00	3.86E-06 ± 9.37E-08	1.01
45.84 -46.28	0.12 ± 0.00	952.44 ± 68.23	-0.65 ± 0.04	-3.44 ± 0.63	1.45E-05 ± 3.03E-07	0.76
46.28 -46.67	0.13 ± 0.00	927.71 ± 77.06	-0.70 ± 0.04	-2.76 ± 0.25	1.52E-05 ± 3.30E-07	1.00
46.67 -47.11	0.13 ± 0.01	591.38 ± 55.78	-0.74 ± 0.05	-2.45 ± 0.19	1.05E-05 ± 3.02E-07	0.91
47.11 -48.51	0.05 ± 0.00	455.80 ± 73.80	-1.01 ± 0.06	-2.15 ± 0.17	3.08E-06 ± 1.05E-07	1.04
48.51 -51.46	0.02 ± 0.01	118.37 ± 39.52	-0.97 ± 0.25	-1.99 ± 0.16	5.99E-07 ± 4.43E-08	1.02
GRB 150220A (bn150220598)						
-2.37 -3.55	0.03 ± 0.01	115.57 ± 25.94	-0.70 ± 0.20	-1.91 ± 0.14	5.39E-07 ± 3.82E-08	1.00
3.55 -6.82	0.03 ± 0.01	159.13 ± 48.57	-0.87 ± 0.16	-1.78 ± 0.14	8.91E-07 ± 5.61E-08	0.99
6.82 -9.35	0.03 ± 0.01	182.18 ± 33.72	-0.89 ± 0.11	-2.38 ± 0.60	9.13E-07 ± 8.53E-08	1.08
9.35 -12.76	0.03 ± 0.01	157.98 ± 38.31	-0.85 ± 0.14	-1.89 ± 0.17	8.59E-07 ± 5.75E-08	1.05
12.76 -15.26	0.00 ± 0.00	199.21 ± 0.00	-1.47 ± 0.17	-1.81 ± 0.46	2.23E-07 ± 5.34E-08	1.08
15.26 -17.75	0.03 ± 0.01	234.90 ± 49.65	-0.71 ± 0.11	-1.98 ± 0.30	1.27E-06 ± 8.09E-08	0.95
17.75 -18.53	0.10 ± 0.02	200.59 ± 30.16	-0.53 ± 0.11	-2.11 ± 0.26	2.80E-06 ± 1.67E-07	0.86
18.53 -19.35	0.10 ± 0.02	183.19 ± 37.05	-0.51 ± 0.15	-1.75 ± 0.12	2.97E-06 ± 1.43E-07	0.93

Table 2—Continued

Timebin (s)	Amplitude	E_p (keV)	α	β	Flux (erg/s.cm ²)	χ_r^2
19.35 -24.26	0.03 ± 0.02	88.19 ± 21.40	-0.78 ± 0.24	-1.98 ± 0.14	4.76E-07 ± 3.57E-08	0.90
GRB 150306A (bn150306993)						
-1.66 -3.23	0.06 ± 0.01	271.91 ± 18.90	-0.12 ± 0.13	-2.58 ± 0.19	1.92E-06 ± 5.01E-08	1.06
3.23 -4.40	0.19 ± 0.03	221.42 ± 12.13	0.04 ± 0.13	-3.07 ± 0.30	4.04E-06 ± 1.22E-07	1.11
4.40 -5.94	0.19 ± 0.04	178.84 ± 13.07	0.02 ± 0.16	-2.68 ± 0.19	2.93E-06 ± 9.36E-08	0.94
5.94 -8.25	0.15 ± 0.04	146.08 ± 12.27	-0.21 ± 0.17	-2.67 ± 0.20	1.91E-06 ± 6.88E-08	1.03
8.25 -12.28	0.09 ± 0.03	131.23 ± 13.50	-0.43 ± 0.18	-2.50 ± 0.17	1.25E-06 ± 4.84E-08	0.86
12.28 -30.59	0.02 ± 0.01	59.70 ± 8.08	-1.18 ± 0.27	-2.88 ± 0.50	2.46E-07 ± 1.98E-08	1.17
GRB 150314A (bn150314205)						
0.00 -0.92	0.13 ± 0.01	483.06 ± 33.27	-0.32 ± 0.06	-2.28 ± 0.09	1.04E-05 ± 2.42E-07	1.10
0.92 -1.38	0.31 ± 0.02	346.41 ± 19.73	-0.19 ± 0.07	-2.55 ± 0.14	1.56E-05 ± 3.61E-07	0.93
1.38 -1.71	0.36 ± 0.02	391.92 ± 24.42	-0.35 ± 0.06	-2.49 ± 0.12	2.11E-05 ± 4.97E-07	1.00
1.71 -2.09	0.35 ± 0.03	335.06 ± 21.25	-0.32 ± 0.07	-2.46 ± 0.12	1.67E-05 ± 4.01E-07	1.08
2.09 -2.44	0.37 ± 0.03	321.67 ± 23.55	-0.44 ± 0.07	-2.28 ± 0.09	1.73E-05 ± 4.19E-07	1.05
2.44 -2.76	0.37 ± 0.03	347.37 ± 23.02	-0.48 ± 0.06	-2.55 ± 0.16	1.87E-05 ± 4.63E-07	1.06
2.76 -3.12	0.46 ± 0.05	235.91 ± 17.33	-0.36 ± 0.08	-2.29 ± 0.09	1.41E-05 ± 3.60E-07	0.99
3.12 -3.59	0.33 ± 0.03	255.06 ± 16.47	-0.45 ± 0.07	-2.70 ± 0.22	1.07E-05 ± 2.96E-07	0.96
3.59 -4.25	0.25 ± 0.03	195.18 ± 19.69	-0.59 ± 0.09	-2.20 ± 0.10	6.88E-06 ± 2.01E-07	1.06
4.25 -4.92	0.20 ± 0.02	263.82 ± 24.51	-0.68 ± 0.07	-2.26 ± 0.12	7.80E-06 ± 2.15E-07	1.07
4.92 -5.64	0.17 ± 0.01	297.88 ± 26.32	-0.73 ± 0.06	-2.43 ± 0.18	7.45E-06 ± 2.12E-07	0.93
5.64 -6.79	0.13 ± 0.01	246.74 ± 25.71	-0.69 ± 0.07	-2.18 ± 0.11	4.79E-06 ± 1.40E-07	0.88
6.79 -8.21	0.07 ± 0.01	450.79 ± 58.71	-0.95 ± 0.05	-2.21 ± 0.14	4.70E-06 ± 1.47E-07	0.98
8.21 -10.27	0.06 ± 0.00	518.49 ± 62.04	-0.90 ± 0.05	-2.27 ± 0.16	4.01E-06 ± 1.24E-07	1.15
10.27 -15.04	0.03 ± 0.00	333.61 ± 58.22	-1.08 ± 0.06	-2.33 ± 0.33	1.41E-06 ± 5.95E-08	1.07
GRB 150403A (bn150403913)						
-0.33 -1.70	0.01 ± 0.00	383.99 ± 170.79	-0.66 ± 0.22	-1.70 ± 0.14	7.15E-07 ± 5.63E-08	1.07
1.70 -3.74	0.02 ± 0.00	946.66 ± 192.02	-0.79 ± 0.07	-2.11 ± 0.19	1.96E-06 ± 8.10E-08	0.88
3.74 -5.77	0.03 ± 0.00	669.64 ± 92.49	-0.77 ± 0.05	-1.94 ± 0.09	2.97E-06 ± 9.20E-08	1.03
5.77 -7.76	0.06 ± 0.00	335.47 ± 32.82	-0.66 ± 0.06	-2.03 ± 0.09	3.04E-06 ± 7.57E-08	1.03
9.47 -10.47	0.07 ± 0.01	419.83 ± 68.54	-0.74 ± 0.08	-1.89 ± 0.07	4.33E-06 ± 1.39E-07	1.02
10.47 -11.04	0.09 ± 0.01	687.53 ± 93.78	-0.79 ± 0.06	-2.10 ± 0.11	8.04E-06 ± 2.55E-07	1.03
11.04 -11.48	0.10 ± 0.00	1138.63 ± 146.31	-0.86 ± 0.04	-2.36 ± 0.17	1.13E-05 ± 3.02E-07	0.95
11.48 -11.94	0.11 ± 0.01	575.44 ± 83.32	-0.78 ± 0.06	-2.02 ± 0.09	8.77E-06 ± 2.83E-07	0.94
11.94 -12.44	0.15 ± 0.02	346.98 ± 38.76	-0.48 ± 0.09	-2.05 ± 0.08	8.08E-06 ± 2.38E-07	0.89
12.44 -12.92	0.16 ± 0.02	314.38 ± 36.57	-0.48 ± 0.09	-2.01 ± 0.08	7.78E-06 ± 2.30E-07	0.94
12.92 -13.60	0.10 ± 0.01	341.31 ± 41.01	-0.80 ± 0.07	-2.45 ± 0.26	4.77E-06 ± 1.71E-07	0.75
13.60 -14.60	0.08 ± 0.01	266.35 ± 38.84	-0.79 ± 0.09	-2.13 ± 0.14	3.26E-06 ± 1.16E-07	0.95
14.60 -16.14	0.05 ± 0.01	224.11 ± 53.36	-0.90 ± 0.12	-1.85 ± 0.08	2.20E-06 ± 8.03E-08	1.00
16.14 -20.03	0.03 ± 0.01	173.21 ± 53.11	-0.95 ± 0.15	-1.79 ± 0.07	1.05E-06 ± 4.23E-08	1.02
GRB 150514A (bn150514774)						
-0.96 -0.96	0.07 ± 0.03	109.15 ± 21.97	-0.72 ± 0.20	-2.23 ± 0.31	1.06E-06 ± 1.15E-07	0.85
0.96 -1.62	0.35 ± 0.21	55.36 ± 6.97	-0.57 ± 0.28	-2.58 ± 0.25	1.54E-06 ± 1.27E-07	0.88
1.62 -2.71	0.27 ± 0.28	37.06 ± 6.15	-0.71 ± 0.42	-2.37 ± 0.16	9.97E-07 ± 7.98E-08	1.05
2.71 -8.00	0.01 ± 0.04	23.33 ± 19.55	-1.51 ± 1.15	-2.09 ± 0.13	2.65E-07 ± 3.14E-08	0.94
GRB 1507212A (bn1507212421)						
-1.79 -3.76	0.09 ± 0.02	145.10 ± 10.50	0.14 ± 0.13	-2.14 ± 0.14	9.91E-07 ± 4.96E-08	0.90
3.76 -5.04	1.04 ± 0.28	81.53 ± 3.25	0.59 ± 0.15	-2.89 ± 0.18	1.51E-06 ± 6.52E-08	1.11
5.04 -6.07	1.30 ± 0.36	74.63 ± 2.79	0.52 ± 0.15	-3.04 ± 0.20	1.61E-06 ± 6.56E-08	1.00
6.07 -7.23	1.87 ± 0.65	62.98 ± 2.56	0.59 ± 0.17	-2.82 ± 0.14	1.45E-06 ± 5.61E-08	1.10
7.23 -8.48	1.85 ± 0.61	56.63 ± 1.80	0.52 ± 0.16	-3.48 ± 0.27	1.03E-06 ± 3.74E-08	1.11
8.48 -10.35	3.66 ± 1.63	45.34 ± 1.45	0.77 ± 0.20	-3.27 ± 0.18	7.41E-07 ± 2.55E-08	1.21
10.35 -13.19	1.11 ± 0.41	42.30 ± 1.20	0.24 ± 0.17	-3.84 ± 0.40	4.83E-07 ± 1.66E-08	1.01
13.19 -15.58	2.39 ± 1.18	38.15 ± 1.24	0.49 ± 0.22	-3.44 ± 0.23	5.06E-07 ± 1.82E-08	1.08
15.58 -18.24	0.49 ± 0.19	34.26 ± 1.06	-0.31 ± 0.17	-3.85 ± 0.47	4.41E-07 ± 1.58E-08	1.08
18.24 -23.32	0.03 ± 0.09	20.33 ± 10.96	-1.39 ± 0.93	-2.00 ± 0.00	5.17E-07 ± 1.06E-08	1.88

Table 3. Results of the spectral lag analysis for 92 pulses.

GRB (Timebin/s)	Energy band ^a	$\hat{\tau}$ (s)	GRB(Timebin/s)	Energy band	$\hat{\tau}$ (s)
bn080906212 (0.0-6.0)	①	0.20 ± 0.08	bn0810091401 (0.0-10.0)	①	0.08 ± 0.02
	②	0.35 ± 0.07		②	0.29 ± 0.03
	③	0.44 ± 0.07		③	0.53 ± 0.04
	④	0.68 ± 0.14	bn081125496 (0.0-15.0)	①	0.36 ± 0.17
bn0810091402 (36.0-52.0)	①	0.47 ± 0.07		②	0.99 ± 0.16
	②	0.83 ± 0.13		③	1.70 ± 0.17
	③	0.58 ± 0.53		④	2.33 ± 0.28
bn081222204 (0.0-20.0)	①	0.04 ± 0.17	bn081224887 (0.0-20.0)	①	0.36 ± 0.23
	②	0.34 ± 0.16		②	1.13 ± 0.21
	③	0.79 ± 0.17		③	1.79 ± 0.21
	④	0.79 ± 0.60		④	2.43 ± 0.25
bn0901310901 (2.6-5.0)	①	0.04 ± 0.03		⑤	2.48 ± 0.22
	②	0.16 ± 0.04	bn0901310903 (22.5-26.0)	①	0.09 ± 0.03
	③	0.24 ± 0.07		②	0.13 ± 0.03
bn0901310902 (6.7-10.0)	①	0.07 ± 0.02		③	0.21 ± 0.04
	②	0.12 ± 0.02	bn0905243461 (4.0-20.0)	①	0.12 ± 0.27
	③	0.11 ± 0.06		②	0.44 ± 0.26
bn090520876 (-3.0-20.0)	⑦	0.58 ± 0.26		③	0.52 ± 0.26
	⑧	0.94 ± 0.29	bn090530760 (0.0-50.0)	⑦	2.89 ± 0.65
	⑨	1.198 ± 0.36		⑧	5.904 ± 0.78
bn0905243462 (40.0-60.0)	⑦	0.14 ± 0.26		⑨	7.55 ± 1.34
	⑧	0.27 ± 0.31	bn0906183531 (0.0-50.0)	①	2.35 ± 0.77
	⑨	-0.18 ± 0.43		②	4.01 ± 0.73
	⑩	0.87 ± 0.49		③	7.23 ± 0.81
bn0906183532 (105.0-150.0)	①	0.79 ± 0.20		④	8.10 ± 0.93
	②	1.67 ± 0.23	bn090620400 (0.0-15.0)	①	1.02 ± 0.22
	③	3.13 ± 0.34		②	1.21 ± 0.20
bn090626189 (0.0-12.0)	①	0.37 ± 0.08		③	1.80 ± 0.20
	②	0.86 ± 0.069		④	1.69 ± 0.22
	③	1.35 ± 0.07	bn090719063 (4.2-12.0)	①	0.19 ± 0.21
	④	1.62 ± 0.20		②	0.50 ± 0.19
	⑤	1.68 ± 0.09		③	0.72 ± 0.18
bn090804940 (0.0-10.0)	⑥	-0.02 ± 0.16		④	1.06 ± 0.25
	⑦	0.11 ± 0.141		⑤	1.05 ± 0.18
	⑧	0.24 ± 0.15	bn090809978 (0.0-15.0)	①	0.62 ± 0.12
	⑨	0.31 ± 0.14		②	1.20 ± 0.11
	⑩	0.30 ± 0.13		③	1.78 ± 0.11
bn090922539 (-1.0-15.0)	①	0.05 ± 0.18		④	2.65 ± 0.31
	②	0.28 ± 0.19		⑤	2.30 ± 0.16
	③	0.37 ± 0.19	bn091208410 (7.0-13.0)	①	0.06 ± 0.05
bn091020900 (0.0-20.0)	①	0.23 ± 0.45		②	0.10 ± 0.05
	②	0.58 ± 0.46		③	0.13 ± 0.05
	③	0.75 ± 0.43	bn100528075 (0.0-25.0)	①	0.66 ± 0.24
bn100122616 (18.0-30.0)	④	-0.03 ± 0.05		②	0.88 ± 0.23
	⑤	-0.17 ± 0.05		③	1.26 ± 0.21
	⑥	-0.24 ± 0.05		④	1.62 ± 0.23
	⑦	-0.19 ± 0.07	bn100707032 (0.0-20.0)	⑤	1.21 ± 0.12
bn100612726 (0.0-10.0)	①	0.49 ± 0.07		⑥	2.25 ± 0.11
	②	0.86 ± 0.08		⑦	2.92 ± 0.10
	③	1.39 ± 0.09		⑧	2.84 ± 1.67
bn101126198 (6.5-25.0)	①	0.20 ± 0.15	bn101208498 (-0.5-3.0)	①	0.05 ± 0.03
	②	0.58 ± 0.15		②	0.05 ± 0.023
	③	0.63 ± 0.17		③	0.12 ± 0.03
	④	1.18 ± 1.16	bn101216721 (-0.5-3.0)	①	0.09 ± 0.05
	⑤	0.91 ± 0.38		②	0.16 ± 0.04
bn110318552 (0.0-20.0)	①	0.46 ± 0.20		③	0.27 ± 0.04
	②	1.25 ± 0.22	bn110521478 (0.0-10.0)	①	0.24 ± 0.11
	③	2.45 ± 0.28		②	0.64 ± 0.10
bn110505203 (0.0-10.0)	①	0.08 ± 0.09		③	0.94 ± 0.11
	②	0.12 ± 0.08		④	1.14 ± 0.19
	③	0.23 ± 0.14	bn110622158 (12.5-35.0)	①	-0.13 ± 0.23
	④	0.24 ± 0.18		②	-0.38 ± 0.23
bn110605183 (-0.5-25.0)	②	0.85 ± 0.49		③	-0.01 ± 0.24
	③	1.73 ± 0.41	bn110709463 (15.0-21.0)	①	-0.03 ± 0.08
	④	2.48 ± 0.41		②	0.15 ± 0.07
bn1106258811 (10.0-13.0)	①	0.11 ± 0.07		③	0.17 ± 0.08
	②	0.25 ± 0.08	bn110721200	①	0.40 ± 0.11

Table 3—Continued

GRB (Timebin/s)	Energy band ^a	$\hat{\tau}$ (s)	GRB(Timebin/s)	Energy band	$\hat{\tau}$ (s)
	③	0.41 ± 0.07	(0.0-20.0)	②	0.82 ± 0.10
	④	0.54 ± 0.09		③	1.24 ± 0.10
	④	0.52 ± 0.07		④	1.90 ± 0.15
bn1106258812	①	0.13 ± 0.03		④	1.75 ± 0.10
(22.0-26.5)	②	0.22 ± 0.03		⑥	2.25 ± 0.12
	③	0.34 ± 0.03	bn1109030091	⑦	0.08 ± 0.04
	④	0.49 ± 0.07	(-1.0-2.5)	⑧	0.19 ± 0.04
	④	0.44 ± 0.04		⑨	0.20 ± 0.05
bn1109030092	⑦	0.02 ± 0.05		③	0.37 ± 0.12
(3.0-10.0)	①	0.28 ± 0.05	bn1109030093	①	0.60 ± 0.13
	⑧	0.52 ± 0.08	(20.0-30.0)	②	0.87 ± 0.12
	⑨	0.55 ± 0.12		③	1.44 ± 0.13
bn110920546	②	1.22 ± 1.27	bn111009282	①	0.37 ± 0.12
(0.0-100.0)	③	5.12 ± 1.21	(0.0-20.0)	②	0.87 ± 0.13
	④	9.54 ± 1.33		③	1.33 ± 0.15
	④	9.69 ± 1.22		⑤	1.81 ± 0.27
bn111017657	①	0.21 ± 0.18	bn120102095	①	0.08 ± 0.12
(0.0-15.0)	②	0.48 ± 0.16	(3.5-12.0)	②	0.15 ± 0.11
	③	0.86 ± 0.15		③	0.15 ± 0.12
	④	1.61 ± 0.28		④	0.34 ± 0.15
	④	1.40 ± 0.17	bn120217808	①	0.27 ± 0.14
bn120206949	①	0.20 ± 0.08	(-0.5-5.0)	②	0.48 ± 0.14
(4.0-8.0)	⑦	0.26 ± 0.09		③	0.68 ± 0.12
	⑧	0.413 ± 0.08	bn120222021	①	0.017 ± 0.04
	③	0.36 ± 0.08	(0.0-2.0)	②	0.00 ± 0.03
	④	0.42 ± 0.09		③	0.06 ± 0.05
bn120304061	①	0.28 ± 0.07	bn120308588	①	0.08 ± 0.10
(0.0-10.0)	②	0.40 ± 0.10	(-0.5-6.0)	②	-0.11 ± 0.14
	③	0.85 ± 0.15		③	-0.01 ± 0.18
bn120326056	①	0.40 ± 0.19	bn1203282681	①	0.21 ± 0.12
(0.0-15.0)	②	0.95 ± 0.22	(3.5-15.0)	②	0.56 ± 0.11
	③	1.02 ± 0.41		③	1.11 ± 0.11
bn1203282682	①	0.34 ± 0.14		④	1.65 ± 0.21
(17.0-25.0)	②	0.46 ± 0.14		④	1.60 ± 0.13
	③	0.83 ± 0.13	bn120402669	①	0.05 ± 0.08
	④	1.18 ± 0.18	(-2.0-6.0)	②	-0.01 ± 0.10
bn120412920	①	0.35 ± 0.13		③	-0.31 ± 0.16
(0.0-10.0)	②	0.69 ± 0.13	bn120427054	①	0.36 ± 0.18
	③	1.00 ± 0.30	(0.0-10.0)	②	0.89 ± 0.17
bn120426090	①	0.18 ± 0.03		③	1.21 ± 0.16
(0.0-5.0)	②	0.36 ± 0.03	bn120727681	①	-0.17 ± 0.16
	③	0.51 ± 0.03	(0.0-15.0)	②	0.17 ± 0.16
	④	0.82 ± 0.09		③	0.62 ± 0.19
bn120625119	①	0.15 ± 0.13	bn120919309	①	0.35 ± 0.16
(2.0-10.0)	②	0.34 ± 0.12	(0.0-10.0)	②	0.57 ± 0.13
	③	0.53 ± 0.12		③	0.87 ± 0.14
	④	0.79 ± 0.15		④	1.25 ± 0.17
bn120921877	①	0.28 ± 0.18	bn121223300	①	1.41 ± 0.41
(0.0-10.0)	②	0.57 ± 0.15	(0.0-15.0)	②	3.24 ± 0.35
	③	0.86 ± 0.15		③	4.29 ± 0.37
bn130206482	①	0.03 ± 0.22	bn130518580	①	0.11 ± 0.10
(0.0-15.0)	①	0.47 ± 0.18	(20.0-40.0)	②	0.37 ± 0.08
	②	0.60 ± 0.18		③	0.65 ± 0.08
	③	0.88 ± 0.19		④	1.10 ± 0.15
bn130325203	①	0.41 ± 0.13		④	1.09 ± 0.09
(0.0-10.0)	②	0.73 ± 0.12		⑥	1.64 ± 0.23
	③	0.98 ± 0.12	bn130609902	①	0.43 ± 0.15
	④	1.49 ± 0.19	(4.0-14.0)	②	0.52 ± 0.24
bn130606497	①	0.05 ± 0.12		③	0.85 ± 0.25
(49.0-70.0)	②	0.24 ± 0.11		④	0.97 ± 0.15
	③	0.39 ± 0.14		⑥	1.13 ± 0.32
	④	0.69 ± 0.16	bn130701060	①	0.24 ± 0.36
bn130612456	①	-0.02 ± 0.07	(0.0-10.0)	②	0.55 ± 0.32
(0.0-8.0)	②	-0.09 ± 0.064		③	0.85 ± 0.31
	③	0.10 ± 0.07		④	1.10 ± 0.32
bn130815660	①	0.22 ± 0.07	bn130828808	①	0.60 ± 0.12
(30.0-40.0)	②	0.60 ± 0.07	(-1.0-10.0)	②	1.13 ± 0.10

Table 3—Continued

GRB (Timebin/s)	Energy band ^a	$\hat{\tau}$ (s)	GRB(Timebin/s)	Energy band	$\hat{\tau}$ (s)
	⑦	0.76 ± 0.09		③	1.60 ± 0.10
	⑧	0.88 ± 0.27	bn131214705	①	-1.27 ± 0.10
	⑨	0.92 ± 0.11	(55.0-85.0)	②	-2.41 ± 0.12
bn131216081	④	0.75 ± 0.26		③	-2.44 ± 0.15
(0.0-10.0)	②	0.01 ± 0.22	bn140102887	①	0.03 ± 0.06
	③	0.30 ± 0.17	(0.0-1.7)	②	0.07 ± 0.02
	④	0.51 ± 0.16		③	0.08 ± 0.02
bn140209313	①	0.07 ± 0.01	bn140213807	①	0.14 ± 0.06
(1.2-3.0)	②	0.13 ± 0.01	(5.0-15.0)	②	0.25 ± 0.06
	③	0.19 ± 0.02		③	0.32 ± 0.09
	④	0.25 ± 0.03	bn1403292951	①	0.04 ± 0.05
bn140311618	①	0.03 ± 0.14	(-0.5-2.0)	②	0.07 ± 0.08
(-0.5-10.0)	②	0.27 ± 0.14		③	0.08 ± 0.17
	③	0.53 ± 0.19		④	0.13 ± 0.07
bn1403292952	①	0.08 ± 0.03	bn140430716	①	-0.04 ± 0.18
(23.3-30.0)	②	0.17 ± 0.03	(0.0-12.0)	②	0.14 ± 0.19
	③	0.27 ± 0.03		③	0.45 ± 0.17
	④	0.39 ± 0.05	bn141004150	①	1.03 ± 0.16
	④	0.38 ± 0.03	(0.0-15.0)	②	1.94 ± 0.18
	⑥	0.40 ± 0.07		③	3.13 ± 0.38
bn141028455	①	1.10 ± 0.27	bn141222691	①	-0.52 ± 0.24
(0.0-40.0)	②	1.51 ± 0.24	(0.0-12.0)	②	-0.30 ± 0.22
	③	2.47 ± 0.26		③	-0.10 ± 0.24
	④	3.42 ± 0.51		⑤	0.46 ± 0.24
	④	3.06 ± 0.28	bn141229492	②	0.25 ± 0.22
	⑥	3.44 ± 0.55	(0.0-12.0)	③	0.66 ± 0.21
bn150118409	①	0.11 ± 0.07		④	0.82 ± 0.19
(44.0-51.0)	②	0.30 ± 0.06	bn150220598	①	0.01 ± 0.15
	③	0.40 ± 0.06	(15.0-23.0)	②	0.18 ± 0.12
	④	0.50 ± 0.09		③	0.36 ± 0.11
	④	0.50 ± 0.06		⑤	0.51 ± 0.14
	⑥	0.41 ± 0.09	bn150306993	①	2.19 ± 0.71
bn150314205	①	0.54 ± 0.08	(-1.0-30.0)	②	4.17 ± 0.81
(0.0-15.0)	②	0.89 ± 0.08		③	5.69 ± 0.88
	③	1.23 ± 0.08	bn150403913	①	0.14 ± 0.12
	④	1.65 ± 0.16	(10.0-20.0)	②	0.37 ± 0.11
	④	1.58 ± 0.08		③	0.46 ± 0.11
	⑥	2.24 ± 0.50		④	0.95 ± 0.16
bn150514774	①	0.29 ± 0.07		④	0.89 ± 0.11
(0.0-10.0)	②	0.60 ± 0.07		⑥	1.17 ± 0.17
	③	0.73 ± 0.11			
bn150721242	⑦	0.38 ± 0.13			
(0.0-10.0)	⑧	1.10 ± 0.17			
	⑨	1.90 ± 0.25			

^a ①: 25-50 keV (NaI); ②: 50-100 keV (NaI); ③: 100-300 keV (NaI); ④: 300-1000 keV (NaI);
 ⑤: 250-1000 keV (BGO); ⑥: 1000-5000 keV (BGO); ⑦: 25-40 keV (NaI); ⑧: 40-60 keV (NaI);
 ⑨: 60-100 keV (NaI); ⑩: 16-25 keV

Table 4. Values of $\hat{\tau}_{31}$, W , $k_{\hat{\tau}}$ and k_E for 92 pulses.

GRB	Evolution ^a	$\hat{\tau}_{31}$	W	$k_{\hat{\tau}}$	k_E
bn080906212	H	0.24 ± 0.05	1.86	0.37 ± 0.11	-0.38 ± 0.14
bn0810091402	H	0.40 ± 13.99	5.97	1.36 ± 0.60	-0.69 ± 0.09
bn081125496	H	1.37 ± 0.10	5.25	1.74 ± 0.25	-0.71 ± 0.07
bn081222204	H	0.76 ± 0.16	6.84	0.98 ± 0.31	-0.58 ± 0.26
bn081224887	H	1.47 ± 0.11	5.67	1.68 ± 0.22	-0.68 ± 0.05
bn0901310901	H	0.18 ± 0.05	0.84	0.31 ± 0.10	-0.83 ± 0.18
bn0901310903	H	0.12 ± 0.03	0.81	0.18 ± 0.07	-0.28 ± 0.09
bn0905243461	H	0.47 ± 0.18	4.91	0.54 ± 0.54	-0.24 ± 0.14
bn0905243462	H	0.54 ± 0.58	5.40	0.74 ± 0.86	-0.57 ± 0.20
bn090530760	H	7.08 ± 0.45	55.63	14.80 ± 3.90	-0.47 ± 0.06
bn0906183531	H	4.60 ± 0.52	28.83	5.67 ± 1.02	-0.72 ± 0.09
bn090626189	H	0.98 ± 0.06	3.71	1.10 ± 0.09	-0.81 ± 0.06
bn090719063	H	0.54 ± 0.07	4.13	0.69 ± 0.19	-0.54 ± 0.03
bn090809978	H	1.19 ± 0.09	5.24	1.49 ± 0.15	-1.10 ± 0.13
bn090922539	H	0.24 ± 0.12	4.77	0.46 ± 0.38	-0.54 ± 0.12
bn091020900	H	0.39 ± 0.36	7.40	0.74 ± 0.89	-1.55 ± 0.58
bn091208410	H	0.09 ± 0.04	0.99	0.10 ± 0.10	-0.23 ± 0.16
bn100612726	H	0.89 ± 0.08	4.50	1.31 ± 0.16	-0.64 ± 0.10
bn100707032	H	1.38 ± 0.08	5.82	2.87 ± 0.27	-0.85 ± 0.03
bn101216721	H	0.18 ± 0.04	0.84	0.26 ± 0.09	-0.81 ± 0.24
bn110318552	H	1.86 ± 0.21	6.95	2.88 ± 0.49	-1.04 ± 0.24
bn110505203	H	0.11 ± 0.12	1.51	0.11 ± 0.12	-0.26 ± 0.21
bn110521478	H	0.74 ± 0.10	2.39	0.81 ± 0.16	-1.18 ± 0.24
bn110605183	H	1.48 ± 0.42	21.95	2.03 ± 0.79	-0.77 ± 0.14
bn1106258811	H	0.21 ± 0.02	1.26	0.35 ± 0.07	-0.68 ± 0.08
bn110709463	H	0.19 ± 0.07	1.69	0.27 ± 0.16	-0.73 ± 0.28
bn110721200	H	0.85 ± 0.07	4.41	1.04 ± 0.08	-1.32 ± 0.08
bn1109030091	H	0.26 ± 0.11	1.12	0.36 ± 0.13	-0.70 ± 0.15
bn1109030093	H	0.83 ± 0.11	2.46	1.22 ± 0.26	-1.22 ± 0.41
bn110920546	H	8.62 ± 1.52	45.29	9.41 ± 1.70	-0.63 ± 0.02
bn111009282	H	0.95 ± 0.14	6.97	1.33 ± 0.22	-0.83 ± 0.15
bn111017657	H	0.66 ± 0.13	4.72	1.06 ± 0.18	-0.77 ± 0.19
bn120102095	H	0.11 ± 0.08	2.37	0.20 ± 0.15	-0.39 ± 0.23
bn120206949	H	0.16 ± 0.05	0.97	0.17 ± 0.09	-0.80 ± 0.31
bn120217808	H	0.51 ± 0.10	1.55	0.60 ± 0.27	-0.70 ± 0.37
bn120304061	H	0.58 ± 0.16	3.22	0.73 ± 0.23	-0.56 ± 0.28
bn120326056	H	0.67 ± 0.36	5.68	1.13 ± 0.61	-0.78 ± 0.21
bn1203282681	H	0.91 ± 0.08	4.76	1.19 ± 0.13	-0.77 ± 0.07
bn120412920	H	0.64 ± 0.22	1.94	1.00 ± 0.43	-0.69 ± 0.17
bn120426090	H	0.33 ± 0.02	1.81	0.49 ± 0.05	-0.83 ± 0.06
bn120427054	H	0.95 ± 0.09	3.33	1.20 ± 0.35	-0.75 ± 0.10
bn120625119	H	0.41 ± 0.08	2.10	0.54 ± 0.15	-0.42 ± 0.15
bn120921877	H	0.51 ± 0.09	1.49	0.83 ± 0.33	-0.63 ± 0.21
bn121223300	H	2.42 ± 0.23	7.87	4.03 ± 0.78	-0.54 ± 0.05
bn130325203	H	0.53 ± 0.10	2.97	0.87 ± 0.18	-0.56 ± 0.24
bn130606497	H	0.33 ± 0.10	5.56	0.52 ± 0.15	-0.67 ± 0.07
bn130609902	H	0.65 ± 0.22	10.66	0.72 ± 0.25	-0.90 ± 0.16
bn130701060	H	0.55 ± 0.21	4.73	0.71 ± 0.37	-0.26 ± 0.28
bn130815660	H	0.25 ± 0.05	3.19	0.74 ± 0.12	-0.37 ± 0.08
bn130828808	H	1.10 ± 0.12	2.15	1.41 ± 0.22	-1.12 ± 0.14
bn131216081	H	0.22 ± 0.19	2.32	0.54 ± 0.29	-0.60 ± 0.22
bn140209313	H	0.11 ± 0.01	0.45	0.15 ± 0.02	-0.69 ± 0.08
bn140311618	H	0.51 ± 0.19	3.67	0.74 ± 0.34	-0.42 ± 0.16
bn1403292951	H	-0.53 ± 1.09	0.35	0.13 ± 0.10	-0.48 ± 0.20
bn140430716	H	0.49 ± 0.15	2.65	0.71 ± 0.35	-0.50 ± 0.25
bn141004150	H	1.89 ± 0.27	6.06	3.03 ± 0.53	-0.89 ± 0.13
bn141028455	H	1.41 ± 0.18	9.26	1.59 ± 0.24	-1.25 ± 0.13
bn141222691	H	0.44 ± 0.15	4.19	0.87 ± 0.29	-1.02 ± 0.19
bn141229492	H	0.55 ± 0.16	1.97	0.61 ± 0.32	-0.91 ± 0.19
bn150220598	H	0.37 ± 0.10	3.10	0.45 ± 0.17	-0.83 ± 0.28
bn150306993	H	2.64 ± 0.26	9.98	5.10 ± 1.64	-0.58 ± 0.05
bn150314205	H	0.68 ± 0.05	4.50	0.87 ± 0.08	-0.30 ± 0.04
bn150514774	H	0.46 ± 0.08	2.07	0.70 ± 0.18	-0.61 ± 0.15
bn150721242	H	2.51 ± 0.98	8.54	2.54 ± 0.40	-0.72 ± 0.04
bn090520876	T	-0.50 ± 5.32	8.94	1.63 ± 1.14	-0.80 ± 0.27
bn0810091401	T	0.48 ± 0.04	4.15	0.66 ± 0.06	-0.47 ± 0.02
bn0901310902	T	0.02 ± 0.05	0.93	0.11 ± 0.07	-0.25 ± 0.07

Table 4—Continued

GRB	Evolution ^a	$\hat{\tau}_{31}$	W	$k_{\hat{\tau}}$	k_E
bn0906183532	T	2.38 ± 0.33	16.40	3.32 ± 0.56	-0.67 ± 0.09
bn090620400	T	0.87 ± 0.13	5.73	0.71 ± 0.27	-1.23 ± 0.16
bn090804940	T	0.19 ± 0.09	4.22	0.35 ± 0.20	-0.61 ± 0.08
bn100528075	T	0.62 ± 0.18	10.36	0.90 ± 0.28	-0.93 ± 0.59
bn101126198	T	0.44 ± 0.16	8.69	0.59 ± 0.26	-0.64 ± 0.20
bn1106258812	T	0.20 ± 0.03	2.45	0.27 ± 0.04	-1.93 ± 0.14
bn1109030092	T	-0.11 ± 0.38	1.90	0.97 ± 0.15	-1.08 ± 0.10
bn1203282682	T	0.53 ± 0.09	5.94	0.74 ± 0.18	-1.01 ± 0.20
bn120727681	T	0.75 ± 0.16	6.27	1.15 ± 0.35	-0.67 ± 0.12
bn120919309	T	0.55 ± 0.09	3.34	0.76 ± 0.18	-0.76 ± 0.11
bn130206482	T	0.40 ± 0.11	3.71	0.81 ± 0.28	-1.18 ± 0.26
bn130518580	T	0.55 ± 0.07	6.49	0.81 ± 0.08	-0.77 ± 0.09
bn140102887	T	0.05 ± 0.05	0.55	0.04 ± 0.06	-1.35 ± 0.41
bn140213807	T	0.14 ± 0.08	3.00	0.26 ± 0.15	-0.68 ± 0.08
bn1403292952	T	0.19 ± 0.02	1.66	0.23 ± 0.03	-1.09 ± 0.08
bn150118409	T	0.30 ± 0.05	2.09	0.20 ± 0.05	-1.95 ± 0.26
bn150403913	T	0.30 ± 0.08	4.28	0.60 ± 0.09	-1.65 ± 0.18
bn130612456	T	0.10 ± 0.05	2.23	0.19 ± 0.14	-0.36 ± 0.16
bn100122616	T	-0.03 ± 0.07	3.00	-0.21 ± 0.08	0.72 ± 0.11
bn131214705	T	-0.94 ± 0.15	8.18	-1.88 ± 0.25	0.46 ± 0.03
bn120308588	T	-0.10 ± 0.21	1.47	-0.19 ± 0.29	0.57 ± 0.13
bn120222021	T	0.02 ± 0.05	0.61	0.02 ± 0.46	-0.15 ± 0.36
bn120402669	T	-0.35 ± 0.21	1.89	-0.45 ± 0.24	0.02 ± 0.09
bn101208498	T	0.08 ± 0.02	0.70	0.09 ± 0.05	0.07 ± 0.20
bn110622158	T	0.17 ± 0.24	15.02	0.21 ± 0.49	-0.05 ± 0.08

^aH: H2S spectral evolution pattern; T: Tracking spectral evolution pattern.

REFERENCES

- Ackermann, M., Asano, K., Atwood, W. B., et al. 2010, *ApJ*, 716, 1178
- Arimoto, M., Kawai, N., Asano, K., et al. 2010, *PASJ*, 62, 487
- Band, I. M., & Trzhaskovskaya, M. B. 1993, *Atomic Data and Nuclear Data Tables*, 55, 43
- Band, D. L. 1997, *ApJ*, 486, 928
- Bernardini, M. G., Ghirlanda, G., Campana, S., et al. 2015, *MNRAS*, 446, 1129
- Cheng, L. X., Ma, Y. Q., Cheng, K. S., Lu, T., & Zhou, Y. Y. 1995, *A&A*, 300, 746
- Colgate, S. A. 1974, *ApJ*, 187, 333
- Deng, W., & Zhang, B. 2014, *ApJ*, 785, 112
- Deng, W., Li, H., Zhang, B., & Li, S. 2015, *ApJ*, 805, 163
- Eichler, D., Livio, M., Piran, T., & Schramm, D. N. 1989, *Nature*, 340, 126
- Fishman, G. J., Bhat, P. N., Mallozzi, R., et al. 1994, *Science*, 264, 1313
- Gehrels, N., Norris, J. P., Barthelmy, S. D., et al. 2006, *Nature*, 444, 1044
- Golenetskii, S. V., Mazets, E. P., Aptekar, R. L., & Ilinskii, V. N. 1983, *Nature*, 306, 451
- Hakkila, J., Giblin, T. W., Norris, J. P., Fragile, P. C., & Bonnell, J. T. 2008, *ApJ*, 677, L81
- Hakkila, J., & Nemiroff, R. J. 2009, *ApJ*, 705, 372
- Hakkila, J., & Preece, R. D. 2011, *ApJ*, 740, 104
- Hakkila, J. E., & Preece, R. D. 2013, *AAS/High Energy Astrophysics Division #13*, 13, 124.01
- Hakkila, J., & Preece, R. D. 2014, *ApJ*, 783, 88
- Hakkila, J., Lien, A., Sakamoto, T., et al. 2015, *ApJ*, 815, 134
- Hakkila, J., Horváth, I., Hofesmann, E., & Lesage, S. 2018, *ApJ*, 855, 101
- Hu, Y.-D., Liang, E.-W., Xi, S.-Q., et al. 2014, *ApJ*, 789, 145
- Kocevski, D., Ryde, F., & Liang, E. 2003, *ApJ*, 596, 389
- Kumar, P., & Zhang, B. 2015, *Phys. Rep.*, 561, 1
- Lazarian, A., Zhang, B., & Xu, S. 2018, *ApJ*, submitted (arXiv:1801.04061)
- Liang, E., & Kargatis, V. 1996, *Nature*, 381, 49

- Liang, E.-W., Zhang, B.-B., Stamatikos, M., et al. 2006, *ApJ*, 653, L81
- Lu, R.-J., Hou, S.-J., & Liang, E.-W. 2010, *ApJ*, 720, 1146
- Lu, R.-J., Wei, J.-J., Liang, E.-W., et al. 2012, *ApJ*, 756, 112
- Margutti, R., Guidorzi, C., Chincarini, G., et al. 2010, *MNRAS*, 406, 2149
- McBreen, S., Foley, S., Watson, D., et al. 2008, *ApJ*, 677, L85
- Narayan, R., Paczynski, B., & Piran, T. 1992, *ApJ*, 395, L83
- Norris, J. P., & Bonnell, J. T. 2006, *ApJ*, 643, 266
- Norris, J. P., Share, G. H., Messina, D. C., et al. 1986, *ApJ*, 301, 213
- Norris, J. P., Nemiroff, R. J., Bonnell, J. T., et al. 1996, *ApJ*, 459, 393
- Norris, J. P., Marani, G. F., & Bonnell, J. T. 2000, *ApJ*, 534, 248
- Norris, J. P., Bonnell, J. T., Kazanas, D., et al. 2005, *ApJ*, 627, 324
- Paczynski, B. 1986, *ApJ*, 308, L43
- Page, K. L., Willingale, R., Osborne, J. P., et al. 2007, *ApJ*, 663, 1125
- Preece, R. D., Briggs, M. S., Mallozzi, R. S., et al. 2000, *ApJS*, 126, 19
- Preece, R., Goldstein, A., Bhat, N., et al. 2016, *ApJ*, 821, 12
- Qin, Y., Liang, E.-W., Liang, Y.-F., et al. 2013, *ApJ*, 763, 15
- RÁCZ, I. I., Balázs, L. G., Horvath, I., Tóth, L. V., & Bagoly, Z. 2018, *MNRAS*, 475, 306
- Schaefer, B. E. 2007, *ApJ*, 660, 16
- Sonbas, E., MacLachlan, G. A., Shenoy, A., Dhuga, K. S., & Parke, W. C. 2013, *ApJ*, 767, L28
- Sultana, J., Kazanas, D., & Fukumura, K. 2012, *ApJ*, 758, 32
- Uhm, Z. L., & Zhang, B. 2016, *ApJ*, 825, 97
- Uhm, Z. L., Zhang, B., & Racusin, J. L. 2018, *ApJ*, submitted (arXiv:1801.09183)
- Ukwatta, T. N., Stamatikos, M., Dhuga, K. S., et al. 2010, *ApJ*, 711, 1073
- Ukwatta, T. N., Dhuga, K. S., Stamatikos, M., et al. 2012, *MNRAS*, 419, 614
- Wheaton, W. A., Ulmer, M. P., Baity, W. A., et al. 1973, *ApJ*, 185, L57
- Woosley, S. E., & Bloom, J. S. 2006, *ARA&A*, 44, 507

Woosley, S. E. 1993, *ApJ*, 405, 273

Yi, T., Liang, E., Qin, Y., & Lu, R. 2006, *MNRAS*, 367, 1751

Zhang, B., & Yan, H. 2011, *ApJ*, 726, 90

Zhang, B., & Zhang, B. 2014, *ApJ*, 782, 92

Zhang, B., Zhang, B.-B., Virgili, F. J., et al. 2009, *ApJ*, 703, 1696

Zhang, B.-B., Zhang, B., Liang, E.-W., et al. 2011, *ApJ*, 730, 141